UNIVERSITAT DE BARCELONA

Desarrollo de formulaciones de Apremilast para el tratamiento de patologías en piel y mucosas

Development of Apremilast formulations for the treatment of skin and mucous membrane pathologies

Paulo Cesar Sarango Granda

UNIVERSITAT DE BARCELONA

FACULTAD DE FARMACIA Y CIENCIAS DE LA ALIMENTACIÓN

**DEPARTAMENTO DE FARMACIA,
TECNOLOGÍA FARMACÉUTICA Y FISICOQUÍMICA**

Unidad de Biofarmacia y Farmacocinética

Desarrollo de formulaciones de Apremilast para el tratamiento de patologías en piel y mucosas

«Development of Apremilast formulations for the treatment of skin and mucous membrane pathologies»

PAULO CESAR SARANGO GRANDA

2023

UNIVERSITAT DE BARCELONA

FACULTAD DE FARMACIA Y CIENCIAS DE LA ALIMENTACIÓN

PROGRAMA DE DOCTORADO EN INVESTIGACIÓN,
DESARROLLO Y CONTROL DE MEDICAMENTOS

Desarrollo de formulaciones de Apremilast para el tratamiento de patologías en piel y mucosas

«Development of Apremilast formulations for the treatment of skin and mucous membrane pathologies»

Memoria presentada por Paulo Cesar Sarango Granda, para optar al título de doctor por la Universidad de Barcelona

Directoras de Tesis:

Ana Cristina Calpena Campmany	Josefa Badía Palacín	Lupe Carolina Espinoza Tituana

Doctorando:	**Tutora:**
Paulo Cesar Sarango Granda	Ana Cristina Calpena Campmany

2023

Con todo mi corazón a los amores de mi vida Celina, Rocío y Rosa, pues sin ellas no lo habría logrado. Sus bendiciones a lo largo de mi vida me protegen y me llevan por el mejor camino.

AGRADECIMIENTOS

«Gracias, Señor, por darme la vida y por todas las bendiciones que has derramado sobre mí. Estoy agradecido por el amor que me has demostrado todos los días de mi vida».

(Salmo 136:1-3).

Primeramente, quiero dar las gracias a Dios y la Virgen del Cisne que han estado continuamente presentes, desde los momentos más felices hasta aquellos días en donde me sentía perdido y sin rumbo; siempre me han apoyado en mi caminar y me han sabido guiar y poner en el camino a personas maravillosas que me han ayudado en mí crecimiento personal.

Han transcurrido tres años desde aquel momento en el que decidí iniciar el programa doctoral y, al fin se acerca el día de ver cumplida esta meta que me había planteado. Ha sido una etapa muy enriquecedora para mi vida, me permitió compartir y receptar conocimiento de personas maravillosas, a quien deseo extender mis sentimientos de gratitud:

A mis directoras de tesis:

Dra. Ana Calpena, quien desde el primer momento que nos conocimos me extendió su mano y apoyo, desde el inicio me hizo sentir como en casa, siempre guiándome, compartiendo su conocimiento, brindándome consejos y teniendo paciencia conmigo; para mí, se ha convertido en un gran referente de la cual no solamente resalto su potencial académico sino también su gran calidez humana.

Dra. Josefa Badia, Pepita que me acogió como su tesista doctoral y que desde el inicio me brindó todo su apoyo para el desarrollo de mi tesis y que en

determinados momentos supo comprender por las situaciones que atravesaba, agradezco sus consejos y paciencia conmigo.

PhD. Carolina Espinoza, quien me ha apoyado desde el inicio, compartiendo su conocimiento, brindándome su mano amiga para mi desarrollo no solamente académico, sino también como persona, dándome consejos y siempre con las palabras apropiadas en el momento justo.

Al grupo de profesionales de diferentes áreas que se enmarcaron dentro de esta investigación como lo son Marcelle Silva-Abreu, Lyda Halbaut, Mª José Rodríguez, Mª José Fábregas, Natalia Díaz, Laura Baldomá, Helen Alvarado y Mireia Mallandrich.

Un agradecimiento a Lyda, que ha sido una de las personas que me ha brindado su apoyo desde el inicio cuando comencé la maestría hasta el desarrollo de la tesis doctoral; asimismo un agradecimiento especial para Mireia que compartimos grandes momentos académicos y laborales, gracias a ella y Ana me guiaron para mi desarrollo profesional en el extranjero y del cual aprendí muchísimo y obtuve una gran experiencia, definitivamente no sabría como retribuirles lo cuan buenas han sido conmigo.

Asimismo, extender mi agradecimiento a Kymos S.L y a todo su personal que me abrió sus puertas y me permitió experimentar en el campo laboral europeo, sobre todo mi agradecimiento por su paciencia, enseñanzas y calidad humana que me brindaron a Digna, Emma, Sandra y demás compañeros del departamento de Bioanalysis & Permeation.

A la Universidad Técnica Particular de Loja a través del Departamento de Química que me abrieron las puertas y con su visión y misión me permiten contribuir en la formación de profesionales integrales, asimismo por la

oportunidad que me brindan en mi desarrollo tanto personal como académico. En especial, gracias a mis compañeros Vladimir, Santiago y Lupe por su apoyo.

Esta tesis es motivo de felicidad ya que se ve reflejado el trabajo realizado durante estos años; agradezco desde lo más profundo de mi corazón a mi madre Rocío, por brindarme el apoyo incondicional desde siempre, ese apoyo que una madre puede dar a sus hijos. Así como también a mi mami Celina y a la Chochita que con su infinito amor me criaron, cuidaron y guiaron para que vaya por el buen camino, paso a paso consiguiendo las cosas. A mi ñaña Mónica y Fabián, que siempre estuvo al pendiente de mí, apoyándome y dándome ánimos, y como no a los pequeños Jordi e Ian, que me alegraban los fines de semana con sus ocurrencias.

A mis amigas que me acompañaron durante este recorrido y que hicieron ameno todo este trabajo, con especial atención a Marcelinha, María y Carolina, que compartimos momentos inolvidables, conocimiento, viajes, risas y frustraciones. Asimismo, con Cynthia, Aphy y Tefys que el tiempo que compartimos en el extranjero estrechó mucho más nuestros lazos de amistad. Gracias por todo.

Un agradecimiento también a todas las personas con las que me tope en mi camino y que contribuyeron a mi crecimiento personal y profesional, la lista es enorme, pero mi cariño y respeto siempre estará para todos ustedes.

Paulo Cesar Sarango Granda

ÍNDICE DE CONTENIDOS

RESUMEN

Apremilast (APR) es un inhibidor selectivo de la fosfodiesterasa 4 que se administra por vía oral para el tratamiento de la psoriasis en placas de moderada a grave y la artritis psoriásica activa. La baja solubilidad y permeabilidad de este fármaco dificultan su administración dérmica. Uno de los propósitos de este estudio fue diseñar y caracterizar una microemulsión cargada con apremilast como terapia tópica para la inflamación local de la piel. Su composición se determinó mediante diagramas pseudoternarios. Se realizaron caracterizaciones físicas, químicas y biofarmacéuticas. Se estudió la estabilidad de esta formulación durante 90 días. Se evaluó la tolerabilidad de APR-ME en voluntarios sanos y se estudió su potencial antiinflamatorio mediante modelos *in vitro* e *in vivo*. Se obtuvo una formulación homogénea con comportamiento newtoniano y gotas de tamaño nanométrico y forma esférica. APR-ME liberó el fármaco incorporado siguiendo una cinética de primer orden y facilitó la retención del fármaco en la piel, asegurando un efecto local. Se observó potencial antiinflamatorio por su capacidad para disminuir la producción de IL-6 e IL-8 en el modelo *in vitro*. Este efecto se confirmó en el modelo *in vivo* histológicamente por la reducción de la infiltración de células inflamatorias e inmunológicamente por la disminución de las citocinas inflamatorias IL-8, IL-17A y TNFα. En consecuencia, estos resultados sugieren que esta formulación podría utilizarse como un atractivo tratamiento tópico para la inflamación cutánea. Por otro lado, la escasa solubilidad en agua de APR es el principal impedimento para la penetración del fármaco a través de la barrera cutánea. Otro de los objetivos del estudio era evaluar la permeabilidad de APR en diferentes soluciones enriquecidas con promotores de la penetración en muestras *ex vivo* de piel humana, y evaluar además su tolerancia *in vivo*. Para ello, se desarrollaron soluciones de APR con un 5% de promotor y se evaluó la capacidad del fármaco para penetrar en muestras de piel abdominal humana; los

coeficientes de permeabilidad, las cantidades acumuladas permeadas y el flujo fueron algunos de los parámetros evaluados. Asimismo, se evaluó la tolerancia *in vitro* e *in vivo* de las soluciones. Los resultados obtenidos mostraron que las soluciones que contenían escualeno como promotor mejoraban la penetración de la APR en comparación con los otros promotores evaluados; del mismo modo, a escala *in vitro* en células HaCaT los promotores no resultaron tóxicos, encontrándose una viabilidad celular superior al 80% en las diferentes diluciones evaluadas. En las pruebas *in vivo* realizadas con APR-Escualeno presentó los mejores resultados. El escualeno se convierte en un excelente candidato para mejorar la permeabilidad del fármaco en el caso del desarrollo de una formulación tópica; además, se confirmó que este potenciador de la penetración no es ni tóxico ni irritante en contacto con la piel en ensayos *in vivo*.

ABSTRACT

Apremilast (APR) is a selective phosphodiesterase-4 inhibitor that is administered orally for the treatment of moderate to severe plaque psoriasis and active psoriatic arthritis. The low solubility and permeability of this drug make dermal administration difficult. One of the purposes of this study was to design and characterize an apremilast-loaded microemulsion as a topical therapy for local skin inflammation. Its composition was determined using pseudoternary diagrams. Physical, chemical and biopharmaceutical characterizations were performed. The stability of this formulation was studied for 90 days. The tolerability of APR-ME was evaluated in healthy volunteers and its anti-inflammatory potential was studied by *in vitro* and *in vivo* models. A homogeneous formulation with Newtonian behavior and droplets of nanometer size and spherical shape was obtained. APR-ME released the incorporated drug following first-order kinetics and facilitated drug retention in the skin, ensuring a local effect. Anti-inflammatory potential was observed due to its ability to decrease IL-6 and IL-8 production in the *in vitro* model. This effect was confirmed in the *in vivo* model histologically by the reduction of inflammatory cell infiltration and immunologically by the decrease of inflammatory cytokines IL-8, IL-17A and TNFα. Consequently, these results suggest that this formulation could be used as an attractive topical treatment for cutaneous inflammation. On the other hand, the poor water solubility of APR is the main impediment to the penetration of the drug through the skin barrier. Another objective of the study was to evaluate the permeability of APR in different solutions enriched with penetration promoters in ex vivo samples of human skin, and also to evaluate its in vivo tolerance. For this purpose, APR solutions with 5% promoter were developed and the ability of the drug to penetrate human abdominal skin samples was evaluated; permeability coefficients, permeated cumulative

amounts and flux were some of the parameters evaluated. The *in vitro* and *in vivo* tolerance of the solutions was also evaluated. The results obtained showed that the solutions containing squalene as promoter improved the penetration of APR compared to the other promoters evaluated; likewise, at *in vitro* scale in HaCaT cells the promoters were not toxic, finding a cell viability higher than 80% in the different dilutions evaluated. In the *in vivo* tests carried out with APR-Squalene, it presented the best results. Squalene becomes an excellent candidate to improve drug permeability in the case of the development of a topical formulation; in addition, it was confirmed that this penetration enhancer is neither toxic nor irritating in contact with the skin *in vivo* tests.

RESUM

Apremilast (APR) és un inhibidor selectiu de la fosfodiesterasa 4 que s'administra per via oral per al tractament de la psoriasi en plaques de moderada a greu i l'artritis psoriàsica activa. La baixa solubilitat i permeabilitat d'aquest fàrmac en dificulten l'administració dèrmica. Un dels propòsits d'aquest estudi va ser dissenyar i caracteritzar una microemulsió carregada amb apremilast com a teràpia tòpica per a la inflamació local de la pell. La seva composició es va determinar mitjançant diagrames pseudoternaris. Es van realitzar caracteritzacions físiques, químiques i biofarmacèutiques. Es va estudiar aquesta estabilitat durant 90 dies. Es va avaluar la tolerabilitat d'APR-ME en voluntaris sans i se'n va estudiar el potencial antiinflamatori mitjançant models *in vitro* i *in vivo*. Es va obtenir una formulació homogènia amb comportament newtonià i gotes de mida nanomètrica i forma esfèrica. APR-ME va alliberar el fàrmac incorporat seguint una cinètica de primer ordre i va facilitar la retenció del fàrmac a la pell, assegurant un efecte local. Es va observar potencial antiinflamatori per la seva capacitat per disminuir la producció d'IL-6 i IL-8 al model *in vitro*. Aquest efecte es va confirmar en el model *in vivo* histològicament per la reducció de la infiltració de cèl·lules inflamatòries i immunològicament per la disminució de les citocines inflamatòries IL-8, IL-17A i TNFα. En conseqüència, aquests resultats suggereixen que aquesta formulació es podria utilitzar com un atractiu tractament tòpic per a la inflamació cutània. D'altra banda, la solubilitat escassa en aigua d'APR és el principal impediment per a la penetració del fàrmac a través de la barrera cutània. Un altre dels objectius de l'estudi era avaluar la permeabilitat d'APR en diferents solucions enriquides amb promotors de la penetració en mostres *ex vivo* de pell humana, i avaluar a més la seva tolerància *in vivo*. Per això, es van desenvolupar solucions d'APR amb un 5% de promotor i es va avaluar la capacitat del fàrmac per penetrar en mostres de pell abdominal

humana; els coeficients de permeabilitat, les quantitats acumulades permeades i el flux van ser alguns dels paràmetres avaluats. Així mateix, es va avaluar la tolerància *in vitro* i *in vivo* de les solucions. Els resultats obtinguts van mostrar que les solucions que contenien esqualè com a promotor milloraven la penetració de l'APR en comparació amb els altres promotors avaluats; de la mateixa manera, a escala *in vitro* en cèl·lules HaCaT els promotors no van resultar tòxics, i es va trobar una viabilitat cel·lular superior al 80% en les diferents dilucions avaluades. A les proves *in vivo* realitzades amb APR-Esqualè va presentar els millors resultats. L'esqualè es converteix en un candidat excel·lent per millorar la permeabilitat del fàrmac en el cas del desenvolupament d'una formulació tòpica; a més, es va confirmar que aquest potenciador de la penetració no és ni tòxic ni irritant en contacte amb la pell en assaigs *in vivo*.

CAPÍTULO 1

INTRODUCCIÓN

1.1. INFLAMACIÓN

El término inflamación se toma de la palabra latina *"inflammare"* que significa *quemar*. La inflamación es una respuesta que posee el organismo a diferentes agresiones endógenas o exógenas (1) , en otras palabras, es un proceso generado para la defensa de las células animales contra ciertas lesiones o infecciones microbianas (2). Dependiendo del tiempo de evolución pueden ser de tipo agudas o crónicas. La inflamación se caracteriza por cinco signos como calor, rubor, dolor, tumoraciones e impotencia funcional, causadas principalmente por la acumulación de proteínas plasmáticas y leucocitos en los tejidos extravasculares donde se está produciendo la infección provocada o no por los agentes patógenos (3).

La inflamación aguda comprende diferentes mecanismos estructurales y moleculares, suele iniciar en poco tiempo y participa directamente la respuesta inmune innata que a su vez activa a la respuesta inmune adquirida. La presencia de pus en la dermis, esputo de coloración amarillento se asocian a signos de respuesta inflamatoria aguda por algún agente (4). Mientras que la inflamación crónica suele ocurrir días después cuando no se ha eliminado completamente al agente patógeno o factor de daño, en este caso participa inicialmente la respuesta inmunitaria innata, sin embargo, es la respuesta inmunitaria adquirida la que mantendrá todo el proceso en cuanto a tiempo como en daño tisular generado (5)

Según Devarajan et al 2014, mencionan que las afecciones inflamatorias pueden ser enfermedades autoinmunes, infecciones persistentes, exposición

prolongada a tóxicos (6). Entre algunas encontramos la psoriasis, esclerosis múltiple, infecciones por virus, bacterias, exposiciones a humos, productos químicos, entre otras.

1.1.1. Mecanismos de la inflamación

El mecanismo de la inflamación corresponde a una cadena de respuestas dinámicas organizadas en donde se producen eventos celulares y vasculares donde se incluyen secreciones humorales específicas (7). Esta cadena de respuesta implica cambiar o mover la ubicación de los monocitos, basófilos, eosinófilos y neutrófilos al sitio inflamado. Las células de defensa inmunitaria que posee el organismo libera un grupo de mediadores y otras moléculas de señalización al mecanismo que ayudará a la inflamación (8). Entre las moléculas que favorecen el desarrollo de la inflamación encontramos a las citocinas, quimiocinas, metabolitos lipídicos, selectinas, integrinas, inmunoglobulinas, complemento, entre otras (9).

Sea lo que sea, la respuesta inflamatoria se desencadena a través de dos fases: (a) aguda y (b) crónica, y cada una está aparentemente mediada por un mecanismo diferente. Estas respuestas inmunes que participan en la inflamación aguda se pueden dividir en vasculares y celulares.

Las respuestas que ocurren en la microvasculatura normalmente aparecen en pocos minutos después de una lesión tisular o infección microbiana en presencia de otros estímulos inflamatorios llamados eventos vasculares (10). La ocurrencia de estos procesos es rápida y eventualmente conducirá a la vasodilatación y, posteriormente, hará que los vasos se vuelvan más permeables. Estos procesos darán lugar a la entrada de mediadores inflamatorios y produce edema intersticial.

La inflexión de los glóbulos blancos del sistema circulatorio es esencial durante las respuestas inflamatorias (11). Un grupo de agentes quimiotácticos, como las endotoxinas microbianas que contienen grupos N-formil metionilo amino terminal, el fragmento del complemento C5a y las interleucinas junto con las secreciones de basófilos como el factor activador de plaquetas, la histamina y el leucotrieno B pueden estimular la infiltración intensa de leucocitos en pocos minutos (12). Entre los leucocitos, los neutrófilos son las primeras células inflamatorias que se reclutan en el sitio de inflamación aguda. La infiltración de células inmunes se desencadena a través de un mecanismo complicado en el que los glóbulos blancos trabajan junto con el endotelio en las vénulas postcapilares.

Los eventos celulares abarcan la captura sucesiva, el movimiento y la afirmación de una adhesión al endotelio microvascular. Estos eventos en la vía de movilización están organizados por moléculas de adhesión celular (CAM). Estas CAM incluyen moléculas de adhesión intracelular (ICAM)-1, ICAM-2, integrinas y selectina. El grupo selectin de CAM contiene tres familias; P-selectina y E-selectina producidas por células endoteliales y L-selectina producidas por glóbulos blancos. La adhesión de alta afinidad presentada sobre los glóbulos blancos en el endotelio está mediada por la interacción entre integrinas (CDII/CDI8) y moléculas de adhesión (CAM-l y CAM-2) expresadas en glóbulos blancos y células endoteliales, respectivamente (13). Después de un período de adhesión estacionaria, los glóbulos blancos pueden salir de las vénulas postcapilares extendiendo seudópodos entre las células endoteliales y llegar al espacio subendotelial. Este evento complejo a menudo se conoce como extravasaciones de glóbulos blancos y migración transendotelial.

La inflamación de los eventos crónicos se distingue por la infiltración de células mononucleares (por ejemplo, monocitos y linfocitos), la proliferación de fibroblastos, las fibras de colágeno y la formación de tejido conectivo (14). Con la

inflamación crónica, la degeneración tisular normalmente está mediada por especies de nitrógeno, proteasas y otras especies reactivas de oxígeno liberadas de células inflamatorias infiltradas. Ciertamente, las alteraciones genómicas en p53 fueron aprobadas como causas de muchas enfermedades inflamatorias crónicas (por ejemplo, enfermedades inflamatorias intestinales y artritis reumatoide) además de cánceres (15,16).

1.1.2. Monofosfato de adenosina cíclico

El monofosfato de adenosina cíclico (cAMP) es un segundo mensajero que regula una amplia variedad de funciones celulares, incluido el crecimiento celular, la diferenciación, la proliferación, la migración, el transporte de iones, la regulación del pH y la expresión génica (17,18). La señalización del cAMP se inicia en respuesta a diversos estímulos y afecta a las funciones antes mencionadas a través de sus proteínas efectoras: proteína quinasa A (PKA), proteína de intercambio activada por cAMP (EPAC) y canales iónicos dependientes de nucleótidos cíclicos (19). En las células de mamíferos, el cAMP se produce a partir de ATP por dos tipos distintos de adenilil ciclasas (AC): una familia de adenilil ciclasas transmembrana (tmAC), compuesta por nueve miembros (ADCY1-9), y la adenilil ciclasa soluble descubierta más recientemente (sAC), que está codificada por un solo gen (ADCY10) (20,21).

La señalización de cAMP ocurre en microdominios intracelulares distintos y altamente localizados. Una vez generado, el cAMP es degradado fácilmente por las PDE, asegurando que el cAMP solo active los efectores de cAMP asociados espacialmente (22). Los microdominios de cAMP dependen de las proteínas de anclaje que atan las proteínas de señalización de cAMP a áreas específicas de la célula. PKA, el efector de cAMP mejor caracterizado, está atado a varios sitios intracelulares por proteínas de anclaje de A-quinasa. Dado que la activación de la señalización de cAMP no se debe a un aumento uniforme en los niveles de

cAMP en toda la célula, diferentes subconjuntos de efectores de cAMP anclados están expuestos a diferentes microdominios de cAMP (23–25). Esto permite que solo se active selectivamente el subconjunto apropiado de objetivos. Estos modelos ayudan a explicar cómo un solo segundo mensajero es capaz de llevar a cabo una gran cantidad de funciones simultáneamente.

Las proteínas llamadas fosfodiesterasas son esenciales para establecer microdominios de cAMP, ya que crean una barrera de difusión para cAMP. Entre sus once isoformas, ocho (PDE4, PDE7 y PDE8 específicas de cAMP, y PDE1, PDE2, PDE3, PDE10 y PDE11 selectivas de cAMP y cGMP) hidrolizan el cAMP (26,27). Fundamental para el estricto control espacio-temporal de la dinámica de señalización de cAMP es la compartimentación de las PDE. Es bien sabido que las isoformas específicas de PDE se localizan en distintos compartimentos subcelulares y regulan las vías diferenciales de señalización de cAMP (28). También se informa que las PDE forman interacción proteína-proteína con varias proteínas efectoras de cAMP, proteínas unidas a la membrana y proteínas de andamiaje. Un ejemplo bien establecido es el anclaje de la isoforma PDE4D3 junto con PKA a la proteína de andamiaje mAKAP en sitios perinucleares y la regulación positiva de PDE4 por fosforilación mediada por PKA. El aumento de la señalización de cAMP en estos sitios perinucleares asociados a mAKAP, por lo tanto, aumenta la actividad del grupo local de PDE4D3, creando una barrera de difusión con una fuerza proporcional a la intensidad de la señalización de cAMP (29–31). Estos ejemplos de cómo se integran isoformas específicas de PDE en microdominios de señalización de cAMP únicos resaltan su papel esencial en el mantenimiento de la especificidad de las funciones llevadas a cabo por diferentes microdominios de señalización de cAMP.

Dentro de una célula existe una serie de microdominios cAMP espacialmente restringidos. Los microdominios de cAMP localizados en la membrana

plasmática generalmente se inician mediante un GPCR, que se activa mediante la unión del ligando, seguido de la liberación de Gsα que conduce a la activación de la adenilil ciclasa y la regulación positiva del cAMP en sitios cercanos a la membrana plasmática. Los diferentes GPCR tienen distintas localizaciones en la membrana plasmática e inician diferentes respuestas objetivo de señalización de cAMP, lo que sugiere que este compartimento de membrana casi plasmática se puede subdividir en distintos microdominios de cAMP (32–34). Además, la evidencia reciente muestra que los GPCR internalizados en los endosomas mantienen su capacidad para activar la producción de cAMP, definiendo un microdominio cAMP mediado por GPCR adicional que está más lejos de la membrana plasmática.

1.1.3. Fosfodiesterasa-4

Las fosfodiesterasas (PDE), que constan de 11 familias (PDE1–PDE11), están disponibles para la degradación de nucleótidos cíclicos. Las distribuciones de las subfamilias de PDE son diversas en diferentes células y tejidos, lo que puede proporcionar un apoyo sustancial para su investigación farmacológica en el campo de la inflamación, la cognición, la lipogénesis, la proliferación, la apoptosis y la diferenciación (35,36). La PDE4 específica de cAMP se expresa altamente en el cerebro, los tejidos cardiovasculares, los músculos lisos, los queratinocitos y los inmunocitos (incluidas las células T, monocitos, macrófagos, neutrófilos, células dendríticas, eosinófilos). La inhibición de la PDE4 puede elevar el nivel intracelular de cAMP y, posteriormente, modular las respuestas inflamatorias y mantener el equilibrio inmunológico (19,37).

Se ha verificado que dirigirse a la PDE4 es una estrategia terapéutica efectiva para afecciones inflamatorias, como asma, enfermedad pulmonar obstructiva crónica (EPOC), psoriasis, dermatitis atópica (DA), enfermedades inflamatorias intestinales (EII), artritis reumática (AR), lupus y neuroinflamación. A través de

grandes esfuerzos, roflumilast, apremilast y crisaborole fueron aprobados sucesivamente para el tratamiento de enfermedades inflamatorias de las vías respiratorias o de la piel (38–40). Además, también se han desarrollado una serie de nuevos inhibidores de la PDE4 para la regulación de la inflamación, y mostraron eficacias terapéuticas satisfactorias.

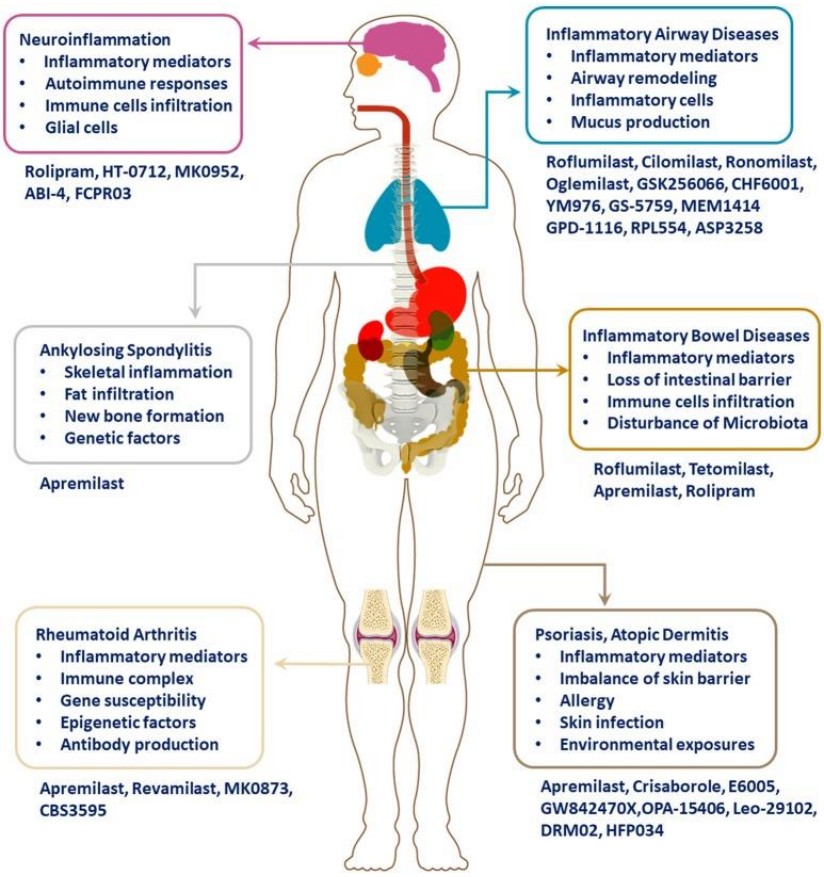

Ilustración 1. *Manifestaciones patológicas e inhibidoras de la PDE4 en enfermedades inflamatorias (41)*

La creciente evidencia demostró que los pacientes que sufrían de enfermedades inflamatorias mostraron una mayor expresión de PDE4 que los individuos sanos. Hay cuatro subtipos de PDE4, a saber, PDE4A-PDE4D, que son altamente específicos para la degradación de cAMP pero no para cGMP. La inhibición de la PDE4 da como resultado la acumulación de cAMP intracelular y, posteriormente, activa PKA, canales iónicos dependientes de nucleótidos cíclicos y Epac1/2 (42–45). Estos están involucrados en la regulación de la síntesis de citoquinas proinflamatorias y antiinflamatorias, la activación de las células T, la

desgranulación de neutrófilos, el rendimiento de la presentación del antígeno y la integridad epitelial a través del inicio de múltiples elementos.

La liberación de la subunidad catalítica de la subunidad reguladora tras la activación de PKA podría aumentar posteriormente la fosforilación de la proteína de unión al elemento sensible al cAMP (CREB), activando el factor de transcripción 1 (ATF-1) y el modulador del elemento sensible a cAMP (CREM) y reclutar la proteína de unión a CREB (CBP) o la proteína homóloga p300, lo que lleva a la reducción de citoquinas inflamatorias y al aumento de citoquinas antiinflamatorias (46,47).

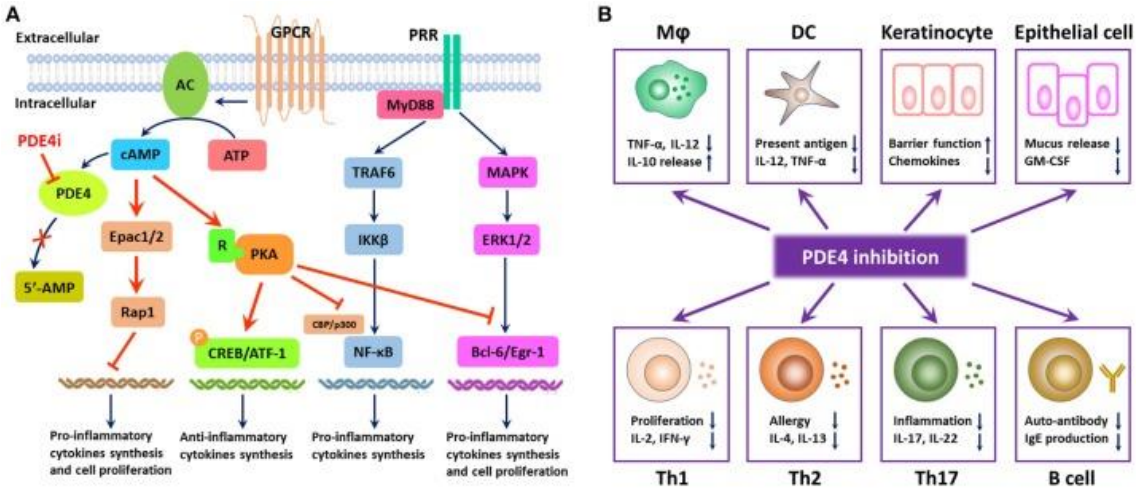

Ilustración 2. *Modo de inhibición de la PDE4 en la regulación de la respuesta inflamatoria.* ***(A)*** *La PDE4 regula la producción de citoquinas proinflamatorias y antiinflamatorias y la proliferación celular a través de la degradación del AMPc.* ***(B)*** *La inhibición de la PDE4 tiene un amplio espectro de efectos antiinflamatorios. Debido a la distribución de PDE4 en el cuerpo humano, la inhibición de PDE4 puede inhibir las respuestas inflamatorias de macrófagos, DC, células Th1, Th2 y Th17, aumentar la producción de citoquinas antiinflamatorias de los macrófagos e interferir con el fenotipo y la función de las células B también. Además, la inhibición de la PDE4 también puede promover la función de barrera de los queratinocitos y las células epiteliales a través de la supresión de la producción de mediadores inflamatorios (41).*

1.1.4. Mediadores

Una variedad de mediadores químicos del sistema circulatorio, las células inflamatorias y el tejido lesionado contribuyen activamente y ajustan la respuesta inflamatoria. Los mediadores químicos liberados incluyen: (I) aminas vasoactivas como histamina y serotonina, (II) péptidos y (III) eicosanoides (48,49).

1.2. BREVE REVISIÓN DE LA ANATOMÍA Y FISIOLOGÍA DE LA PIEL

La piel es el órgano más grande del sistema tegumentario (1.5 – 2 m^2 de superficie), comprende aproximadamente el 10% de la masa corporal total de una persona promedio. La función de la piel es proporcionar una barrera entre el cuerpo y el ambiente externo hostil (50). La función barrera protege contra la penetración de los rayos UV, productos químicos, microorganismos, alérgenos, y contra la pérdida de humedad y nutrientes corporales (51). Además, la piel cumple in rol importante en la homeostasis, regulando la temperatura corporal y la sangre (52). La piel es un órgano sensorial en contacto con el medio ambiente, de esta forma detecta la estimulación en forma de temperatura, presión y dolor.

Se sabe que la piel proporciona un sitio ideal para la administración de fármacos para efectos locales y en algunos casos sistémicos, sin embargo, presenta una barrera formidable para la penetración de muchos de los fármacos (53). Las rutas de penetración de los fármacos a través de la piel se describen más adelante en la sección. El comprender la estructura y funcionabilidad de la piel es fundamental para el diseño de óptimas formas farmacéuticas tópicas y transdérmicas.

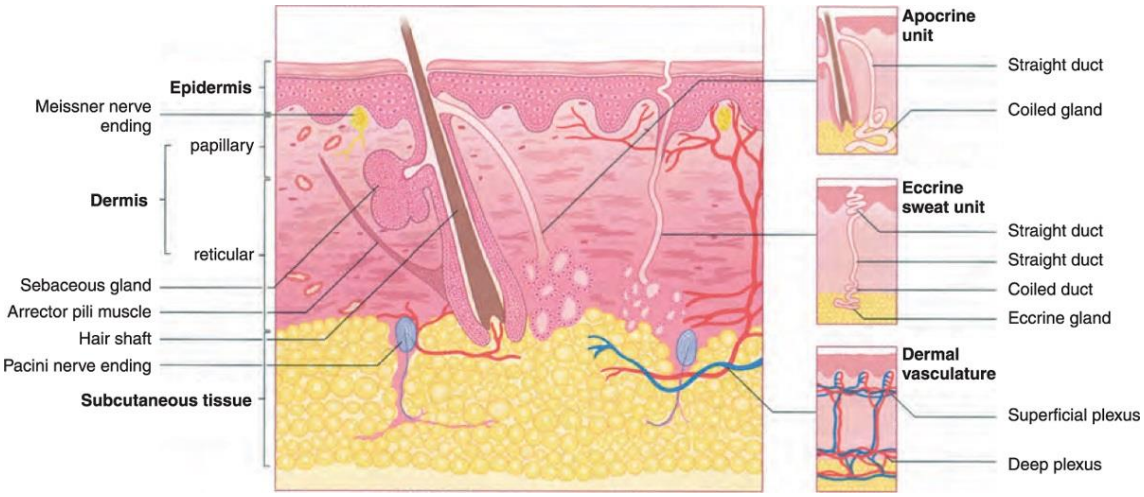

Ilustración 3. *Sección transversal de la piel y el panículo (54)*

La piel se compone de tres capas: la epidermis, la dermis y el tejido subcutáneo. El nivel más externo (epidermis) consiste en una constelación específica de células conocidas como queratinocitos, que funcionan para sintetizar queratina, una proteína larga y filiforme con un papel protector. La capa media (dermis) está formada fundamentalmente por la proteína estructural fibrilar conocida como colágeno. La dermis se encuentra en el tejido subcutáneo, opanículo, que contiene pequeños lóbulos de células grasas conocidas como lipocitos. El grosor de estas capas varía considerablemente, dependiendo de la ubicación geográfica en la anatomía del cuerpo. El párpado, por ejemplo, tiene la capa más delgada de la epidermis, que mide menos de 0.1 mm, mientras que las palmas y las plantas de los pies tienen la capa epidérmica más gruesa, midiendo aproximadamente 1.5 mm. La dermis es más gruesa en la espalda, donde es 30-40 veces más gruesa que la epidermis suprayacente (55)

1.2.1. Epidermis

La epidermis es una capa de epitelio escamoso estratificado que se compone principalmente de dos tipos de células: queratinocitos y células dendríticas. Los queratinocitos se diferencian de las células dendríticas "claras" por poseer puentes intercelulares y grandes cantidades de citoplasma teñible (56). La

epidermis alberga una serie de otras poblaciones celulares, como melanocitos, células de Langerhans y células de Merkel, pero el tipo de célula de queratinocitos comprende la mayoría de las células con diferencia. La epidermis comúnmente se divide en cuatro capas de acuerdo con la morfología y la posición de los queratinocitos, ya que se diferencian en células córneas, incluida la capa de células basales (estrato germinativo), la capa de células escamosas (estrato espinoso), la capa de células granulares (estrato granuloso) y la capa de células cornificadas o córneas (estrato córneo) (57–59).

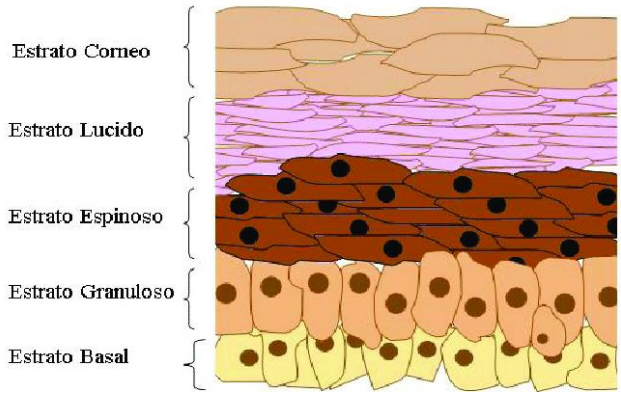

Ilustración 4. *Estructura de la epidermis (60)*

La epidermis es una capa que se renueva continuamente y da lugar a estructuras derivadas, como aparatos pilosebáceos, uñas y glándulas sudoríparas. Las células basales de la epidermis sufren ciclos de proliferación que proporcionan la renovación de la epidermis externa. La epidermis es un tejido dinámico en el que las células están constantemente en movimiento no sincronizado, ya que las diferentes poblaciones celulares individuales pasan no solo entre sí, sino también los melanocitos y las células de Langerhans a medida que se mueven hacia la superficie de la piel.

1.2.1.1. Queratinocitos

El proceso de diferenciación que ocurre cuando las células migran de la capa basal a la superficie de la piel da como resultado la queratinización, un proceso en el que el queratinocito pasa primero a través de una fase sintética y luego una fase degradativa (61,62).

En la fase sintética, la célula acumula un suministro citoplasmático de queratina, un filamento intermedio fibroso dispuesto en un patrón de bobina alfa-helicoidal que sirve como parte del citoesqueleto de la célula. Los haces de estos filamentos de queratina convergen y terminan en la membrana plasmática formando las placas de unión intercelular conocidas como desmosomas.

Durante la fase degradativa de la queratinización, los orgánulos celulares se pierden, el contenido de la célula se consolida en una mezcla de filamentos y envolturas celulares amorfas, y la célula finalmente se conoce como célula córnea o corneocitos (63). El proceso de maduración que resulta en la muerte celular se conoce como diferenciación terminal.

1.2.1.2. Capa basal

La capa basal, también conocida como estrato germinativo, contiene queratinocitos en forma de columna que se adhieren a la zona de la membrana basal con su eje largo perpendicular a la dermis. Estas células basales forman una sola capa y se adhieren entre sí, así como a las células escamosas más superficiales a través de uniones desmosómicas (64). Otras características distintivas de las células basales son sus núcleos ovalados o alargados de tinción oscura y la presencia de pigmento de melanina transferido desde melanocitos adyacentes.

La capa basal es la ubicación primaria de las células mitóticamente activas en la epidermis que dan lugar a las células de las capas epidérmicas externas. Sin

embargo, no todas las células basales tienen el potencial de dividirse. Las células madre epidérmicas en la capa basal son células clonogénicas con una larga vida útil que progresan a través del ciclo celular muy lentamente en condiciones normales. Las condiciones hiperplasiógenas, como las heridas, pueden aumentar el número de células cíclicas en la epidermis al estimular la división de las células madre. El daño al ADN causado por agentes cancerígenos puede mutar la maquinaria de proliferación celular y también puede afectar la tasa de división celular. La migración de una célula basal de la capa basal a la capa cornificada en humanos toma al menos 14 días, y el tránsito a través de la capa cornificada a la epidermis más externa requiere otros 14 días (65,66).

1.2.1.3. Capa de células escamosas

Sobre la capa de células basales hay una capa de la epidermis que tiene 5-10 células de espesor y se conoce como capa de células escamosas o estrato espinoso. La capa escamosa se compone de una variedad de células que difieren en forma, estructura y propiedades subcelulares dependiendo de su ubicación (67). Las células espinosas suprabasales, por ejemplo, son de forma poliédrica y tienen un núcleo redondeado, mientras que las células de las capas espinosas superiores son generalmente de mayor tamaño, se vuelven más planas a medida que se empujan hacia la superficie de la piel y contienen gránulos lamelares. Los gránulos lamelares son orgánulos unidos a la membrana que contienen glicoproteínas, glicolípidos, fosfolípidos, esteroles libres y varias hidrolasas ácidas, incluidas lipasas, proteasas, fosfatasas ácidas y glicosidasas (68). La abundancia de enzimas hidrolíticas indica que los gránulos lamelares son un tipo de lisosoma. Aunque los gránulos lamelares son activos principalmente en las células en la interfaz entre las capas granular y cornificada, también funcionan en las células de la capa espinosa superior para entregar precursores de lípidos del estrato córneo en el espacio intercelular (69,70).

Los espacios intercelulares entre las células espinosas están unidos por abundantes desmosomas que promueven el acoplamiento mecánico entre las células de la epidermis y proporcionan resistencia a las tensiones físicas. Organizados concéntricamente alrededor del núcleo, los filamentos de queratina en el citoplasma están unidos a placas desmosómicas en un extremo y permanecen libres en el extremo más cercano al núcleo. Las placas desmosómicas están compuestas por seis polipéptidos que se encuentran en el lado citoplasmático de la membrana celular que son importantes en la regulación del calcio requerido para el ensamblaje y mantenimiento desmosómico. La apariencia espinosa de los numerosos desmosomas a lo largo de los márgenes celulares es de donde el estrato espinoso deriva su nombre (70).

Las uniones gap son otro tipo de conexión entre las células epidérmicas. Esencialmente formando un poro intercelular, estas uniones permiten la comunicación fisiológica a través de señales químicas que es vital en la regulación del metabolismo, crecimiento y diferenciación celular.

1.2.1.4. Capa granular

La capa más superficial de la epidermis que contiene células vivas, la capa granular o estrato granuloso, está compuesta por células aplanadas que contienen abundantes gránulos querato hialinos en su citoplasma. Estas células son responsables de la síntesis y modificación de proteínas implicadas en la queratinización. La capa granular varía en grosor en proporción a la de la capa de células córneas suprayacente. Por ejemplo, bajo áreas delgadas de capa cornificada, la capa granular puede tener solo 1-3 capas celulares de espesor, mientras que debajo de las palmas de las manos y las plantas de los pies, la capa granular puede tener 10 veces este grosor. Una capa granular muy delgada o ausente puede conducir a una para queratosis extensa en la que los núcleos de

los queratinocitos persisten a medida que las células se mueven hacia el estrato córneo, lo que resulta en psoriasis.

Los gránulos querato hialinos son profundamente basófilos e irregulares en forma y tamaño, y son necesarios en la formación tanto de la matriz interfibrilar que mantiene unidos los filamentos de queratina como del revestimiento interno de las células córneas. La acción enzimática de los gránulos de queratohialina da como resultado la producción de queratina "suave" en la epidermis al proporcionar un corte periódico de los filamentos de queratina. En contraste, el cabello y las uñas no contienen gránulos querato hialinos, y los filamentos tonofibrillos que atraviesan el citoplasma celular se endurecerán debido a la incorporación de enlaces disulfuro, produciendo queratina "dura" en esas estructuras.

Las enzimas lisosomales presentes solo en pequeñas cantidades en el estrato basal y el estrato espinoso se encuentran en niveles altos en el estrato granuloso porque la capa granular es una zona queratógena de la epidermis. Aquí, la disolución de los orgánulos celulares se prepara a medida que las células de la capa granular se someten al proceso abrupto de diferenciación terminal a una célula córnea de la capa cornificada (71,72).

1.2.1.5. Capa cornificada

Las células córneas (corneocitos) de la capa cornificada proporcionan protección mecánica a la epidermis subyacente y una barrera para evitar la pérdida de agua y la invasión de sustancias extrañas. Los corneocitos, ricos en proteínas y bajos en contenido lipídico, están rodeados por una matriz lipídica extracelular continua. Las células córneas grandes, planas, de forma poliédrica han perdido sus núcleos durante la diferenciación terminal y técnicamente se consideran muertas.

Las propiedades físicas y bioquímicas de las células en la capa cornificada varían de acuerdo con la posición para promover la descamación que se mueve hacia afuera. Por ejemplo, las células en el medio tienen una capacidad mucho mayor para la unión al agua que las capas más profundas debido a la alta concentración de aminoácidos libres que se encuentran en el citoplasma de las células de la capa media. Las células profundas también son más densamente compactas y muestran una mayor variedad de uniones intercelulares que las capas más superficiales. Los desmosomas sufren degradación proteolítica a medida que las células progresan hacia el exterior, contribuyendo al desprendimiento de corneocitos durante la descamación (73–75).

1.2.1.6. Células no queratinocíticas de la epidermis

1.2.1.6.1. Melanocitos

El melanocito es una célula dendrítica, sintetizadora de pigmento, derivada de la cresta neural y confinada en la piel predominantemente a la capa basal. Al ramificarse en capas más superficiales, las extensiones del melanocito entran en contacto con los queratinocitos pero no forman uniones celulares. Los melanocitos son responsables de la producción del pigmento melanina y su transferencia a los queratinocitos. La melanina se produce en un orgánulo redondeado unido a la membrana conocido como melanosoma a través de una serie de reacciones mediadas por receptores, estimuladas por hormonas y catalizadas por enzimas (76).

Los melanosomas se mueven al final de los procesos de melanocitos que se encuentran más cerca de la superficie de la piel y se transfieren a los queratinocitos. En la piel blanca, estos melanosomas se agregan en complejos de melanosoma unidos a la membrana que contienen dos o tres melanosomas, mientras que los melanosomas tienden a eliminarse de estos complejos más rápidamente en los queratinocitos de individuos con piel oscura. La piel muy

pigmentada puede atribuirse a la mayor producción de melanosomas en los melanocitos, el mayor grado de melanización en cada melanosoma, el mayor tamaño de los melanosomas, la mayor cantidad de dispersión de melanosomas en los queratinocitos y la tasa más lenta de degradación del melanosoma en comparación con la piel clara

El aumento de la exposición a la luz ultravioleta estimula un aumento en la melanogénesis y un aumento correspondiente en la transferencia de melanosomas a los queratinocitos donde los melanosomas se agregarán hacia el lado superficial del núcleo. Esta respuesta, que resulta en el bronceado de la piel, aumenta la capacidad de la célula para absorber la luz y, por lo tanto, proteger la información genética en el núcleo de la radiación dañina (77–79).

1.2.1.6.2. Células de Merkel

Las células de Merkel son mecanorreceptores de tipo I de forma ovalada, de adaptación lenta, ubicados en sitios de alta sensibilidad táctil que están unidos a los queratinocitos basales por uniones desmosómicas (79). Las células de Merkel se encuentran en los dedos, los labios, las regiones de la cavidad oral y la vaina externa de la raíz del folículo piloso y, a veces, se ensamblan en estructuras especializadas conocidas como discos táctiles o cúpulas táctiles. Las deformaciones relativamente pequeñas de los queratinocitos adyacentes son estímulos suficientes para hacer que las células de Merkel secreten una señal química que genera un potencial de acción en la neurona aferente adyacente, que transmite la señal al cerebro. La alta concentración de células de Merkel en ciertas regiones, como las yemas de los dedos, da como resultado campos receptivos más pequeños y más densamente empaquetados y, por lo tanto, una mayor resolución táctil y sensibilidad (80,81).

1.2.1.6.3. Células de Langerhans

Las células de Langerhans están involucradas en una variedad de respuestas de células T. Derivadas de la médula ósea, estas células migran a una posición suprabasal en la epidermis temprano en el desarrollo embrionario y continúan circulando y repoblando la epidermis durante toda la vida (82). Las células son dendríticas y no forman uniones celulares con células vecinas. Las células de Langerhans constituyen el 2% -8% de la población total de células epidérmicas y mantienen números y distribuciones casi constantes en un área particular del cuerpo. En la epidermis, las células se distribuyen principalmente entre las capas escamosas y granulares con menos células en la capa basal. Se encuentran en otros epitelios escamosos además de la epidermis, incluyendo la cavidad oral, el esófago y la vagina, así como en los órganos linfoides y en la dermis normal.

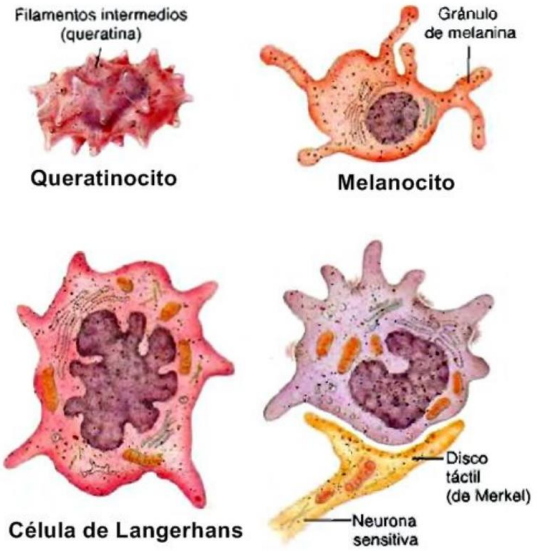

Ilustración 5. *Células no queratinocitos de la epidermis*

Las células de Langerhans deben reconocer y procesar antígenos solubles que se encuentran en el tejido epidérmico. Cuando se ingiere un antígeno unido a la membrana a través de endocitosis, se forman gránulos celulares. El contenido de estos gránulos se entrega a los fagolisosomas en el citoplasma que contiene enzimas hidrolíticas similares a las que se encuentran en los macrófagos. En la

primera etapa de la vida, las células de Langerhans son estimuladores débiles de células T no preparadas, pero son capaces de ingerir y procesar antígenos. Más tarde, una vez que la célula se ha convertido en un activador eficaz de las células T, la activación a través del contacto con el antígeno no desencadenará fagocitosis, sino que estimulará la migración celular (83–85).

1.2.1.7. Apéndices epidérmicos

Los anexos de la piel son una agrupación de apéndices derivados ectodérmicos, que incluyen glándulas ecrinas y apocrinas, conductos y unidades pilosebáceas que se originan como crecimientos descendentes de la epidermis durante el desarrollo. Después de la lesión, todas las estructuras anexiales son capaces de reepitelización a través de la migración de queratinocitos desde el epitelio anexial a la superficie de la epidermis. Debido a que áreas como la cara y el cuero cabelludo contienen una gran cantidad de unidades pilosebáceas, la reepitelización ocurre más rápidamente después de una lesión en estas áreas que en áreas con menos estructuras anexiales, como la espalda (86,87).

1.2.2. Dermis

La dermis es un sistema integrado de tejido conectivo fibroso, filamentoso y amorfo que acomoda la entrada inducida por estímulos por redes nerviosas y vasculares, apéndices derivados de la epidérmica, fibroblastos, macrófagos y mastocitos. Otras células transmitidas por la sangre, incluidos los linfocitos, las células plasmáticas y otros leucocitos, también ingresan a la dermis en respuesta a diversos estímulos. La dermis comprende la mayor parte de la piel y proporciona su flexibilidad, elasticidad y resistencia a la tracción. Protege al cuerpo de lesiones mecánicas, se une al agua, ayuda en la regulación térmica e incluye receptores de estímulos sensoriales. La dermis interactúa con la epidermis en el mantenimiento de las propiedades de ambos tejidos. Las dos regiones colaboran durante el desarrollo en la morfogénesis de la unión dérmica-

epidérmica y los apéndices epidérmicos e interactúan en la reparación y remodelación de la piel a medida que se curan las heridas. La dermis no sufre una secuencia obvia de diferenciación paralela a la diferenciación epidérmica, pero la estructura y organización de los componentes del tejido conectivo son predecibles de una manera dependiente de la profundidad. Los componentes de la matriz, incluyendo el colágeno y el tejido conectivo elástico, también varían de manera dependiente de la profundidad y sufren renovación y remodelación en la piel normal, en procesos patológicos y en respuesta a estímulos externos (88,89).

Los constituyentes de la dermis son de origen mesodérmico, excepto los nervios, que, como los melanocitos, derivan de la cresta neural. Hasta la sexta semana de vida fetal, la dermis es simplemente un grupo de células de forma dendrítica llenas de mucopolisacáridos ácidos, que son los precursores de los fibroblastos. En la semana 12, los fibroblastos sintetizan activamente fibras de retículo, fibras elásticas y colágeno. Se desarrolla una red vascular y han aparecido células grasas debajo de la dermis en la semana 24. La dermis infantil se compone de pequeños haces de colágeno, mientras que la dermis adulta contiene haces más gruesos de colágeno. Muchos fibroblastos están presentes en la dermis infantil, pero pocos persisten en la edad adulta. En la dermis encontramos una vasculatura, musculatura, nervios y mastocitos (90–92).

1.2.2.1. Mastocitos

Los mastocitos son células secretoras especializadas derivadas de la médula ósea y distribuidas en los tejidos conectivos de todo el cuerpo. Aunque están presentes en mayor número en la dermis papilar, también están presentes en la grasa subcutánea (93). En la dermis normal, los mastocitos aparecen como células ovaladas a en forma de huso con un núcleo redondo a ovalado ubicado centralmente. Numerosos mastocitos se encuentran alrededor de los vasos

sanguíneos, especialmente las vénulas postcapilares. Tras la ampliación, los mastocitos revelan numerosas vellosidades grandes y largas en su periferia. Los gránulos de mastocitos son estructuras redondas, ovaladas o angulares unidas a la membrana que contienen histamina, heparina, serina proteinasas y ciertas citoquinas. La superficie de la célula contiene cientos de miles de sitios receptores de glicoproteína para la inmunoglobulina E. Los mastocitos de tipo I o tejido conectivo se encuentran en la dermis y la submucosa. Los mastocitos tipo II o mucosas se encuentran en la mucosa del tracto respiratorio y en el intestino.

Los mastocitos se acumulan en la piel debido a la proliferación anormal, la migración y la falla de la apoptosis cuando ocurre la mastocitosis. Tradicionalmente asociadas con la respuesta alérgica, estudios más recientes sugieren que estas células también pueden ser capaces de regular la inflamación, la defensa del huésped y la inmunidad innata. Los mastocitos pueden sufrir activación por antígenos o alérgenos que actúan a través del receptor de alta afinidad para inmunoglobulina E, superóxidos, proteínas del complemento, neuropéptidos y lipoproteínas. Después de la activación, los mastocitos expresan histamina, leucotrienos, prostanoides, proteasas y muchas citoquinas y quimiocinas. Estos mediadores pueden ser fundamentales para la génesis de una respuesta inflamatoria. En virtud de su ubicación y expresión mediadora, se cree que los mastocitos desempeñan un papel activo en muchas afecciones como alergias, enfermedades parasitarias, aterosclerosis, neoplasia maligna, asma, fibrosis pulmonar y artritis (94,95).

1.3. PERMEABILIDAD DE LA PIEL

La permeación transdérmica se refiere al paso de una sustancia a través de la piel y se divide en tres pasos: penetración, permeación y absorción (96–98).

La penetración es un proceso por el cual la sustancia entra en contacto con el estrato córneo. El proceso implica una disolución inicial del fármaco y una difusión a la interfase vehículo-estrato córneo, con una posterior liberación del fármaco del vehículo y una partición entre el vehículo-estrato córneo. Por lo tanto, se necesita un vehículo adecuado para permitir la liberación del fármaco.

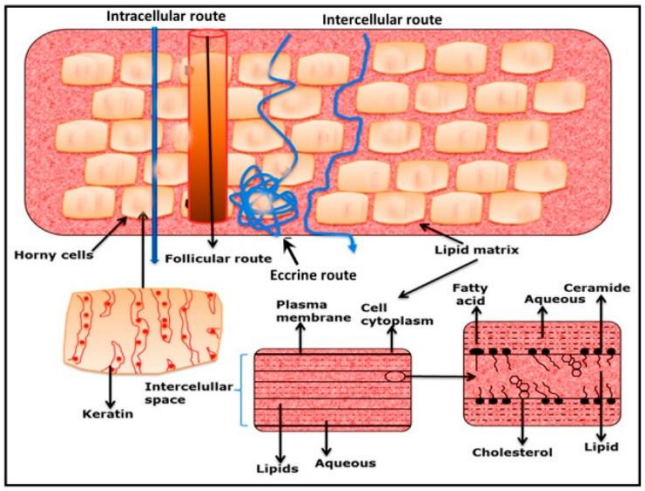

***Ilustración 6**. Rutas de penetración de fármacos a través de la piel humana (99)*

La permeación es el paso en el que el fármaco atraviesa las siguientes capas de la piel a través de un mecanismo de difusión pasiva, desde el compartimento con mayor concentración, hasta el de menor concentración. El cruce de la epidermis puede producirse por dos vías diferentes:

a) ***La vía apendicular***, se produce cuando las sustancias pasan principalmente por los folículos pilosos y las glándulas sebáceas. Aunque los folículos pilosos sólo ocupan el 0,1% de la superficie total de la piel, la vía apendicular constituye una ruta significativa para los fármacos esteroideos y las moléculas de estructura similar, las sustancias hidrófilas, los compuestos de difusión lenta y los fármacos de elevado peso molecular (100).

b) ***La vía epidérmica***, es la ruta principal, y el paso de los fármacos depende de las propiedades fisicoquímicas del fármaco, como su peso molecular, su solubilidad en agua y lípidos, y su pKa (101). Otros aspectos que influyen en la vía epidérmica son el metabolismo del fármaco, el grosor del estrato córneo, la hidratación e integridad de la piel y los excipientes. El paso de las sustancias a través de la epidermis puede tener lugar, a su vez, a través de dos vías:

- *La ruta intracelular*, es la más utilizada por las sustancias hidrofílicas, y se produce cuando el fármaco atraviesa la célula.
- *La ruta intercelular*, que se produce cuando el fármaco atraviesa las matrices lipídicas, entre las células del estrato córneo, y es utilizada principalmente por las sustancias hidrofóbicas.

1.4. SISTEMA DE ENTREGA TRANSDÉRMICA DE FÁRMACOS

Los sistemas de entrega transdérmica son un método indoloro de administración de fármacos mediante la aplicación de una forma farmacéutica sobre la piel. El fármaco o fármacos penetran inicialmente a través del estrato córneo para luego atravesar la epidermis y la dermis, dependiendo del tamaño de la molécula (102).

Este tipo de sistemas de entrega tienen muchas ventajas sobre otras vías convencionales de administración de fármacos, entre ellas podemos resaltar una alternativa no invasiva a las vías parenterales, evitando problemas de fobias a agujas, asimismo la gran superficie que posee la piel favorece la facilidad de acceso, permitiendo muchas opciones de colocación del fármaco en la piel para su absorción; además, los perfiles farmacocinéticos de los fármacos administrados por esta vía son más uniformes, con menos picos, lo que minimiza el riesgo de efectos secundarios tóxicos. Entre otras ventajas se constituye el

mejoramiento del cumplimiento del paciente al tratamiento debido a la reducción de las frecuencias de dosificación, así como también es adecuado para aquellos pacientes que se encuentran inconscientes o vomitan, o para aquellos dependientes. Cabe recalcar que, la administración de fármacos por vía transdérmica evita el metabolismo presistémico, mejorando así la biodisponibilidad. Las células dendríticas desempeñan un papel central en las respuestas inmunitarias, estas se encuentran tanto en la epidermis como en la dermis de la piel, los sistemas de entrega transdérmica resultan una vía atractiva para la administración de fármacos a esta escala (103,104).

El mayor desafío para la administración transdérmica es que solo un número limitado de fármacos al momento son capaces de administrarlos por esta vía. Desde una perspectiva general, los sistemas de administración transdérmico han ido evolucionando y al momento podemos detectar tres generaciones de desarrollo, desde la primera, donde se produjeron parches mediante la selección cuidadosa de medicamentos que puedan atravesar la piel a tasas terapéuticas poco o nada determinadas, para luego pasar a una segunda generación que produjo avances en la administración de las moléculas a través de la permeabilidad de la piel y las fuerzas impulsoras para el transporte transdérmico; a la tercera generación que permitirá la administración transdérmica de medicamentos a través de la permeabilización dirigida del estrato córneo de la piel (105–107).

1.4.1. Factores que influyen en la permeación de los fármacos

Entre los factores que influyen en la permeación de los fármacos encontramos a los factores fisicoquímicos de la piel y fármacos, en otros casos podemos encontrar una interacción por parte de los vehículos y factores fisicopatológicos (53,108–111).

1.4.1.1. Factores fisicoquímicos de la piel

a) ***Temperatura,*** un aumento de la temperatura de la piel implica un aumento del flujo sanguíneo y, por consiguiente, de la velocidad de permeación y absorción del fármaco. Además, el aumento de la temperatura de 32 a 35°C modifica el empaquetamiento de los lípidos en el estrato córneo, pasando de un empaquetamiento ortorrómbico a uno hexagonal, lo que aumenta la permeabilidad.
b) ***pH,*** los valores normales de pH de la piel pueden afectar al grado de disociación del fármaco y, por tanto, a su capacidad para atravesar las membranas. Por ejemplo, las sustancias no ionizadas pueden permeabilizar la piel más fácilmente.

1.4.1.2. Factores fisicoquímicos del fármaco

a) ***El coeficiente de partición*** se define como la proporción de fármaco que se disuelve en dos disolventes inmiscibles. En este caso, la proporción disuelta entre el estrato córneo y el vehículo es de gran importancia, ya que la capa córnea se comporta como una membrana lipídica. Cuando el valor del coeficiente de partición se acerca a 1, la permeabilidad es adecuada. Es bien sabido que las moléculas con un log P comprendido entre 1 y 3 (una solubilidad predominante en los lípidos), y con una buena solubilidad en los aceites y el agua, muestran una permeabilidad cutánea adecuada.
b) ***El coeficiente de permeabilidad*** es una constante proporcional al coeficiente de partición y al coeficiente de difusión (P_2) del fármaco. A su vez, el P_2 es inversamente proporcional al peso molecular. Es bien sabido que el peso molecular es un factor determinante en la permeabilidad de

los fármacos, siendo los menores de 500 Da los que pueden permeabilizar la piel.

1.4.1.3. Factores del vehículo

a) ***Excipientes,*** la naturaleza del vehículo puede modificar la permeación cutánea del fármaco debido a la interacción con la estructura del estrato córneo, a través de un aumento en la hidratación, temperatura o una alteración del empaquetamiento de los lípidos. Además, la interacción vehículo-fármaco como, por ejemplo, el pH de la formulación afecta al grado de disociación de las moléculas según su pKa, lo que a su vez afecta al coeficiente de partición de la sustancia.
b) ***Propiedades reológicas,*** un vehículo con un comportamiento viscoelástico se considera óptimo debido a su comportamiento fluido.
c) ***Concentración del fármaco,*** dado que la penetración y la permeación del fármaco se producen mediante un mecanismo de difusión pasiva, dependen del gradiente de concentración entre el vehículo y las capas de la piel.

1.5. TÉCNICAS PARA MEJORAR LA PERMEABILIZACIÓN DEL FÁRMACO EN LA PIEL

Las tecnologías utilizadas para modificar las propiedades de barrera del estrato córneo se pueden dividir en metodologías pasivas/químicas o activas/físicas. Los métodos pasivos incluyen la influencia de las interacciones farmacológicas y vehiculares y la optimización de la formulación, con el fin de modificar la estructura del estrato córneo. Los métodos pasivos son relativamente fáciles de incorporar en parches transdérmicos, como potenciadores químicos y emulsiones (92,99).

1.5.1. Promotores de penetración

Uno de los enfoques pasivos más utilizados es el uso de potenciadores químicos de la penetración que facilitan la permeación del fármaco a través de la piel al aumentar la partición del fármaco en el dominio de barrera del estrato córneo, sin daño a largo plazo a la piel (112). Los potenciadores de la penetración tienen varios mecanismos de acción, tales como: aumento de la fluidez de las bicapas lipídicas del estrato córneo, interacción con proteínas intercelulares, interrupción o extracción de lípidos intercelulares, aumento de la actividad termodinámica del fármaco y aumento de la hidratación del estrato córneo.

Se conocen varios tipos de potenciadores de la penetración y se pueden dividir en varios grupos en función de su estructura química, en lugar de su mecanismo de acción. La mayoría de estos tienen modos de acción mixtos, por lo que es difícil clasificarlos de acuerdo con esta característica. Ejemplos de potenciadores de penetración comúnmente investigados son alcoholes, sulfóxidos, azona, pirrolidonas, aceite esencial, terpenos y terpenoides, ácidos grasos, agua y urea. Sin embargo, la principal limitación para los potenciadores de la penetración es que su eficacia a menudo está estrechamente relacionada con la aparición de irritación de la piel (97,113–115).

1.6. ENFERMEDADES INFLAMATORIAS DE LA PIEL

1.6.1. Dermatitis atópica

La dermatitis atópica (DA) es una enfermedad crónica de la piel basada en la disfunción de la barrera cutánea, que conduce junto con factores ambientales y múltiples cambios del sistema inmune a lesiones eccematosas y con picazón en los pliegues de flexión y otras distribuciones típicas (116). Los brotes agudos y las exacerbaciones, así como las lesiones cutáneas eccematosas crónicas en la piel seca acompañadas de prurito intensivo caracterizan el curso. La DA puede variar de formas leves a formas moderadas y graves y el diagnóstico, así como la

gravedad, se pueden definir con la ayuda de criterios estandarizados y sistemas de puntuación. Aunque el cuadro clínico, caracterizado por brotes agudos de lesiones eccematosas y pruriginosas en la piel seca con predilección típica, como los pliegues de flexión, es bastante homogéneo, los factores desencadenantes de la enfermedad son diversos y la red fisiopatológica involucrada es bastante compleja (117,118). Se puede observar un aumento de la infiltración de células T, subtipos de células dendríticas, macrófagos, mastocitos y eosinófilos en las lesiones de DA, así como una mayor cantidad de diferentes citoquinas y quimiocinas (119).

El papel de la barrera cutánea en la patogénesis de la EA ha sido un tema de debate durante mucho tiempo (120). Se ha demostrado hasta ahora la asociación genética más fuerte con la DA para mutaciones de pérdida de función en el gen de la filagrina (FLG), que codifica la importante proteína de barrera (pro-) filagrina. En pacientes europeos caucásicos con DA, las mutaciones nulas FLGR501X y 2282del4 se asociaron con mayor frecuencia con la enfermedad. Además, se ha demostrado que, en particular, los pacientes con DA con mutaciones de pérdida de función en el gen FLG sufren formas graves de DA con cursos crónicos. La exposición a alérgenos ambientales particulares, como los alérgenos de los gatos durante los primeros momentos de la vida, podría aumentar el riesgo de desarrollo de eccema en portadores de la mutación FLG. Además de las mutaciones de pérdida de función en el gen FLG, varios otros factores, como el estado de metilación del ADN o las variaciones del número de copias de FLG, factores ambientales que incluyen irritación de la piel y daño mecánico, baja humedad, pero también el medio de citoquinas en la piel con reducción de la expresión de filagrina por citoquinas Th2, IL-17, IL-22, IL-25 o IL-31, así como microorganismos que colonizan la piel y el tratamiento tópico y sistémico son capaces de modular la expresión de filagrina secundariamente (121–123).

La piel inflamatoria de la EA contiene un gran número de células inmunes residentes e infiltradas, como LC, células dendríticas epidérmicas inflamatorias (IDEC), mastocitos, macrófagos, neutrófilos, basófilos, eosinófilos, células linfoides innatas (ILC), células asesinas naturales, fibroblastos y varios subconjuntos de células T (124). Las interacciones funcionales de las células inmunes de la piel son esenciales para la patogénesis de la DA. El papel de la IgE en la DA sigue siendo un tema de debate, porque no está claro si desempeña un papel central en la patogénesis de la DA o representa solo un fenómeno espectador. De hecho, la IgE específica de alérgenos a alimentos o aeroalérgenos es detectable en la infancia de pacientes con DA y el desafío alérgeno en forma de provocación oral o exposición epicutánea conduce al desarrollo o deterioro de lesiones cutáneas. Recientemente, se ha observado que las ILC se infiltran en la piel de AD y liberan citoquinas de tipo Th2 IL-5, IL-9 e IL-13 para promover la inflamación local después de la estimulación con alérgenos, TSLP o IL-33.

Tras la estimulación con alérgenos, la barrera cutánea derivada de TSLP estimula las CD para derivar respuestas Th2. Se observó infiltración de células T Th2 en la piel aguda de la EA, junto con una infiltración moderada con células Th22 y pocas células Th17. Los datos de las pruebas de parches de atopia y otros estudios han demostrado que la EA crónica se asocia con una respuesta inmune mixta que consiste en células Th2 / Th1 / Th22 que se infiltran en la piel (125–127).

1.6.2. Rosácea

La rosácea es una enfermedad crónica e inflamatoria con una serie de manifestaciones cutáneas faciales, que incluyen enrojecimiento, eritema no transitorio, pústulas, telangiectasias y cambios fimatosos (128). Las manifestaciones secundarias, como picazón, ardor o escozor, a menudo se observan en pacientes con rosácea. La rosácea generalmente comienza entre los 30 y 50 años de edad, pero puede ocurrir a cualquier edad. Las tasas de

prevalencia entre las poblaciones varían de < 1 a 22%, pero es probable que estos porcentajes estén influenciados por las diferencias en el diseño del estudio, la metodología, la población, la ubicación geográfica y las diferencias culturales y sociales en la percepción de la enfermedad. En 2002, la rosácea se clasificó en los siguientes cuatro subtipos: eritemato-angiectásica, papulopustular, fimatosa y ocular (129,130).

Las vías inflamatorias actuales relevantes para la patogénesis de la rosácea incluyen la desregulación de los mecanismos inmunes (innatos, adaptativos, inflamasoma) y neurocutáneos. La susceptibilidad genética con la reactividad inmune modificada se sugiere por la asociación de la rosácea con polimorfismos de un solo nucleótido en genes asociados con el complejo principal de histocompatibilidad (131).

La activación inmune innata y adaptativa puede ser desencadenada por microbios, incluidas las especies de Demodex y varias bacterias, como Bacillus oleronius y Staphylococcus epidermidis. La activación inmune innata conduce a una regulación positiva del receptor tipo toll 2 derivado de queratinocitos (TLR2) y el receptor 2 activado por proteinasa (PAR2). Estos promueven la expresión del péptido antimicrobiano catelicidina, que posteriormente se activa a LL-37 bioactivo por la proteasa calicreína 5 (KLK-5), lo que lleva al eritema y la angiogénesis. TLR2 facilita la activación del inflamasoma NLRP3 que conduce a la formación de pústulas, dolor y respuesta vascular a través de la interleucina-1β y el factor de necrosis tumoral alfa (TNF-α); y liberación de prostaglandina E2. Además, TLR2 puede provocar eritema, telangiectasia e inflamación a través de la expresión de citoquinas, quimiocinas, proteasas y factores angiogénicos. La activación de PAR2 conduce a inflamación, prurito y dolor combinados con el reclutamiento de linfocitos T y neutrófilos, la desgranulación de los mastocitos y

la liberación adicional de quimiocinas inflamatorias, citoquinas y prostaglandinas (131–133).

Aunque la terapia combinada es una práctica común entre los dermatólogos y ampliamente recomendada, solo hay evidencia limitada que respalde su eficacia.

1.6.3. Síndrome de Behçet o Enfermedad de Behçet

La Enfermedad de Behçet (EB) o también conocido como Síndrome de Behçet (SB), es una enfermedad caracterizada por vasculitis inflamatoria compleja, recurrente, crónica y remitente de etiología desconocida, se presenta con episodios recurrentes de úlceras orales, genitales, lesiones cutáneas, oculares, entre otras (134), y puede cursar con más problemas graves como meningitis, coágulos de sangre, inflamación del sistema digestivo y ceguera (135). Esta enfermedad puede comenzar con uno o dos de los síntomas indicados anteriormente, pero a medida que pasa el tiempo, el resto de los síntomas se van desencadenando gradualmente (136).

La mayor prevalencia se da en países como Turquía (80-370 personas por 100 000 habitantes) (137) seguido de Irán (80 personas por 100 000 habitantes) (138). En Israel, Irak, Arabia Saudí, China y Japón la prevalencia está entre 11.9 y 20 personas por 100.000 habitantes (139–142), mientras que en Europa Occidental y Estados Unidos la prevalencia está entre 0.6 y 5.2 personas por 100.000 habitantes, es señaló que la prevalencia en estos países aumenta dependiendo de si las personas son descendientes directas de los países del Medio Oriente (143–146).

Aunque factores genéticos y ambientales están directamente involucrados en la patogenia de la EB, aún se desconoce la causa principal, a pesar de esto se cree que la enfermedad se debe a un proceso autoinmune desencadenado por un

agente infeccioso o ambiental en una persona genéticamente predispuesta (147). Se ha encontrado que las células T son los principales linfocitos implicados en la patogenia de la SB, y la IL-8 producida por las células T se ha correlacionado con la actividad de la enfermedad y la enfermedad vascular (148,149). La EB también ha sido considerado una enfermedad autoinflamatoria y esto se corrobora por las similitudes con la Enfermedad de Crohn, siendo esta considerada una enfermedad autoinflamatoria (150,151). Un estudio del genoma realizado en pacientes con EB informó una asociación para EB de IL-4, IL-10, IL-12, IL-13, Interferón-γ y loci IL23R – IL12RB2. De manera similar, se identificaron dos asociaciones en los cromosomas 1p31.3 (IL23R-IL12RB2) y 1q32.1 (IL10), cromosomas que predisponen a las personas con EB (152,153). EB está asociado con una región entre IL23R e IL12RB2, también se encontró un aumento en las células T Th1, Th17, CD4+ y CD8+, y se observó actividad en las células T γ δ + tanto en suero como en tejidos de pacientes diagnosticados con EB, lo que sugiere que la inmunidad innata y adaptativa están involucradas en la patogenia de esta enfermedad (154,155).

Actualmente no existe una cura para el EB, sin embargo, los estudios con diversos fármacos para enfocar el tratamiento en la reducción del dolor y la prevención de problemas más graves, por ejemplo, la terapia de primera línea para el tratamiento de manifestaciones clínicas como lesiones mucocutáneas incluye colchicina y corticosteroides (156,157). Un ensayo clínico de fase II realizado en hospitales de Turquía y Estados Unidos entre 2009 y 2011, con un total de 111 pacientes que cumplían los criterios del Grupo Internacional para la Enfermedad de Behçet, una edad media de entre 37.3 ± 0.4 y un número medio de úlceras orales por paciente al inicio del estudio de 3.1 ± 1.3 en el grupo tratado con Apremilast y 3.2 ± 2.1 en el grupo placebo. El tratamiento consistió en la dosis de 30 mg de Apremilast dos veces al día durante 12 semanas por vía oral y luego una observación de 28 días después del tratamiento. Como resultado, se obtuvo

una reducción significativa de ulceraciones orales en el grupo tratado con el fármaco frente al grupo placebo (0.5 ± 1.0 vs. 2.1 ± 2.6, $p < 0.001$) (158–161). En estudios recientes realizados por Luca et al 2020 evaluaron la eficacia y seguridad de apremilast en 12 pacientes con EB que presentaban ulceraciones recurrentes y/o intolerancia a las terapias convencionales, se excluyeron aquellos que presentaban uveítis y afectación gastrointestinal. El estudio demostró una eficacia de apremilast para las úlceras orales y la actividad general de la enfermedad según las puntuaciones basadas en la puntuación de actividad del síndrome de Behçet (BSAS), el formulario de actividad actual de la enfermedad de Behçet (BDCAF), la escala analógica visual (VAS) y los cambios en la calidad de vida de la enfermedad de Behçet (BDQOL) en la semana 12. La diarrea en tres pacientes y la ideación suicida en uno fueron los principales efectos adversos que se presentaron, lo que limitó el estudio, por lo que se decidió suspender la administración (162).

1.7. APREMILAST

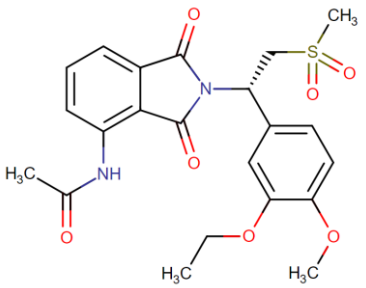

Fórmula química: $C_{22}H_{24}N_2O_7S$

Peso molecular: 460.5 g/mol

Ilustración 7. *Estructura química de apremilast*

1.7.1. Mecanismo de acción

El mecanismo completo de acción de este fármaco no está completamente establecido, sin embargo, se sabe que apremilast es un inhibidor de la fosfodiesterasa 4 (PDE4), que media la actividad del monofosfato de adenosina cíclico (cAMP), un segundo mensajero.

La inhibición de la PDE4 por apremilast conduce a un aumento de los niveles intracelulares de cAMP. Un aumento en el cAMP resulta en la supresión de la inflamación al disminuir la expresión de TNF-α, IL-17, IL-23 y otros mediadores inflamatorios. Los mediadores inflamatorios anteriores se han implicado en diversas afecciones psoriásicas, así como en la enfermedad de Behçet, lo que lleva a sus síntomas inflamatorios indeseables, como úlceras bucales, lesiones cutáneas y artritis. La administración de apremilast conduce a una cascada que eventualmente disminuye los niveles de los mediadores anteriores, aliviando los síntomas inflamatorios (163,164).

1.7.2. Farmacocinética

Una dosis oral de apremilast se absorbe bien y la biodisponibilidad absoluta es de aproximadamente el 73%. Tmax es de aproximadamente 2.5 horas y se ha informado que la Cmax es de aproximadamente 584 ng/ml en un estudio farmacocinético. La ingesta de alimentos no parece afectar a la absorción de apremilast. El volumen de distribución aparente (Vd) promedio es de aproximadamente 87 L, lo que sugiere que apremilast se distribuye en el compartimiento extravascular. La unión a proteínas plasmáticas de apremilast es de aproximadamente 68%. Apremilast se metaboliza en gran medida por varias vías, que incluyen oxidación, hidrólisis, además de la conjugación. Alrededor de 23 metabolitos se producen a partir de su metabolismo. El CYP3A4 media principalmente el metabolismo oxidativo de este fármaco, con contribuciones más pequeñas de las enzimas CYP1A2 y CYP2A6. El metabolito principal de apremilast, M12, es una forma conjugada glucurónida inactiva del fármaco O-desmetilado. Algunos otros metabolitos importantes, M14 y M16, son significativamente menos activos en la inhibición de la PDE4 y los mediadores inflamatorios que su fármaco original, apremilast. Después de una dosis oral, apremilast inalterado (45%) y el metabolito inactivo, O-desmetil apremilast

glucurónido (39%) se encuentran en el plasma. Los metabolitos menores M7 y M17 son activos, pero sólo están presentes en aproximadamente el 2% o menos de las concentraciones de apremilast, y probablemente no contribuyan significativamente a las acciones de apremilast. Sólo el 3% y el 7% de una dosis de apremilast se detectan en la orina y las heces como fármaco inalterado, respectivamente, lo que indica un metabolismo extenso y una alta absorción. La vida media de eliminación promedio de este medicamento varía de 6 a 9 horas (165–168).

1.7.3. Farmacodinamia

Apremilast reduce, pero no inhibe completamente varias citoquinas inflamatorias como IL-1α, IL-6, IL-8, IL-10 MCP-1, MIP-1β, MMP-3 y TNF-α, aliviando los síntomas de la psoriasis y la enfermedad de Behçet, que son causados por un aumento de estos mediadores inflamatorios. Este medicamento también ha demostrado ser eficaz para aliviar el dolor asociado con las úlceras orales en la enfermedad de Behçet.

Apremilast puede causar pérdida de peso no deseada y empeorar la depresión, lo que lleva a pensamientos o acciones suicidas. Es aconsejable controlar los síntomas de depresión y buscar atención médica si ocurren, especialmente en pacientes con depresión preexistente. La necesidad de apremilast debe evaluarse cuidadosamente junto con el riesgo de empeoramiento de la depresión y el suicidio. Si se produce pérdida de peso, se debe evaluar el grado de pérdida de peso y se debe considerar la posible interrupción de apremilast (169–171).

1.7.4. Reacciones adversas

Dentro de las principales reacciones adversas del medicamento administrado por vía oral encontramos bronquitis, nasofaringitis, infección del tracto

respiratorio superior; depresión, disminución del apetito; insomnio; migraña, cefalea; diarrea, náuseas, vómitos, dolor abdominal superior, enfermedad por reflujo gastroesofágico (172).

CAPÍTULO 2

OBJETIVOS

Los objetivos de la presente investigación buscan:

- Validar un método analítico que permita identificar y cuantificar al activo.
- Desarrollar y optimizar una nanoformulación.
- Caracterizar las formulaciones físico y química mente.
- Evaluar la estabilidad de la fórmula a corto plazo.
- Evaluar la toxicidad de los componentes de la formulación a través de ensayos in vitro en cultivos celulares.
- Conocer el perfil de liberación *in vitro* y de permeación de la formulación.
- Valorar la eficacia de la formulación en ensayos de experimentación animal.
- Conocer la tolerancia en la fórmula *in vivo* en humanos
- Evaluar la permeabilidad de apremilast contenido en una solución con diferentes promotores de penetración en muestras *ex vivo* de piel humana
- Realizar estudios de toxicidad de las soluciones preparadas *in vitro* en cultivos celulares
- Ajustar el método analítico para la valoración de apremilast en muestras de IVPT
- Evaluar la tolerancia *in vivo* de las soluciones de apremilast candidata con el promotor idóneo.

CAPÍTULO 3

RESULTADOS

A raíz de la investigación llevada a cabo durante el desarrollo de la presente tesis doctoral, se realizaron las siguientes publicaciones:

Artículo 1	**Apremilast Microemulsion as Topical Therapy for Local Inflammation: Design, Characterization and Efficacy Evaluation** *Pharmaceuticals* 2020, 13 (12): 484
Artículo 2	**Effect of Penetration Enhancers and Safety on the Transdermal Delivery of Apremilast in Skin** *Pharmaceutics* 2022, 14 (5): 1011

En el capítulo 6, se hace mención a otras publicaciones generadas a raíz del tema de tesis que se encuentran enmarcadas como mini revisiones y comunicaciones.

Mini Review	**Apremilast Application as Treatment of Oral Ulcers in Behçet Syndrome** *Biomedical Journal of Scientific & Technical Research* 2021, 34 (5): 27076-27080
Communication	**Efficacy evaluation of a Microemulsion loaded with Apremilast for the Rosacea treatment** *Skin Forum* 2022

3.1. Artículo 1

Journal	*Pharmaceuticals*
Volume	*13*
Issue	*12*
Published date	21 December 2020
Section	*Pharmaceutical Technology*
Special Issue	*Nano Drug Carriers 2021*
ISSN:	1424-8247
Factor de impacto:	5.863
DOI:	10.3390/ph13120484

Afiliaciones:

1 Department of Pharmacy, Pharmaceutical Technology and Physical Chemistry, Faculty of Pharmacy and Food Sciences, University of Barcelona, 08028 Barcelona, Spain
2 Institute of Nanoscience and Nanotechnology (IN2UB), University of Barcelona, 08028 Barcelona, Spain
3 Department of Experimental and Health Sciences, Parc de Recerca Biomèdica de Barcelona, University Pompeu Fabra (UPF), 08005 Barcelona, Spain
4 Department of Biochemistry and Physiology, Faculty of Pharmacy and Food Sciences, University of Barcelona, 08028 Barcelona, Spain
5 Nutrition and Food Safety Research Institute (INSA-UB), 08921 Santa Coloma de Gramenet, Spain
6 Institute of Biomedicine of the University of Barcelona (IBUB), Sant Joan de Déu Research Institute, 08028 Barcelona, Spain
7 Departamento de Química y Ciencias Exactas, Universidad Técnica Particular de Loja, Loja 1101608, Ecuador

pharmaceuticals

MDPI

Article

Apremilast Microemulsion as Topical Therapy for Local Inflammation: Design, Characterization and Efficacy Evaluation

Paulo Sarango-Granda [1,2], Marcelle Silva-Abreu [1,2], Ana Cristina Calpena [1,2,*], Lyda Halbaut [1,2], María-José Fábrega [3], María J. Rodríguez-Lagunas [4,5], Natalia Díaz-Garrido [4,6], Josefa Badia [4] and Lupe Carolina Espinoza [1,2,7]

1 Department of Pharmacy, Pharmaceutical Technology and Physical Chemistry, Faculty of Pharmacy and Food Sciences, University of Barcelona, 08028 Barcelona, Spain; paulogranda92@gmail.com (P.S.-G.); marcellesabreu@gmail.com (M.S.-A.); halbaut@ub.edu (L.H.); lcespinoza@utpl.edu.ec (L.C.E.)
2 Institute of Nanoscience and Nanotechnology (IN2UB), University of Barcelona, 08028 Barcelona, Spain
3 Department of Experimental and Health Sciences, Parc de Recerca Biomèdica de Barcelona, University Pompeu Fabra (UPF), 08005 Barcelona, Spain; mjfabrega.f@gmail.com
4 Department of Biochemistry and Physiology, Faculty of Pharmacy and Food Sciences, University of Barcelona, 08028 Barcelona, Spain; mjrodriguez@ub.edu (M.J.R.-L.); natalia.diaz.garrido@gmail.com (N.D.-G.); josefabadia@ub.edu (J.B.)
5 Nutrition and Food Safety Research Institute (INSA-UB), 08921 Santa Coloma de Gramenet, Spain
6 Institute of Biomedicine of the University of Barcelona (IBUB), Sant Joan de Déu Research Institute, 08028 Barcelona, Spain
7 Departamento de Química y Ciencias Exactas, Universidad Técnica Particular de Loja, Loja 1101608, Ecuador
* Correspondence: anacalpena@ub.edu

Received: 24 November 2020; Accepted: 16 December 2020; Published: 21 December 2020

Abstract: Apremilast (APR) is a selective phosphodiesterase 4 inhibitor administered orally in the treatment of moderate-to-severe plaque psoriasis and active psoriatic arthritis. The low solubility and permeability of this drug hinder its dermal administration. The purpose of this study was to design and characterize an apremilast-loaded microemulsion (APR-ME) as topical therapy for local skin inflammation. Its composition was determined using pseudo-ternary diagrams. Physical, chemical and biopharmaceutical characterization were performed. Stability of this formulation was studied for 90 days. Tolerability of APR-ME was evaluated in healthy volunteers while its anti-inflammatory potential was studied using in vitro and in vivo models. A homogeneous formulation with Newtonian behavior and droplets of nanometric size and spherical shape was obtained. APR-ME released the incorporated drug following a first-order kinetic and facilitated drug retention into the skin, ensuring a local effect. Anti-inflammatory potential was observed for its ability to decrease the production of IL-6 and IL-8 in the in vitro model. This effect was confirmed in the in vivo model histologically by reduction in infiltration of inflammatory cells and immunologically by decrease of inflammatory cytokines IL-8, IL-17A and TNFα. Consequently, these results suggest that this formulation could be used as an attractive topical treatment for skin inflammation.

Keywords: apremilast; phosphodiesterase 4; microemulsion; skin diseases; inflammation

1. Introduction

Inflammation constitutes a defense mechanism of the body. It is the response of the immune system against numerous harmful stimuli, among which include pathogens, toxic compounds and damaged cells [1]. However, inappropriate or excessive inflammatory responses can trigger chronic

inflammation implicated in the pathogenesis of a wide variety of skin disorders [2]. The skin inflammatory response is mediated by cytokine secretions in response to injury, including tumor necrosis factor-alpha (TNF-α) and interleukin (IL) -6, IL-8 and IL-17. Therapeutic treatment involves treating symptoms by interrupting the inflammatory process [3]. The mechanism based on phosphodiesterase 4 (PDE4) enzyme inhibition has been used for the treatment of inflammatory and autoimmune diseases. PDE4 is one of the many classes of phosphodiesterase enzymes (PDE) that participate in the hydrolysis of cAMP [4]. PDE4 inhibition causes a decrease in the expression of pro-inflammatory cytokines, such as interleukin (IL)-17 and tumor necrosis factor alpha (TNF-α), and an increase in anti-inflammatory mediators, such as IL-10 [5]. Apremilast (APR) is a selective PDE4 inhibitor chemically identified as *N*-{2-[(1S)-1-(3-ethoxy-4-methoxyphenyl)-2-(methylsulfonyl) ethyl]-2,3-dihydro-1,3-dioxo-1*H*-isoindole-4-yl} acetamide. It is a small and versatile molecule whose formula and molecular weight are $C_{22}H_{24}N_2O_7S$ and 460.5 g/mol, respectively [6,7]. Figure 1 shows the chemical structure of APR [8]. APR was approved in 2014 by the United States Food and Drug Administration (FDA) as oral therapy for the treatment of moderate-to-severe plaque psoriasis and active psoriatic arthritis [9,10]. This drug causes an intracellular accumulation of cyclic adenosine monophosphate (cAMP), resulting in a modification in the signaling pathways of cells belonging to the innate (monocytes) and adaptive (T cells) immune system as well as non-immune cells (keratinocytes) [11,12]. In the last decade, novel drug delivery systems for APR has been reported in order to improve its solubility and bioavailability including PLGA nanoparticles [13], amorphous solid dispersion [14], nanostructured lipid carriers [15] and nanocrystal-based formulations [16]. Currently, APR is available in tablet form of 10, 20 and 30 mg for oral administration [17]. However, this route of administration presents notable disadvantages related with adverse effects, first-pass metabolism and, moreover, is not suitable for patients with swallowing difficulties. In particular, topical therapy targeting a specific inflammatory mediator on the skin promises a local pharmacological effect with fewer side effects [18]. This route represents a convenient and painless alternative in the treatment of dermatological diseases because it allows drugs to be directed to the affected sites within the skin [19]. However, the main obstacle of topical formulations is to overcome the stratum corneum (SC), which limits the speed of transdermal diffusion of various drugs to achieve the intended therapeutic effect [20–22]. Drug permeation through the skin depends on the physicochemical characteristics of the drug as well as the chemical composition and physical properties of the carrier. APR is categorized as a class IV drug, according to the Biopharmaceutical Classification System (BCS), due to its low solubility and low permeability [23]. Hence, the incorporation of APR into nanotechnology-based drug delivery systems such as microemulsions (MEs) could be used as a strategy to improve its solubility and permeability in order to improve dermal bioavailability and consequently to achieve local anti-inflammatory efficacy [24]. MEs have been proposed as promising nanocarriers to deliver anti-inflammatory drugs in the skin such as cyclosporine, methotrexate and tacrolimus due to their capability to solubilize highly hydrophobic drugs as well as their capability to enhance drug uptake into the skin [25–27].

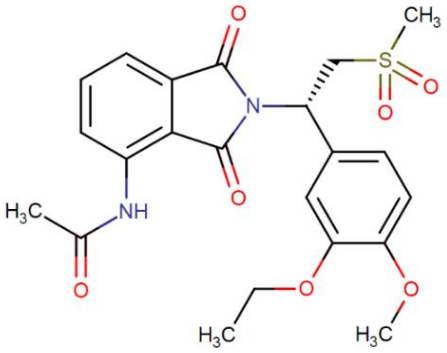

Figure 1. Apremilast chemistry structure.

MEs are thermodynamically stable formulations characterized by being transparent, monophasic optically isotropic systems. They are formed by adequate proportions of water, oil, surfactant and co-surfactant, and usually show small droplets that range from 10 to 100 nm [28]. MEs have a high interfacial stability that optimize the stability of the formulation. Among the benefits offered by this type of system include reduced droplet size and greater solubility, especially for poorly soluble and unstable drugs [29,30]. In addition, due to the nature of the components that are in the formulation, in some cases they can serve as a penetration enhancer, thereby increasing the rate of penetration of the drug through the skin.

Considering that there are currently no complete or relevant studies of drug delivery systems for APR by topical application, the purpose of this study was to design and characterize an APR-ME as a strategy to improve the solubility and permeability of APR in order to provide a topical therapy alternative with a local anti-inflammatory effect on the skin.

2. Results

2.1. Validation of the Analytical Method

The results obtained related to the analytical method can be found in Supplementary Material. The linearity was evaluated from three calibration curves within a range of 1.25 to 200 μg/mL (Table S1). No point was left in the calibration during the validation and the data showed good linearity of the proposed method (Figure S1). The value of r^2 in each of the calibration curves was above 0.999, thus indicating a linear relationship between analyte concentration and peak area. No statistically significant differences were found after the one-way analysis of variance (one-way ANOVA) test of the calibration curves, where p value = 0.91.

The precision and accuracy values were obtained from APR standard concentration ranged from 1.25 to 200 μg/mL. The inter-day precision and accuracy were calculated after analyzing the samples on three different days. The results were reported in Tables S2 and S3. These results showed good precision with values of RSD below 3.77%, while accuracy was shown to have a maximum RE of −8.36% for lowest standard concentration.

Measuring robustness allows recognition of the effect of operational parameters on results and provides an indication of applicability during the study. This parameter was determined by evaluating the retention time of the asset with the variations of concentration change of the mobile phase shown in Table S4.

Specificity (Figure S2) was determined by analysis of the blank mobile phase control, the 100 μg/mL standard, the skin blank as a control, and APR extracted from human skin after permeation study. No interference on the chromatogram with respect to retention time of APR was observed.

The LOD and LOQ were calculated using the standard deviation of response and the slope of the calibration curve from 1.25 to 200 μg/mL, described in Section 4.2. From the flow and the Y-intercept of the three straight lines (Table S5), the LOD for APR was set at 1.13 ± 1.04 μg/mL and LOQ at 3.42 ± 3.16 μg/mL. These results indicate that the method is sensitive enough for the APR determination.

2.2. Pseudo-Ternary Phase Diagrams and APR-ME Preparation

The APR solubility at 25 °C in the different assayed oils, surfactants and co-surfactants are shown in Figure 2. The components that showed the greatest capacity to solubilize the drug were selected as constituents of APR-ME. In this study, Plurol® oleique CC497 (oil, solubility 1.32 ± 0.04 mg/mL), Labrasol® (surfactant, solubility 2.60 ± 0.09 mg/mL) and Transcutol® P (co-surfactant, solubility 2.69 ± 0.07 mg/mL) were used.

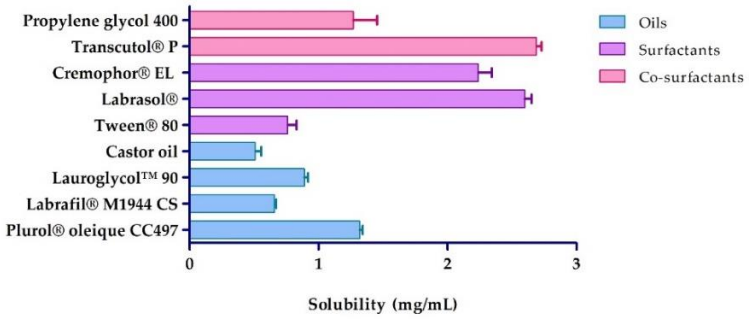

Figure 2. Apremilast solubility in different vehicles (n = 3).

Four pseudoternary phase diagrams were performed to establish the area with the greatest amplitude for the formation of the ME. Various proportions between the amounts of Labrasol® and Transcutol® P were considered (S_{mix} of 1:1, 2:1, 3:1, 1:2) (Figure 3). Results revealed that the maximum area for the formation of an ME occurs with a surfactant and co-surfactant ratio of 2:1; therefore, it was consequently selected as S_{mix} and optimized for the preparation of APR-ME.

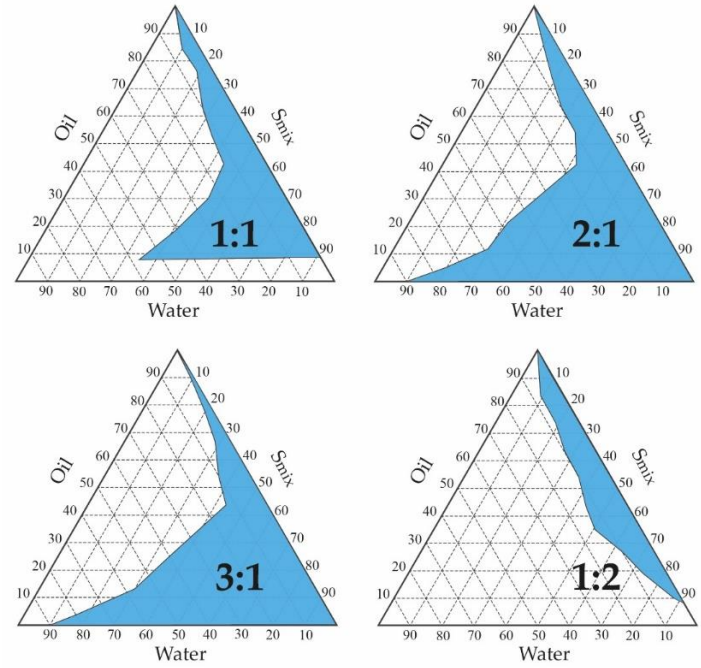

Figure 3. Pseudo-ternary phase diagrams using different ratios of surfactant/co-surfactants (S_{mix}) at 25 °C.

The final composition of APR-ME (Table 1) was obtained by integrating APR in Plurol® oleique CC497 (6%), Labrasol® (29.33%), Transcutol® P (14.67%) and purified water (50%). This formula was homogeneous, transparent and showed no signs of drug precipitation.

Table 1. Formula of apremilast microemulsion (APR-ME).

Components	(%)
Apremilast (1.5 mg/mL)	
Plurol® oleique CC497 (Polyglyceryl-3 dioleate)	6.00
Labrasol® (Caprylocaproyl Polyoxyl-8 glycerides)	29.33
Transcutol® P (Diethylene glycol monoethyl ether)	14.67
Water	50.00

2.3. APR-ME Characterization

Drug content and pH were at 99.30 ± 0.37% and 6.07 ± 0.06, respectively. After 24 h of preparation, the obtained ME was transparent with a monophasic appearance, optically isotropic and droplets with size of 60.53 ± 0.08 nm. The PDI value was 0.39 ± 0.02, which indicated the presence of a homogeneous system with droplets of uniform size. A representative TEM image of APR-ME is shown in Figure 4, in which a system of plainly distinguishable droplets of spherical shape with uniform size as consistent with DLS results can be observed. The droplets appear dark in color against a white background, with random dispersion and little agglomeration in the field.

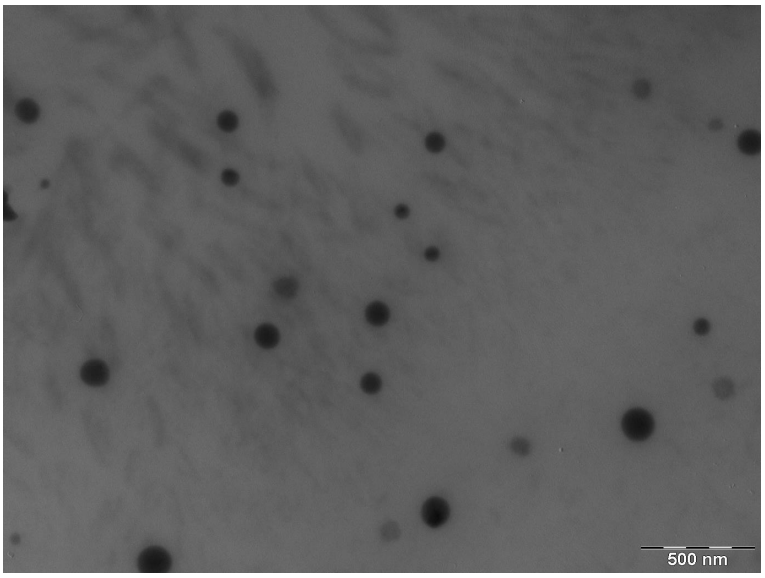

Figure 4. Transmission electron microscopy image of Apremilast microemulsion, magnification 40,000×.

Figure S3 shows the viscosity and rheological behavior of APR-ME. The relationship between the shear stress and the shear rate (flow curve) was linear, while the viscosity remained constant with a value of 21.58 ± 0.05 mPas·s. The mathematical model that best describes the experimental data was the Newtonian model with an $r^2 = 1$.

2.4. Stability Studies

After manufacturing, MEs were stored at different temperatures (4 ± 1 °C, 30 ± 2 °C, and 40 ± 2 °C) for 90 days. The physical stability studies carried out using TurbiScanLab® equipment did not show evidence of destabilization processes such as flocculation, sedimentation or coalescence. Variations greater than 10% in the T signals would indicate destabilization processes; however, as shown in Figure S4, T signals remained constant under the studied conditions, thereby confirming physical stability of the ME system. The peaks that appear on the left and right sides of the graph are formed by the contact between the sample and the glass. As such, the left region of the graph represents the bottom of the vial and the right region corresponds to the top of the vial [31,32].

The chemical stability evaluation (Table 2) showed that the drug content of APR-ME remained stable during the time of the stability study, especially at 4 °C, while at 30 °C and 40 °C there was an insignificant decrease in drug of around 1% and 1.5%, respectively.

Table 2. Chemical stability studies of APR-ME.

Time (days)	Drug Content (%)		
	4 ± 1 °C	**30 ± 2 °C**	**40 ± 2 °C**
1	99.66	99.67	99.67
30	99.66	99.66	99.66
60	99.61	99.12	98.90
90	99.59	98.67	98.14

2.5. In Vitro Release Studies

Figure 5 shows the patterns of release of APR from the ME. The graphical representation of cumulative released amount of APR vs. time indicated a faster diffusion of the drug during the first 20 h followed by a sustained release of the drug, showing a release of 174.32 µg after 74 h, which represents 58% of the drug placed in the donor compartment. The mathematical fitting suggested a first-order kinetic model (Fickian kinetic), with r^2 = 0.97, a maximum release amount (Y_{max}) = 176.5 µg and a release constant (K) = 0.1061 h^{-1}.

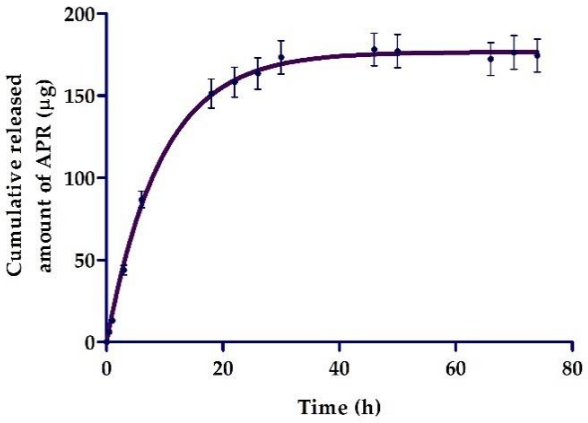

Figure 5. In vitro release profile of apremilast (APR) from microemulsion.

2.6. Permeation and Q_{ret} Studies in Ex Vivo Human Skin

Apremilast was not detected (LOD: 1.13 ± 1.04 µg/mL) in the receptor fluid after 24 h of permeation test. However, it was possible to observe its presence into the skin after its extraction. The retained amount drug in the skin (Q_{ret}) was 479.35 ± 102.85 µg APR/g skin/cm^2.

2.7. In Vitro Anti-Inflammatory Efficacy Studies

In order to evaluate the capability of APR-ME to inhibit the inflammatory response, IL-8 and IL-6 cytokines were measured in supernatants of TNF- α-stimulated HaCaT cells. A cell viability greater than 80% was observed in the dilutions made of APR-ME (Figure 6). In absence of APR-ME (positive control), TNF-α induced a significant increase in both analyzed cytokines. However, a decrease in IL-8 and IL-6 production dependent on drug concentration was observed in HaCaT cells stimulated with different concentrations of APR-ME (Figure 7). Secreted levels of IL-6 were significantly reduced using APR-ME at 6 µg/mL while IL-8 was significantly reduced using 6 µg/mL and 3 µg/mL of APR-ME. Finally, 1.75 and 0.75 µg/mL concentrations showed negligible effects.

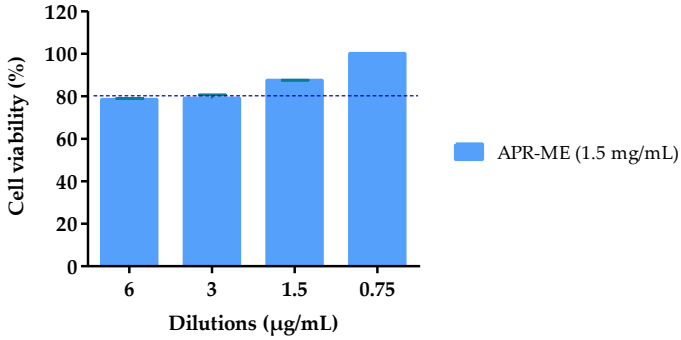

Figure 6. Percentage of cell viability of HaCaT cell line exposed to APR-ME for 24 h at different concentrations ranging from 6 to 0.75 µg/mL. Results obtained with Blank-ME indicated 100% viability.

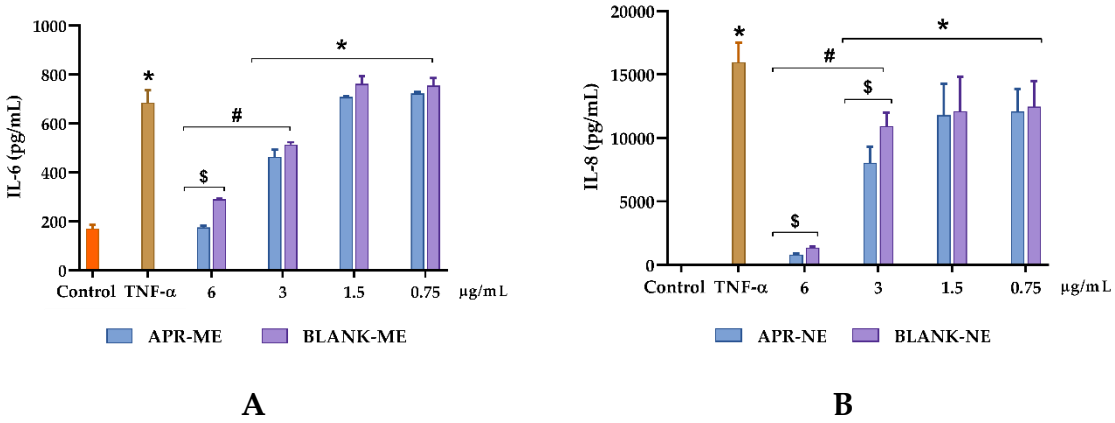

Figure 7. Inhibition of inflammatory response of cytokines in HaCaT cell line. (**A**) Interleukin-6 (IL-6); and (**B**) Interleukin 8 (IL-8). *Control −:* untreated cells; *Control +:* positive control. *APR-ME:* cells treated with apremilast microemulsion; and *Blank-ME:* cells treated with drug free vehicle. Results are expressed as mean ± SD (n = 3) Statistically significant difference: *, comparison with negative control; #, comparison between concentrations; and $, comparison between APR-ME and Blank-ME.

2.8. In Vivo Anti-Inflammatory Efficacy Studies: Arachidonic Acid (Aa)-Induced Inflammation

The evaluation of the anti-inflammatory potential of APR-ME was performed using a model of induction of inflammation in mice ear with AA. Figure 8 shows the inflammatory action of AA, which is manifested by redness and edema in the ears of the positive control group and is substantially more evident when contrasted with those of the negative control group. Figure 9 shows noticeably greater skin thickness in the positive control group compared to the group treated with APR-ME. These results suggest that APR-ME reduces the signs of inflammation induced by the action of AA.

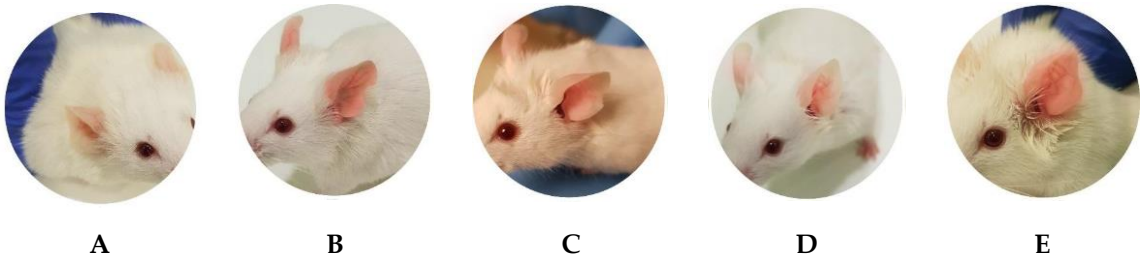

Figure 8. Macroscopic features of the ear's appearance. (**A**) Negative control; (**B**) Positive control (edema and redness); (**C**) Ibuprofen group; (**D**) Apremilast microemulsion (APR-ME) group; and (**E**) Blank-ME group.

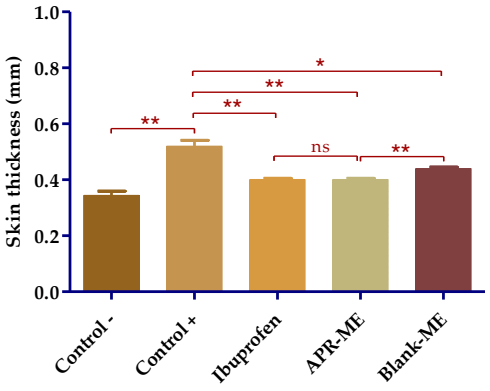

Figure 9. Ear thickness. Results are expressed as mean ± SD (n = 3). Statistically significant differences: *, $p < 0.05$; **, $p < 0.01$; ns, not significant.

2.8.1. Biomechanical Skin Properties Evaluation

After inducing inflammation, stratum corneum hydration (SCH) was not significantly affected across all study groups. However, it is necessary to highlight the evident moisturizing action of different treatments, especially to APR-ME (Figure 10).

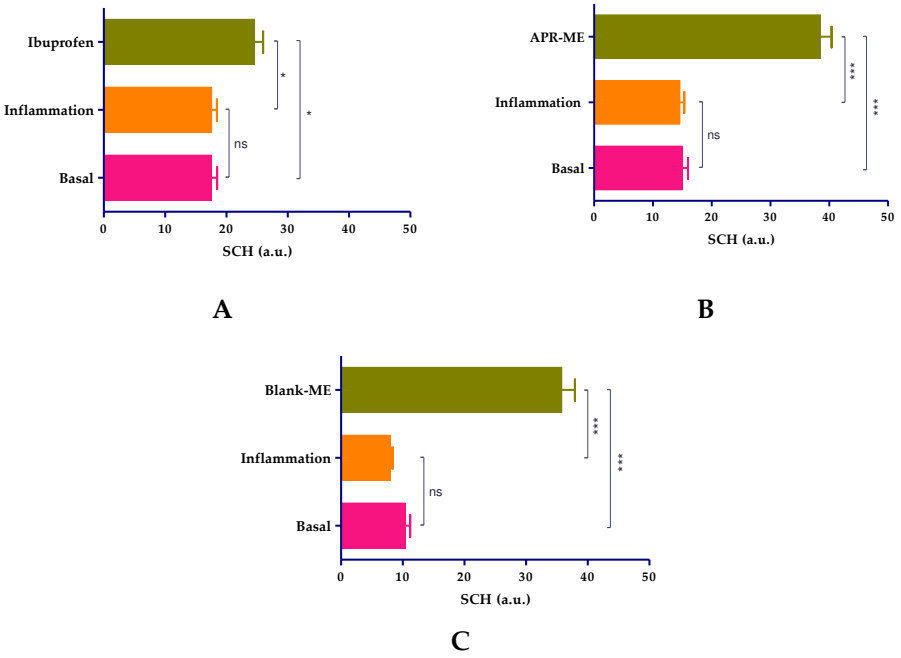

Figure 10. Evaluation of stratum corneum hydration (SCH). (**A**) Ibuprofen treatment group; (**B**) Apremilast microemulsion (APR-ME) treatment group; and (**C**) Blank-ME treatment group. Results are expressed as mean ± SD (n = 3). Statistically significant differences: *, $p < 0.05$; ***, $p < 0.001$; ns, not significant.

2.8.2. Histological Analysis

To examine the anti-inflammatory effect of APR-ME, hematoxylin and eosin staining histologically analyzed the architecture of mouse ear skin. Negative control micrographs consisted of a relatively thin epidermis with a contiguous stratum corneum (SC) and dermis (Figure 11A). Images of positive control exhibited edema as well as presence of leukocytic infiltrate and a slight loss of SC (Figure 11B). Loss of the SC was also evident in ibuprofen-treated mice, along with a leukocyte infiltrate (Figure 11C). When ears were topically treated with APR-ME, a profile with less inflammatory cell infiltrates and a

normal SC resembling the negative control was observed (Figure 11D). Topical application of blank-NE did not improve the inflammatory characteristics induced by AA such as edema and leukocytic infiltrate (Figure 11E).

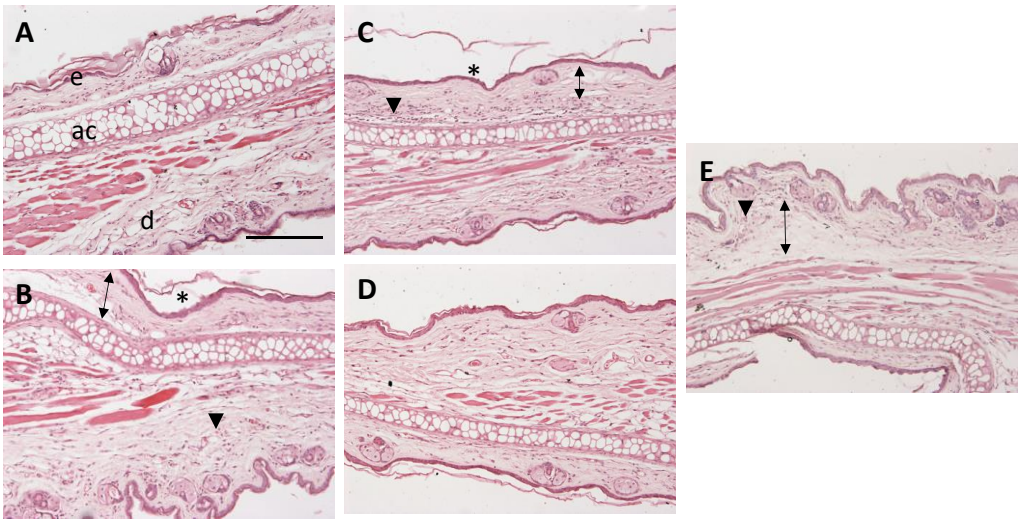

Figure 11. Representative micrographs of mice ear (100× magnification). (**A**) Negative control; (**B**) Positive control; (**C**) Ibuprofen; (**D**) Apremilast microemulsion (APR–ME); and (**E**) Blank–ME. Skin structures: (**e**) epidermis; (**d**) dermis; and (**ac**) auricular cartilage. Arrowheads indicate leukocytic infiltrates, arrows indicate edema, and asterisks (∗) indicate loss of stratum corneum. Scale bar = 200 μM.

2.8.3. Pro-Inflammatory Cytokines Determination

When compared with the negative control, the positive control shows a significant increase in the expression of the pro-inflammatory cytokines IL-8, IL-17A and TNFα as a result of the inflammatory process induced by topical application of AA on mouse ear. The treatment with APR-ME showed anti-inflammatory potential and was evidenced by a decrease in the production of pro-inflammatory interleukins. The anti-inflammatory efficacy between APR-ME and reference anti-inflammatory product (ibuprofen gel) did not show significant differences. Blank-ME did not demonstrate anti-inflammatory capacity; therefore, possible therapeutic action by the excipients of the formulation was discarded (Figure 12).

2.8.4. In Vivo Tolerance

Topical application of APR-ME on the skin of the volunteers demonstrated that the formulation does not cause signs of damage or irritation. Results showed a significant reduction in TEWL and an inversely proportional increase in SCH after APR-ME application, the latter indicating that the fatty components of ME are absorbed into the skin. These studies confirmed that the ME composition does not damage the skin barrier and can be easily absorbed into it (Figure 13).

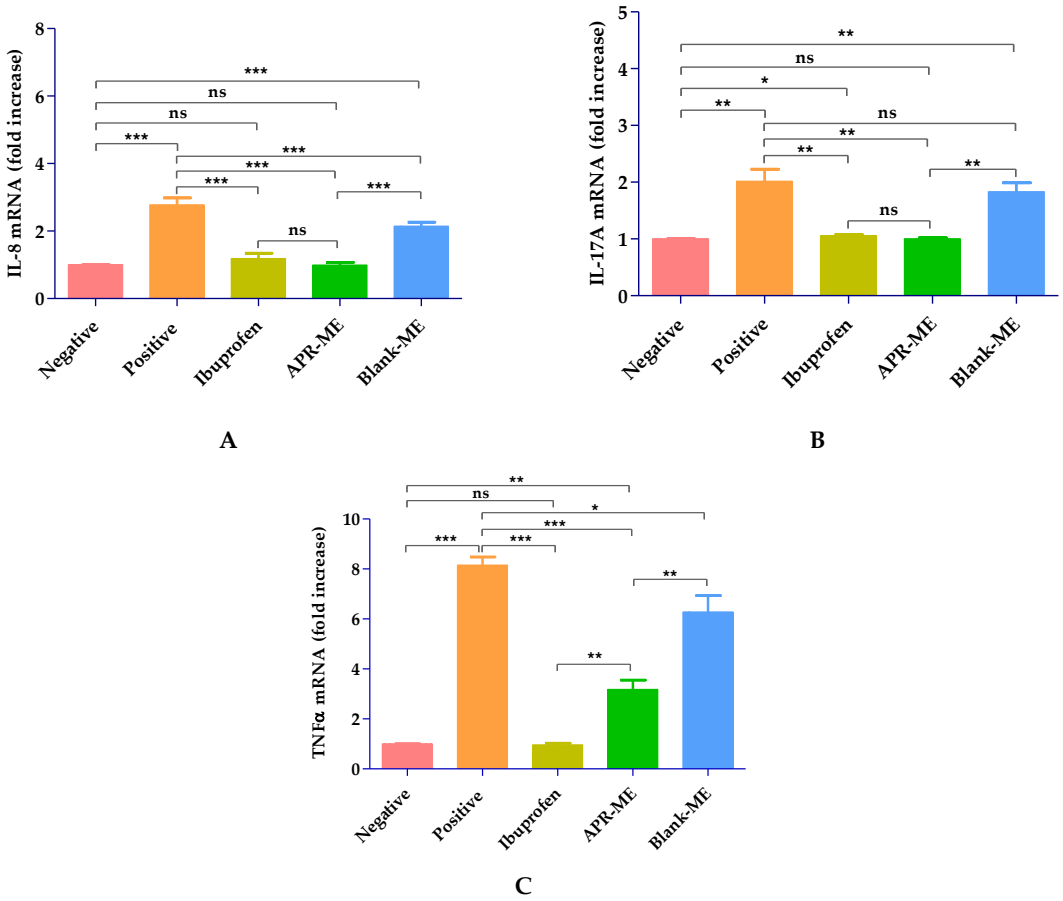

Figure 12. Relative expression of pro-inflammatory cytokines measured by RT-qPCR. (**A**) Interleukin-8 (IL-8); (**B**) Interleukin 17A (IL-17A); and (**C**) Tumor Necrosis Factor alpha (TNFα). *Negative*: untreated mice; *Positive*: AA-treated mice; *Ibuprofen*: mice treated with a reference anti-inflammatory product (ibuprofen gel); *Blank-ME:* mice treated with drug free vehicle; and *APR-ME:* mice treated with apremilast microemulsion. Results are expressed as mean ± SD (n = 4). Statistically significant difference: *, $p < 0.05$; **, $p < 0.01$; ***, $p < 0.001$; ns, not significant.

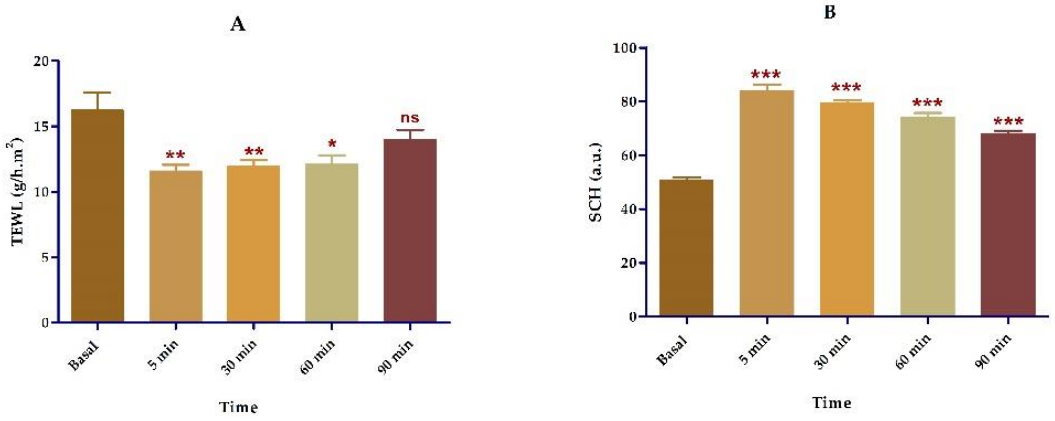

Figure 13. Tolerance studies in human individuals. (**A**) TEWL: Transepidermal water loss; (**B**) SCH: Stratum corneum hydration. Results are expressed as mean ± SD (n = 12). Statistically significant differences in comparison with basal state: *, $p < 0.05$; **, $p < 0.01$; ***, $p < 0.001$; ns, not significant.

3. Discussion

Inflammatory skin diseases affect numerous patients worldwide [33] not only physiologically but also psychologically and socioeconomically [34,35]. APR is an FDA approved oral drug for the treatment of adult patients with active psoriatic arthritis, adult patients with moderate-to-severe plaque psoriasis who are candidates for phototherapy or systemic therapy, and adult patients with oral ulcers associated with Behçet's disease [36,37]. Topical application of APR as an alternative treatment for local skin inflammation was evaluated in this study. Validation of the analytical method was performed in order to obtain a reliable method for drug quantification. The results showed compliance with ICH guidelines, exhibiting good linearity in a range from 1.25 to 200 µg/mL (r^2 = 0.999) in addition to having acceptable precision, accuracy and robustness [38]. Detailed results are shown in the Supplementary Materials. APR is categorized as a class IV drug, according to the Biopharmaceutical Classification System (BCS), due to its low solubility and low permeability [39]. Hence, this study incorporated APR in a ME as a strategy to improve the solubility and permeability of the drug. The formulation was developed using the excipients that showed the highest solubilizing capacity for the drug: Plurol® oleique CC497, Labrasol® and Transcutol® P (Figure 2). The search for the most suitable components with regards to the solubility of the drug is a critical step in the development of a ME in order to ensure its stability and high drug loading capacity [40,41]. Labrasol® is a non-ionic oil/water surfactant characterized by its low irritability for the skin and which is commonly used with Plurol® oleique in dermal formulations [42]. Transcutol® P was selected as a co-surfactant due to its ability to solubilize APR with non-toxic and biocompatible properties with the skin [43]. The pseudo-ternary phase diagram with a surfactant-cosurfactant mixture (S_{mix}) in the ratio 2:1 (*w*:*w*) showed a greater ME region (Figure 3), and therefore was used for drug incorporation. APR-ME (1.5 mg/mL) was prepared by the titration method, where there is a spontaneous emulsification by a low energy process [44]. Final formulation was homogeneous and transparent, with a slightly acidic pH, which is biocompatible with the skin and thus suggests that APR-ME does not have an irritating effect [45]. The physical characterization by DLS and TEM (Figure 4) showed the presence of droplets of nanometric size and spherical shape distributed uniformly. The microemulsion presented isotropic characteristics [46] after its evaluation with a polarized light microscope. The rheological behavior of dermal formulations influences administration properties such as sensory characteristics, spreadness and dosage [47,48]. In ME systems, evaluation of rheological properties provides information on the structural constitution as well as the interactions between droplets [49,50]. The rheological behavior of APR-ME (Figure S3) was determined from the relationship between the shear stress and the shear rate (flow curve), which was linear, while the viscosity remained constant. This result was supported by mathematical modeling which confirmed Newtonian behavior that is typical for this type of formulation and thus providing the possibility of being easily administered by spray.

The transmission profiles obtained by multiple light scattering analysis allowed assessment and demonstration of the physical stability of APR-ME for a period of 90 days due to the fact that no signals of creaming, sedimentation, flocculation or coalescence were detected (Figure S4). Additional evaluation of physical parameters including droplet size, PDI and pH confirmed the high physical stability of the formulation. APR-ME also showed chemical stability, since there were insubstantial changes in the quantified drug content after 90 days at different temperatures, which demonstrates the high compatibility between the components with the drug.

In dermal formulations, release and permeation studies of drug are useful tools to predict drug bioavailability while consequently determining its efficacy [51,52]. In this work, APR was released from NE following a first-order model (Fickian kinetic) in which the release rate is directly proportional to the concentration of the remaining drug (Figure 5). As such, compliance with Fick's law is observed, which establishes that the diffusion rate through a membrane is directly proportional to the concentration gradient of the substance on both sides [53]. This result confirmed that the formulation can release the incorporated drug and thus it does not limit drug permeation through the skin.

Ex vivo permeation studies using human skin and under suitable conditions are successfully used to predict in vivo behavior of topical formulations [54,55]. The results of this assay revealed that APR-ME could be used as an effective local treatment for skin inflammation since the drug was able to cross the SC and remain retained into the skin (479.35 ± 102.85 μg APR/g skin/cm^2) without reaching the receptor compartment. These findings suggest that it is possible to reach adequate drug concentration in the target area while avoiding systemic adverse effects.

Regarding the therapeutic efficacy, both in vitro and in vivo tests APR-ME demonstrated anti-inflammatory potential after its application (Figures 7 and 12). In vitro efficacy studies using HaCaT cell line corroborated the activity of the drug on the expression of previously reported pro-inflammatory interleukins such as IL-6 and IL-8 [56]. The inhibitory effects of APR-ME on the production of inflammatory mediators were accompanied by concentration-dependent decreases in IL-6 and IL-8 mRNA and protein expression levels. Additionally, in vivo efficacy studies were performed using AA to induce inflammation in the mice ear. AA is a long-chain unsaturated essential fatty acid that is formed from the synthesis of linoleic acid in the diet, and is considered one of the precursors of prostaglandins, thromboxanes and leukotrienes [57,58]. Research supports the use of AA for the induction of inflammatory processes because it is an intrinsic component of the inflammatory response, which can subsequently be used in mouse ear edema models for evaluation of anti-inflammatory potential of drugs [59–62]. APR, being a phosphodiesterase 4 inhibitor, elevates intracellular cAMP levels, which in turn intervenes in the regulation of the inflammatory response by modulating the expression of TNFα and IL-17 [63]. The skin inflammatory process promotes skin dryness, induces infiltration of inflammatory cells, increases skin thickening and stimulates the membrane receptors of keratinocytes which promotes the release of various inflammatory mediators such as TNFα, IL-8, IL-1α, IL-6 and IL-12 [64,65]. In our study, SCH results (Figure 10) showed that the SC water content was not altered for the topical application of AA; however, a moisturizing effect was noticeable in mice treated with APR-ME. Nevertheless, AA induced an increase in the skin thickness, which is indicative of edema, hyperplasia and intensified vascular permeability (Figure 8) [66]. This effect was corroborated by histological studies (Figure 11) that showed the presence of edema and leukocytic infiltrate in the positive control. The therapeutic efficacy of the formulation in the treatment of these symptoms was confirmed in this study, since a reduction of skin thickness (Figure 9) as well as in the infiltration of inflammatory cells was observed after topical administration of APR-ME. Regarding the immunological mechanisms involved in the local inflammatory process induced by AA, an increase in the expression of pro-inflammatory cytokines IL-8, IL-17A and TNFα compared to the negative control group was observed (Figure 12). Topical treatment with APR-ME on the inflamed area significantly reduced the expression of these cytokines. The role of IL-8, IL-17A and TNFα in skin inflammation has been widely described in previous studies [67–69]. TNF-α is a multifunctional agent that stimulates the acute phase of an inflammatory reaction and is secreted by different cell types, including monocytes, macrophages, Langerhans cells and microglia [70,71]. This cytokine is one of the most abundant early markers and is considered a "master regulator" in inflammatory processes because it can trigger local expressions of other pro-inflammatory cytokines such as IL-1, IL-6 and IL-8 [72–74]. IL-8 is an inflammatory chemokine that is produced by various cells, including monocytes, fibroblasts, endothelial cells, keratinocytes and chondrocytes [75]. The role of IL-8 in inflammation and inflammatory skin diseases has been confirmed by experimental models that showed a constitutive expression of IL-8 mRNA in normal cultured keratinocytes along with a rapid increase in its level when submitting a stimulus, such as irradiation [76]. Finally, IL-17 plays an important role in the regulation of innate and adaptive immune systems. However, its overexpression is involved in various inflammatory and autoimmune diseases including dermatitis and psoriasis [77–79]. In summary, the efficacy studies carried out in this work confirmed: (i) the therapeutic effect of APR in an in vitro model in HaCaT cell lines; (ii) no apparent cytotoxicity (cell viability [80–82] Figure 6) of APR-ME in concentrations from 6 μg/mL onwards; (iii) the therapeutic potential of APR-ME that was evidenced by a decrease in the expression of the cytokines IL-8, IL-17A and TNFα; reduction in the infiltration

of inflammatory cells as well as in edema and redness; and (iv) moisturizing effect on affected area thanks to the composition of the formulation based on oils and surfactants.

Finally, the tolerance in vivo study (Figure 13) was conducted, where biochemical skin properties were analyzed in healthy volunteers. TEWL and SCH have been used in dermatology to detect possible irritant effects of topical formulations [83–85]. Normal hydration levels maintain SC flexibility and its viscoelastic characteristics in addition to facilitating the enzymatic reactions involved in the maturation of corneocytes [86,87]. Destabilization or damage to the skin surface by exposure to physical or chemical agents can cause changes in TEWL and SCH [88–90]. In this study, the evaluation of these parameters confirmed that APR-ME does not alter sebaceous function nor compromise the integrity of the skin barrier. On the contrary, improved hydration levels were evidenced by a significant reduction of TEWL along with an increase of SCH following topical application of APR-ME, likely due to the moisturizing effect of the formulation.

4. Materials and Methods

4.1. Materials

Apremilast (purity of 99.6% and molecular weight of 460.5 Da) was purchased from Wuhan Senwayer Century Chemical (Wuhan, China). Polyglyceryl-3 dioleate (Plurol® oleique CC497), oleoyl polyoxyl-6 glycerides (Labrafil® M1944 CS), propylene glycol monolaurate-type II (Lauroglycol™ 90), caprylocaproyl polyoxyl-8 glycerides (Labrasol®) and diethylene glycol monoethyl ether (Transcutol® P) were supplied by Gattefossé (Saint-Priest, France). Castor oil (*Ricinus communis* L.), polyethylene glycol sorbitan monooleate (Tween® 80) and propylene glycol 400 were supplied by Sigma-Aldrich (Madrid, Spain). Macrogol glycerol ricinoleate [Cremophor® EL] was supplied by Fagron Iberica (Barcelona, Spain). Reagents for histological procedures were purchased from Sigma and Thermo Fisher Scientific (Barcelona, Spain). HaCaT cell line was purchased from Cell Line Services (Eppelheim, Germany) and the reagents used for cell cultures were obtained from Gibco (Carcavelos, Portugal). Reagents for MTT assay were obtained from Invitrogen Alfagene® (Carcavelos, Portugal). A Millipore Milli-Q® purification system (Millipore Corporation; Burlington MA) was used to obtain ultrapure water for all experiments. Finally, the reagents used in this study were of analytical grade.

4.2. Validation of the Analytical Method

High-performance liquid chromatography (HPLC) method for APR quantification was validated. The HPLC system consisted of a Waters 1525 pump and a UV-VIS 2487 detector (Waters, Milford, MA, USA). Data was collected and processed using Empower Pro software (Waters, Milford, MA, USA). Analysis was performed with a Kromasil C18 chromatographic column (250 mm, 4.6 mm and 5 µm). The mobile phase consisted of a mixture of acetonitrile (ACN) water (70:30 *v*/*v*) filtered with a 0.45 µm PVDF membrane filter (Millipore Corp., Madrid, Spain). The mobile phase was pumped at a flow rate of 1 mL/min and the injection volume was 20 µL. The isocratic elution was carried out at 25 °C and the detection was carried out by UV spectrophotometry at λ = 230 nm.

Conditions Analyzed

Standard stock solution (APR = 250 µg/mL) was prepared daily in ACN. The calibration curve was prepared using mobile phase to obtain dilutions in a concentration range of 1.25 to 200 µg/mL. The method was validated in terms of linearity, precision, accuracy, robustness, sensitivity and specificity. Validation was performed according to the International Conference on Harmonization (ICH) Q2A and Q2B guidelines.

Linearity: The linearity was evaluated by a one-way ANOVA test to compare peak areas versus nominal concentrations of each standard [91]. Differences were considered statistically significant

when $p < 0.05$. The least-square linear regression analysis and mathematical determinations were carried out using GraphPad Prism v5.0 software (GraphPad Software Inc., San Diego, CA, USA).

Accuracy and Precision: Accuracy and precision were investigated by measuring samples in the concentrations of 1.25 to 200 µg/mL. The between-day test for three days was performed to analyze the analyte within all the previously mentioned concentrations. Precision was defined as the relative standard deviation (RSD%) of the measurement, whereas accuracy was expressed as a relative error (RE%), using the equation:

$$RE\% = \frac{X_a - X_r}{X_a} \cdot 100 \quad (1)$$

where: X_a is the theoretical value of the concentration, X_r is the experimental value of the concentration and 100 is the constant.

Robustness: Robustness was determined by changing the experimental conditions of concentration of the mobile phase by varying the proportions by ±1% of acetonitrile and water. The effects of these variations in the experimental conditions were tested for the retention time. SD was calculated.

Specificity: The specificity of the method was evaluated by analyzing any possible interferences due to the components of the skin that are released during the passage of the drug. Different samples were evaluated including drug-free mobile phase and standard 100 µg/mL, as well as two samples obtained from permeation studies: APR retained in the skin and a skin blank (sample extracted from receptor compartment in a Franz cell using drug-free skin) as a control. A volume of 20 µL of each sample was injected and then the chromatographic profiles (λ= 230 nm) were analyzed.

Sensitivity: Sensitivity was analyzed using limit of detection (LOD) and limit of quantification (LOQ). The LOD and LOQ were calculated based on each of the standard deviation of the response and the slope of the calibration curve. LOD and LOQ are calculated using:

$$LOD \text{ or } LOQ = k\frac{SD_{Sa}}{S_b} \quad (2)$$

where: k is the factor related to the level of confidence (k = 3.3 and 10 for LOD and LOQ, respectively). SD_{Sa} is standard deviation of the intercept. S_b is the slope.

4.3. Solubility Studies

The solubility of APR in various oils (Plurol® oleique CC497, Labrafil® M1944 CS, Lauroglycol™ 90 and Castor oil), surfactants (Tween® 80, Labrasol® and Cremophor® EL) and co-surfactants (Transcutol® P and Propylene glycol 400) was determined. An excess of APR was added to the indicated vehicles and mixed under stirring for 4 h. The samples were equilibrated for 24 h and later centrifuged at 9000 rpm for 10 min. The supernatant was diluted with methanol to quantify the amount of APR dissolved using a Thermo Spectronic Helios Beta UV-Visible Spectrophotometer (Thermo Fisher Scientific, Karlsruhe, Germany).

4.4. Pseudo-Ternary Phase Diagrams

Four pseudo-ternary phase diagrams were constructed with the components that presented higher APR solubility capacity by the water titration method [92]. The pseudo-ternary diagrams were constructed using Plurol® oleique CC497 as the oil phase, a mixture of Labrasol® and Transcutol® P (S_{mix}) as surfactants and co-surfactants, respectively, and purified water as the aqueous phase. Labrasol and Transcutol® P were mixed at ratios 1:1, 2:1, 3:1 and 1:2 while oil and S_{mix} were mixed at a fixed weight ratio 9:1, 8:2, 7:3, 6:4, 5:5, 4:6, 3:7, 2:8 and 1:9 (*w*/*w*); Titration with water was carried until turbidity or phase separation was observed in each oil/S_{mix} ratio. The single-phase and transparent combinations were placed within the emulsification area, which made it possible to delimit the ME formation region. The diagram showing the highest emulsification area was selected as S_{mix} optimized.

4.5. Preparation of Apremilast Microemulsion (APR-ME)

APR-ME (1.5 mg/mL) was prepared by incorporating the APR into the oil and S_{mix} under stirring at 700 rpm until drug dissolution. Afterwards, purified water was added dropwise under constant stirring until a transparent ME was obtained.

4.6. Characterization of the Apremilast Microemulsion

4.6.1. Content and pH of APR-ME

The drug content in the ME was quantified using the HPLC method described in Section 4.2. The pH values of the formulation were determined using a calibrated digital pH meter GLP 22 (Crison Instruments, Barcelona, Spain).

4.6.2. Drop Size and Polydispersity Index

The droplet size and polydispersity index (PDI) were determined using 1 mL of APR-ME without dilution at 25 °C by dynamic light scattering technique (DLS) with a Zetasizer Nano ZS kit (Malvern Instruments, Malvern, UK). Previously, the formulation refractive index was measured obtaining a value of 1.397. Values are reported as the mean ± SD of three replicates.

4.6.3. Transmission Electron Microscopy (TEM)

To corroborate droplet size and to examine morphology, the formulation was analyzed by TEM using a JEOL JEM-1010 microscope (JEOL Ltd., Tokyo, Japan). For negative staining, a drop of undiluted ME was deposited on a Formvar coated copper grid for 1 min. After blotting the excess of formulation, the grid was washed with a drop of ultrapure water. Then, the sample was stained with UranyLess® for 1 min. Finally, TEM images were taken after 24 of drying.

4.6.4. Viscosity and Rheological Behavior

Viscosity and rheological behavior were analyzed without dilution at 25 °C using a Haake RheoStress 1 rheometer (Thermo Fisher Scientific, Karlsruhe, Germany). ME was assessed in duplicate using a program consisting of three steps: an increasing period of shear rate (0–50 s^{-1}) for 3 min, followed by a period of constant shear rate at 50 s^{-1} for 1 min, and a period of decreasing shear rate (50–0 s^{-1}) for 3 min. Values are reported as the mean ± SD of three replicates. Results of the flow curves were fitted to various mathematical models:

Newton Equation:

$$\tau = \eta \cdot \dot{\gamma} \quad (3)$$

Bingham Equation:

$$\tau = \eta \cdot \dot{\gamma} \quad (4)$$

$$\tau = \tau_0 + (\eta_p \cdot \dot{\gamma}) \quad (5)$$

Ostwald-de-Waele Equation:

$$\tau = K \cdot \dot{\gamma}^n \quad (6)$$

Herschel-Bulkley Equation:

$$\tau = \tau_0 + K \cdot \dot{\gamma}^n \quad (7)$$

Casson Equation:

$$\tau = \sqrt[n]{\left(\tau_0^n + \left(\eta_0 \cdot \dot{\gamma}\right)^n\right)} \quad (8)$$

Cross Equation:

$$\tau = \dot{\gamma} \cdot (\eta_\infty + (\eta_0 - \eta_\infty) / (1 + (\dot{\gamma} / \dot{\gamma}_0)^n) \quad (9)$$

where: τ is the shear stress (Pa). $\dot{\gamma}$ is the shear rate (1/s). η is the dynamic viscosity (mPa·s). τ_0 is the yield shear stress (Pa). η_0 is the zero-shear rate viscosity. η_p is a constant plastic viscosity (mPa·s). η_∞ is the infinity shear rate viscosity. η is the flow index. K is the consistency index.

4.7. Stability Study

The physical stability of APR-ME was evaluated by analyzing transmission profiles (T) obtained by multiple light scattering using the TurbiScanLab® equipment (Formulation, L'Union, France), whose light source is near-infrared (λ = 880 nm). The TurbiScanLab® is an optical instrument that characterizes emulsions and dispersions which is based on the measurement of backscatter (BS) and transmission (T) signals in order to early detect destabilization phenomena such as droplet aggregation or their migration [93]. The T profiles of the APR-ME samples (20 mL) stored at 4, 30 and 40 °C were measured at predetermined time intervals (1, 30, 60 and 90 days).

The chemical stability of APR-ME was evaluated by the quantification of the drug present in the formula at all the indicated time intervals and storage temperatures. To that end, 1 mL of ME was taken and diluted with ACN at a ratio of 1:100. This sample was analyzed according to the method described in Section 4.2.

4.8. In Vitro Release Study

The release study of APR from ME was performed using Franz vertical diffusion cells of 13 mL capacity (Franz Diffusion Cells 400; Crown Glass, Somerville, NJ) and dialysis membranes (MWCO 12 KDa) previously hydrated for 24 h with methanol/water (50:50 *v*/*v*), which were washed with water and mounted between the donor and receptor compartment. The effective diffusion area was 2.54 cm^2. The receptor compartment was filled with Transcutol® P/water medium (60:40 *v*/*v*), which was kept under continuous stirring (700 r.p.m.). 0.2 mL samples of APR-ME were placed in the donor compartment and the system was maintained at 32 ± 0.5 °C, to simulate skin conditions in vivo. Aliquots of 0.2 mL were withdrawn from the receptor compartment at predetermined time intervals up to 74 h, which were subsequently replaced by the same volume of receptor medium. The concentration of released APR from ME was quantified by HPLC (Section 4.2). Values are reported as the mean ± SD of three replicates. The data were fitted to various mathematical models to determine the release kinetics, where the model was selected based on the correlation coefficient (r^2):

Zero Order Equation:

$$Q_t = K_0 \cdot t + Q_\infty \tag{10}$$

First Order Equation:

$$Q_t = Q_\infty \left(1 - e^{-K_f \cdot t}\right) \tag{11}$$

Higuchi's Equation:

$$Q_t = K_H \, t^{\frac{1}{2}} \tag{12}$$

Korsmeyer–Peppas Equation:

$$Q_t = K_k \, t^n \tag{13}$$

where: Q_t is the amount of released drug at time t. Q_∞ is the maximum amount of release drug. K_0, K_f, K_H, K_k are the constants of release rate. t is time in hours. n is the exponent of release (related to the drug release mechanism) $n \leq 0.43$ (Fickian diffusion), $0.43 < n < 0.85$ (abnormal transport) and ≥ 0.85 (case II transport; zero-order release kinetic). r^2 is the determination coefficient.

4.9. Ex Vivo Skin Permeation Study

This assay was performed using human skin from an abdominal lipectomy of a healthy 38-year-old woman (Hospital de Barcelona, SCIAS, Barcelona, Spain) under prior written consent in accordance with the Ethics Committee of the Hospital de Barcelona (number 001, dated January 20, 2016). The integrity of the skin samples was evaluated based on transepidermal water loss (TEWL) using Tewameter TM

300 (Courage & Khazaka Electronics GmbH, Cologne, Germany) and those with results less than 10 g/m^2/h were used [94]. For the experiment, the skin samples were cut with the help of an Aesculap GA 630 dermatome (Aesculap, Tuttlingen, Germany) in order to obtain skin samples 0.4 mm thick, which were then placed between the donor and receptor compartment of Franz diffusion cells (6 mL) with a diffusion area of 0.64 cm^2. The receptor medium consisted of a solution of Transcutol® P/water (60:40, *v*/*v*) at 32 ± 0.5 °C and stirring at 700 r.p.m. to guarantee sink conditions. 0.2 mL samples of APR-ME (1.5 mg/mL) were placed in the donor compartment in contact with the outer surface of the skin. Aliquots of 0.2 mL were withdrawn from the receptor compartment at predetermined time intervals up to 30 h, which were then replaced by the same volume of receptor medium. The amount of permeated APR was quantified by HPLC (Section 4.2). Values are reported as the mean ± SD of three replicates.

Determination of the Amount of Drug Retained in the Skin

At the end of the permeation study, the amount of APR retained in the skin (Q_{ret} µg/g skin/cm^2) was extracted by ultrasound-assisted extraction. The skin samples were removed from Franz diffusion cells and cleaned with gauze soaked in a 0.05% solution of dodecyl sulfate and washed with distilled water. The skin permeation area was cut, weighed and immersed in 1 mL of ACN for 30 min using an ultrasonic bath. Solvent samples were filtered and quantified by HPLC (described in Section 4.2).

4.10. In Vitro Anti-Inflammatory Efficacy Studies in HaCaT Cell Line

4.10.1. Cell Culture

All assays were performed with immortalized keratinocytes HaCaT cell line. The cells were grown in Dubelcco's Modified Eagle's Medium (DMEM) with high glucose content buffered with 25 mM HEPES, and supplement with 1% non-essential amino acids, 100 U/mL penicillin, 100 g/mL streptomycin and 10% heat inactivated Fetal Bovine Serum (FBS). The cells were growth until 80–90% confluence at 37 °C under 5% CO_2 atmosphere. The culture medium was changed every 3 days.

4.10.2. Cell Viability Assay

The effect of APR-ME on cell viability was evaluated using an Methylthiazolyldiphenyl-tetrazolium bromide assay (MTT assay). HaCaT cell line (2×10^5 cells/mL) were seeded in 96-well plates (Corning) while being kept in a humidified incubator at 37 °C under a 5% CO_2 atmosphere for 48 h to allow adhesion. Experiments were performed at 80%–90% confluence.

APR-ME (1500 µg/mL) was diluted to obtain a concentration range of 6 to 0.75 µg/mL in order to select the concentrations that guarantee a cell viability greater than 80% for posterior in vitro anti-inflammatory studies. After 24 h of incubation with these dilutions, the HaCaT cells were washed with 1% sterile PBS and incubated with MTT (Sigma-Aldrich Chemical Co, St. Louis, MO, USA) solution (5 mg/mL) for 2 h at 37 °C. Afterwards, the medium was carefully removed and 0.1 mL of Dimethyl sulfoxide (DMSO, purity 99%) was add to lyse the cells and dissolve the purple MTT crystals. Cell viability was measured at 570 nm in a microplate photometer Varioskan™ LUX (Thermo Scientific, Waltham, MS, USA). In parallel, a negative control (cells without any stimulation or treatment) was processed for comparison. The results were expressed as percentage of cell survival relative to the control (untreated HaCaT cells, 100% viability) using the following equation:

$$\text{Cell viability} = \left[\frac{\text{ABS treated cells}}{\text{ABS control cells}}\right] \times 100 \quad (14)$$

4.10.3. In Vitro Anti-Inflammatory Efficacy

In order to determine the in vitro anti-inflammatory effect of APR-ME, HaCaT cells (2×10^5 cell/mL) were seeded in a 12-well plate and grown until 80%–90% confluence. Different

concentrations of APR-ME were added in presence of TNF-α (50 ng/mL). Cells only stimulated with TNF- α were considered as positive control and untreated cells as the negative control. After 24 h of incubation, supernatants were collected and centrifuged (10,000× *g* for 15 min at 4 °C) and stored at −80 °C until use. Secreted levels of the pro-inflammatory cytokines IL-8 and IL-6 were measured using enzyme-linked immunosorbent assay (ELISA) sets (BD Biosciences, CA, USA), according to manufacturer's instructions. The results were expressed as pg/mL.

4.11. In Vivo Anti-Inflammatory Efficacy Studies: Arachidonic Acid (AA)-Induced Inflammation

4.11.1. Animals and Study Protocol

The study protocol was approved by the Animal Experimentation Ethics Committee of the University of Barcelona (CEEA/UB ref. 4/16 and Generalitat ref. 8756. Date: 28 January 2016). The experiment was performed to evaluate the efficacy of APR-ME for the treatment of skin inflammation using BALB/c mice (4–5 months old) (n = 12) divided into four cages according to experimental groups (n = 3) in a temperature and humidity-controlled room with food and water *ad libitum*. These groups included: negative control (untreated healthy animals), positive control (treatment only with AA), APR-ME group (treatment with APR-ME after inducing inflammation), Blank-ME group (treatment with the vehicle after inducing inflammation) and ibuprofen group (treatment with ibuprofen gel 50 mg/g; reference: 886192.7 after inducing inflammation). Inflammation was induced in the mice corresponding to the following groups: APR-ME, Blank-ME, Ibuprofen, and positive control, by direct application of 60 µL of AA dissolved in PBS (5 mg/mL). After 20 min, biomechanical properties were analyzed and APR-ME, Blank-ME, or ibuprofen gel was topically applied over the inflamed area. The trial concluded 20 min later with biomechanical properties, evaluation, and sacrifice by cervical dislocation of the animals. Additionally, a negative control group (healthy mice) without any treatment was used to compare the results. Extraction of the biopsy samples from mice ears was performed for histological examination and analysis of gene expression of pro-inflammatory cytokines by quantitative reverse transcription polymerase chain reaction (RT-qPCR). The thickness of the mice ear of each group was measured using a Digital Thickness Gauge of 0–10 mm (Mitutoyo, Japan).

4.11.2. Biomechanical Skin Properties Evaluation

Stratum corneum hydration (SCH) was measured in basal state as well as after inducing inflammation with AA, and after treatment with APR-ME, Blank-ME, or ibuprofen gel, using a Corneometer CM-825 (Courage & Khazaka Electronics GmbH, Germany).

4.11.3. Histological Analysis

The ear biopsies carefully extracted from mice were stored for 24 h in 4% formaldehyde at room temperature, suspended in PBS for 3 h (replacing it with fresh medium in time intervals of 1 h) and stored in 96% ethanol. Afterwards, the samples were embedded in paraffin blocks, cut into 6 µm sections and stained with hematoxylin and eosin. Finally, the samples were observed under a microscope to assess the structure of the skin and possible inflammatory responses using Olympus BX41 microscope equipped with Olympus XC50 camera.

4.11.4. Pro-Inflammatory Cytokines Study

Total RNA was isolated from ear samples using the TRIZol® method (Thermo Fisher Scientific, Waltham, MA, USA). To do so, small fragments of tissue were homogenized using 1 mL of cold TRIZol reagent and under the Polytron homogenizer for 3 min, as manufacturer instructions specified. RNA concentration and quality were tested using the NanoDropTM 2000/2000c spectrophotometer (Thermo Fisher Scientific, Waltham, MA, USA).

Total RNA (1 μg) was reverse transcribed into cDNA using the Revert Aid First Strand cDNA synthesis kit (Thermo Fisher Scientific, Waltham, MA). Subsequently, qPCR was performed using StepOnePlus Real-Time PCR (Applied Biosystem, Foster City, CA, USA) and the primers for IL8, IL-17A and TNFα (Table 3). GAPDH was used as maintenance, and the conditions of the PCR cycles included: 5 min at 94 °C for denaturation, 30 cycles of amplification at 72 °C for 2 min, 1 min at 94 °C, 1 min at 60 °C and a final cycle at 72 °C for 10 min for the final extension. Finally, the relative gene expression of each gene was normalized with housekeeping GAPDH, and the formula $2^{-\Delta\Delta Ct}$ was used to calculate the changes.

Table 3. Primer sequences used for real-time PCR in *Mus musculus* BALB/c.

Gene	Primer Sequence (5′ to 3′)	Gene Accession Number
GAPDH	FW: AGCTTGTCATCAACGGGAAG RV: TTTGATGTTAGTGGGGTCTCG	BC023196.2
IL-8	FW: GCTGTGACCCTCTCTGTGAAG RV: CAAACTCCATCTTGTTGTGTC	X53798.1
IL-17A	FW: TTTTCAGCAAGGAATGTGGA RV: TTCATTGTGGAGGGCAGAC	NM_010552.3
TNFα	FW: AACTAGTGGTGCCAGCCGAT RV: CTTCACAGAGCAATGACTCC	NM_013693.3

GAPDH = Glyceraldehyde–3–Phosphate Dehydrogenase; IL–8 = Interleukin–8; IL–17A = Interleukin–17A; TNFα = Tumor necrosis factor alpha; FW = forward primer; RV = reverse primer.

4.12. In Vivo Tolerance Study in Humans

A tolerance study was carried out in 12 volunteers (6 men and 6 women) with healthy skin between 20 and 30 years old with prior written informed consent. This study was approved by the Ethics Committee of the University of Barcelona (IRB00003099) in accordance with the recommendations of the Declaration of Helsinki. TEWL and SCH were measured on the ventral forearm area at baseline and after topical application of APR-ME at predetermined time intervals of 5, 30, 60 and 90 min. The readings were recorded using a Tewameter® TM300 and Corneometer® 825 (Courage & Khazaka Electronics GmbH, Cologne, Germany) for TEWL and SCH, respectively.

To measure TEWL, the probe was pressed and held on the skin for 2 min and the results are expressed as g/cm^2/h. For the SCH value, the probe was pressed onto the skin to measure the dielectric constant of the skin in which measurements were given in arbitrary units (AU). TEWL and SCH results were recorded as the mean ± SD (n = 12).

4.13. Statistical Analysis

Statistical analysis was performed with GraphPad Prism, v5.0 software (GraphPad Software Inc., San Diego, CA, USA). The results are presented as the mean ± SD (n = 3). The experimental data obtained was analyzed using a one-way ANOVA followed by Tukey's test to compare the mean values. A value of p less than 0.05 was established to consider statistically significant differences.

5. Conclusions

The results of this study support the topical use of APR-ME as an appealing therapeutic strategy in the treatment of local skin inflammation. This homogeneous and transparent formulation exhibited a Newtonian behavior, thus allowing easy administration via spray or roll-on. Moreover, high tolerability of APR-ME in healthy volunteers was exhibited due to its composition based on approved excipients for dermal formulations with high biocompatibility with the skin. APR-ME demonstrated its capacity to release the incorporated drug following a first-order kinetic model while also guaranteeing a local anti-inflammatory effect with reduced systemic adverse effects due to the high drug retention in the skin. This anti-inflammatory potential was evidenced by a reduction in the production in vitro of IL-6 and IL-8, a decrease in the infiltration of inflammatory cells, less damage to the stratum corneum and

a decrease in the expression of pro-inflammatory cytokines such as TNFα, IL -8 and IL-17 from the in vivo model.

Supplementary Materials: The following are available online at http://www.mdpi.com/1424-8247/13/12/484/s1, Figure S1: Linearity of the average of 3 calibrate curve; Figure S2: Apremilast chromatograms by HPLC; Figure S3: Rheogram of apremilast microemulsion (APR-ME) showing flow and viscosity curves at 25 °C; Figure S4: Transmission profiles of apremilast microemulsion after 1, 30, 60 and 90 days of production; Table S1: Standards of APR to analyze the linearity; Table S2: Precision inter-day; Table S3: Accuracy of the analytical method; Table S4: Robustness of the analytical method; and Table S5: Limit of detection (LOD) and limit of quantification (LOQ) of the analytical method.

Author Contributions: P.S.-G. carried out all the experiments, analyzed the data/results, and wrote the manuscript; M.S.-A. carried out the analytical method and analyzed the data/results; L.H. carried out the rheological studies; M.-J.F., J.B. and N.D.-G. realized the biochemical, viability and in vitro anti-inflammatory efficacy studies; M.J.R.-L. carried out the histological studies; A.C.C. developed the biopharmaceutical studies and analyzed the data/results; and L.C.E. developed the protocol for the entire study, analyzed the data/results obtained and ensured that the goals of the study were met. All authors have read and agreed to the published version of the manuscript.

Funding: This research received no external funding.

Acknowledgments: P.S.-G. appreciates the collaboration of Antonio Boix Montañes for aiding in processing approval of the protocol used in tolerance studies. L.C.E. acknowledges the support of the Universidad Técnica Particular de Loja and the Secretaría de Educación Superior, Ciencia, Tecnología e Innovación (SENESCYT—Ecuador). M.S.-A. also acknowledges the support received from the Coordination for the Improvement of Higher Education Personnel (CAPES), Brazil. The authors would like to express their gratitude to Gattefossé for its provision of pharmaceutical excipients. Finally, the authors also acknowledge Jonathan Proctor (M.Ed) for his review of the use of the English language.

Conflicts of Interest: The authors declare no conflict of interest.

References

1. Chen, L.; Deng, H.; Cui, H.; Fang, J.; Zuo, Z.; Deng, J.; Li, Y.; Wang, X.; Zhao, L. Inflammatory responses and inflammation-associated diseases in organs. *Oncotarget* **2018**, *9*, 7204–7218. [CrossRef] [PubMed]
2. Medzhitov, R. Inflammation 2010: New adventures of an old flame. *Cell* **2010**, *140*, 771–776. [CrossRef] [PubMed]
3. Dainichi, T.; Hanakawa, S.; Kabashima, K. Classification of inflammatory skin diseases: A proposal based on the disorders of the three-layered defense systems, barrier, innate immunity and acquired immunity. *J. Dermatol. Sci.* **2014**, *76*, 81–89. [CrossRef] [PubMed]
4. Mease, P.J. Apremilast: A phosphodiesterase 4 inhibitor for the treatment of psoriatic arthritis. *Rheumatol. Ther.* **2014**, *1*, 1–20. [CrossRef]
5. Raker, V.K.; Becker, C.; Steinbrink, K. The cAMP pathway as therapeutic target in autoimmune and inflammatory diseases. *Front. Immunol.* **2016**, *7*. [CrossRef]
6. Abdulrahim, H.; Thistleton, S.; Adebajo, A.O.; Shaw, T.; Edwards, C.; Wells, A. Apremilast: A PDE4 inhibitor for the treatment of psoriatic arthritis. *Expert Opin. Pharmacother.* **2015**, *16*, 1099–1108. [CrossRef]
7. Zerilli, T.; Ocheretyaner, E. Apremilast (otezla): A new oral treatment for adults with psoriasis and psoriatic arthritis. *Drug Forecast* **2015**, *40*, 495–500.
8. Man, H.-W.; Schafer, P.; Wong, L.M.; Patterson, R.T.; Corral, L.G.; Raymon, H.; Blease, K.; Leisten, J.; Shirley, M.A.; Tang, Y.; et al. Discovery of (S)-*N*-{2-[1-(3-ethoxy-4-methoxyphenyl)-2-methanesulfonylethyl]-1,3-dioxo2,3-dihydro-1*H*-isoindol-4-yl} acetamide (Apremilast), a potent and orally active phosphodiesterase 4 and tumor necrosis factor-α inhibitor. *J. Med. Chem.* **2009**, *52*, 1522–1524. [CrossRef]
9. Afra, T.P.; Razmi, T.M.; Dogra, S. Apremilast in psoriasis and beyond: Big hopes on a small molecule. *Indian Dermatol. Online J.* **2019**, *10*, 1–12. [CrossRef]
10. Butler, T.; Maravent, S.; Boisselle, J.; Valdes, J.; Fellner, C. A review of 2014 cancer drug approvals, with a look at 2015 and beyond. *P T* **2015**, *40*, 191–205.
11. Schafer, P. Apremilast mechanism of action and application to psoriasis and psoriatic arthritis. *Biochem. Pharmacol.* **2012**, *83*, 1583–1590. [CrossRef] [PubMed]
12. Kumar, N.; Goldminz, A.M.; Kim, N.; Gottlieb, A.B. Phosphodiesterase 4-targeted treatments for autoimmune diseases. *BMC Med.* **2013**, *11*, 96. [CrossRef] [PubMed]

13. Anwer, K.; Mohammad, M.; Ezzeldin, E.; Fatima, F.; Alalaiwe, A.; Iqbal, M. Preparation of sustained release apremilast-loaded PLGA nanoparticles: In vitro characterization and in vivo pharmacokinetic study in rats. *Int. J. Nanomed.* **2019**, *14*, 1587–1595. [CrossRef] [PubMed]
14. Muvva, A.; Lakshman, D.; Dwibhashyam, V.S.N.M.; Dengale, S.; Lewis, S.A. In vitro-in silico evaluation of Apremilast solid dispersions prepared via Corotating Twin Screw Extruder. *J. Drug Deliv. Sci. Tech.* **2020**, *59*, 101844. [CrossRef]
15. Madan, J.R.; Khobaragade, S.; Dua, K.; Awasthi, R. Formulation, optimization, and in vitro evaluation of nanostructured lipid carriers for topical delivery of Apremilast. *Dermatol. Ther.* **2020**. [CrossRef]
16. Parmar, P.K.; Bansal, A.K. Novel nanocrystal-based formulations of apremilast for improved topical delivery. *Drug Deliv. Transl. Res.* **2020**. [CrossRef]
17. Fala, L. Otezla (Apremilast), an oral PDE-4 Inhibitor, receives FDA approval for the treatment of patients with active psoriatic arthritis and plaque psoriasis. *Am. Health Drug Benefits* **2015**, *8*, 105–110.
18. Pireddu, R.; Caddeo, C.; Valenti, D.; Marongiu, F.; Scano, A.; Ennas, G.; Lai, F.; Fadda, A.M.; Sinico, C. Diclofenac acid nanocrystals as an effective strategy to reduce in vivo skin inflammation by improving dermal drug bioavailability. *Colloids Surf. B* **2016**, *143*, 64–70. [CrossRef]
19. Brown, M.B.; Martin, G.P.; Jones, S.A.; Akomeah, F.K. Dermal and transdermal drug delivery systems: Current and future prospects. *Drug Deliv.* **2006**, *13*, 175–187. [CrossRef]
20. Hafeez, F.; Chiang, A.; Hui, X.; Zhu, H.; Kamili, F.; Maibach, H.I. Stratum corneum reservoir as a predictive method for in vitro percutaneous absorption: SC reservoir to predict in vitro percutaneous absorption. *J. Appl. Toxicol.* **2016**, *36*, 1003–1010. [CrossRef]
21. Marwah, H.; Garg, T.; Goyal, A.K.; Rath, G. Permeation enhancer strategies in transdermal drug delivery. *Drug Deliv.* **2016**, *23*, 564–578. [CrossRef] [PubMed]
22. Lee, H.; Song, C.; Baik, S.; Kim, D.; Hyeon, T.; Kim, D.-H. Device-assisted transdermal drug delivery. *Adv. Drug Deliv. Rev.* **2018**, *127*, 35–45. [CrossRef] [PubMed]
23. European Medicines Agency. *Assessment Report: Otezla*; EMA: England, UK, 2014; pp. 1–189.
24. Nastiti, C.; Ponto, T.; Abd, E.; Grice, J.; Benson, H.; Roberts, M. Topical Nano and Microemulsions for Skin Delivery. *Pharmaceutics* **2017**, *9*, 37. [CrossRef] [PubMed]
25. Benigni, M.; Pescina, S.; Grimaudo, M.A.; Padula, C.; Santi, P.; Nicoli, S. Development of microemulsions of suitable viscosity for cyclosporine skin delivery. *Int. J. Pharm.* **2018**, *545*, 197–205. [CrossRef] [PubMed]
26. Rahdar, A.; Hajinezhad, M.R.; Nasri, S.; Beyzaei, H.; Barani, M.; Trant, J.F. The synthesis of methotrexate-loaded F127 microemulsions and their in vivo toxicity in a rat model. *J. Mol. Liq.* **2020**, *313*, 113449. [CrossRef]
27. Savić, V.; Todosijević, M.; Ilić, T.; Lukić, M.; Mitsou, E.; Papadimitriou, V.; Avramiotis, S.; Marković, B.; Cekić, N.; Savić, S. Tacrolimus loaded biocompatible lecithin-based microemulsions with improved skin penetration: Structure characterization and in vitro/in vivo performances. *Int. J. Pharm.* **2017**, *529*, 491–505. [CrossRef]
28. Shewaiter, M.A.; Hammady, T.M.; El-Gindy, A.; Hammadi, S.H.; Gad, S. Formulation and characterization of leflunomide/diclofenac sodium microemulsion base-gel for the transdermal treatment of inflammatory joint diseases. *J. Drug Deliv. Sci. Tech.* **2020**, 102110. [CrossRef]
29. Mu, H.; Holm, R.; Müllertz, A. Lipid-based formulations for oral administration of poorly water-soluble drugs. *Int. J. Pharm.* **2013**, *453*, 215–224. [CrossRef]
30. Godin, B.; Touitou, E. Dermal and Transdermal Delivery. In *Encyclopedia of Nanotechnology*; Bhushan, B., Ed.; Springer: Dordrecht, The Netherlands, 2012; pp. 517–526.
31. Yuan, Y.; Gao, Y.; Zhao, J.; Mao, L. Characterization and stability evaluation of β-carotene nanoemulsions prepared by high pressure homogenization under various emulsifying conditions. *Food Res. Int.* **2008**, *41*, 61–68. [CrossRef]
32. Espitia, P.J.P.; Fuenmayor, C.A.; Otoni, C.G. Nanoemulsions: Synthesis, Characterization, and Application in Bio-Based Active Food Packaging. *Compr. Rev. Food Sci. Food Saf.* **2019**, *18*, 264–285. [CrossRef]
33. Karimkhani Aksut, C.; Dellavalle, R.P.; Naghavi, M. 181 Global skin disease morbidity and mortality: An update from the Global Burden of Disease Study 2013. *J. Invest Dermatol.* **2017**, *137*, S31. [CrossRef]
34. Seth, D.; Cheldize, K.; Brown, D.; Freeman, E.E. Global Burden of Skin Disease: Inequities and Innovations. *Curr. Derm. Rep.* **2017**, *6*, 204–210. [CrossRef] [PubMed]

35. Zhang, X.; Wang, A.; Shi, T.; Zhang, J.; Xu, H.; Wang, D.; Feng, L. The psychosocial adaptation of patients with skin disease: A scoping review. *BMC Public Health* **2019**, *19*, 1404. [CrossRef] [PubMed]
36. Zamora, N.V.; Valerio-Morales, I.-A.; Lopez-Olivo, M.A.; Pan, X.; Suarez-Almazor, M.E. Phosphodiesterase 4 inhibitors for psoriatic arthritis. *Cochrane Database Syst. Rev.* **2016**. [CrossRef]
37. Lopalco, G.; Venerito, V.; Leccese, P.; Emmi, G.; Cantarini, L.; Lascaro, N.; Di Scala, G.; Fabiani, C.; Rigante, D.; Iannone, F. Real-world effectiveness of apremilast in multirefractory mucosal involvement of Behçet's disease. *Ann. Rheum. Dis.* **2019**, *78*, 1736–1737. [CrossRef]
38. European Medicines Agency ICH Q2 (R1) Validation of Analytical Procedures: Text and Methodology. Available online: https://www.ema.europa.eu/en/ich-q2-r1-validation-analytical-procedures-text-methodology (accessed on 15 July 2020).
39. Kulkarni, P.; Deshpande, A. Analytical methods for determination of apremilast from bulk, dosage form and biological fluids: A critical review. *Crit. Rev. Anal. Chem.* **2020**, 1–10. [CrossRef]
40. Wadhwa, J.; Nair, A.; Kumria, R. Self-emulsifying therapeutic system: A potential approach for delivery of lipophilic drugs. *Braz. J. Pharm. Sci.* **2011**, *47*, 447–465. [CrossRef]
41. Abbasi, S.; Amiri-Rigi, A. Microemulsions as nano-carriers for nutraceuticals: Current trends and the future outlook. *EC Nutr.* **2017**, *12*, 46–50.
42. Fernández-Campos, F.; Clares Naveros, B.; López Serrano, O.; Alonso Merino, C.; Calpena Campmany, A.C. Evaluation of novel nystatin nanoemulsion for skin candidosis infections: Nystatin nanoemulsion for skin candidosis. *Mycoses* **2013**, *56*, 70–81. [CrossRef] [PubMed]
43. Espinoza, L.C.; Silva-Abreu, M.; Calpena, A.C.; Rodríguez-Lagunas, M.J.; Fábrega, M.-J.; Garduño-Ramírez, M.L.; Clares, B. Nanoemulsion strategy of pioglitazone for the treatment of skin inflammatory diseases. *Nanomed. Nanotechnol. Biol. Med.* **2019**, *19*, 115–125. [CrossRef]
44. Gué, E.; Since, M.; Ropars, S.; Herbinet, R.; Le Pluart, L.; Malzert-Fréon, A. Evaluation of the versatile character of a nanoemulsion formulation. *Int. J. Pharm.* **2016**, *498*, 49–65. [CrossRef] [PubMed]
45. Elmataeeshy, M.E.; Sokar, M.S.; Bahey-El-Din, M.; Shaker, D.S. Enhanced transdermal permeability of Terbinafine through novel nanoemulgel formulation; Development, in vitro and in vivo characterization. *Future J. Pharm. Sci.* **2018**, *4*, 18–28. [CrossRef]
46. Szumała, P. Structure of microemulsion formulated with monoacylglycerols in the presence of polyols and ethanol. *J. Surfactants Deterg.* **2015**, *18*, 97–106. [CrossRef] [PubMed]
47. Ciurlizza, C.; Fernández, F.; Calpena, A.C.; Lázaro, R.; Parra, A.; Clares, B. Semisolid formulations containing cetirizine: Human skin permeation and topical antihistaminic evaluation in a rabbit model. *Arch. Dermatol. Res.* **2014**, *306*, 711–717. [CrossRef] [PubMed]
48. Ali, M.S.; Alam, M.S.; Alam, N.; Siddiqui, M.R. Preparation, characterization and stability study of dutasteride loaded nanoemulsion for treatment of benign prostatic hypertrophy. *Iran J. Pharm. Res.* **2014**, *13*, 1125–1140.
49. Zhang, Z.; McClements, D.J. Overview of Nanoemulsion Properties: Stability, Rheology, and Appearance. In *Nanoemulsions*; Elsevier: Amsterdam, The Netherlands, 2018; pp. 21–49.
50. Mehrnia, M.-A.; Jafari, S.-M.; Makhmal-Zadeh, B.S.; Maghsoudlou, Y. Rheological and release properties of double nano-emulsions containing crocin prepared with Angum gum, Arabic gum and whey protein. *Food Hydrocoll.* **2017**, *66*, 259–267. [CrossRef]
51. Salamanca, C.; Barrera-Ocampo, A.; Lasso, J.; Camacho, N.; Yarce, C. Franz diffusion cell approach for pre-formulation characterisation of ketoprofen semi-solid dosage forms. *Pharmaceutics* **2018**, *10*, 148. [CrossRef]
52. Dahan, A.; Miller, J.M. The solubility–permeability interplay and its implications in formulation design and development for poorly soluble drugs. *AAPS J.* **2012**, *14*, 244–251. [CrossRef]
53. Mallandrich, M.; Fernández-Campos, F.; Clares, B.; Halbaut, L.; Alonso, C.; Coderch, L.; Garduño-Ramírez, M.L.; Andrade, B.; del Pozo, A.; Lane, M.E.; et al. Developing transdermal applications of ketorolac tromethamine entrapped in stimuli sensitive block copolymer hydrogels. *Pharm. Res.* **2017**, *34*, 1728–1740. [CrossRef]
54. Lai, J.; Maibach, H.I. Experimental models in predicting topical antifungal efficacy: Practical aspects and challenges. *Skin Pharmacol. Physiol.* **2009**, *22*, 231–239. [CrossRef]
55. Abd, E.; Yousef, S.A.; Pastore, M.N.; Telaprolu, K.; Mohammed, Y.H.; Namjoshi, S.; Grice, J.E.; Roberts, M.S. Skin models for the testing of transdermal drugs. *Clin. Pharmacol.* **2016**, *8*, 163–176. [CrossRef] [PubMed]

56. Schafer, P.H.; Chen, P.; Fang, L.; Wang, A.; Chopra, R. The pharmacodynamic impact of apremilast, an oral phosphodiesterase 4 inhibitor, on circulating levels of inflammatory biomarkers in patients with psoriatic arthritis: Substudy results from a phase III, randomized, placebo-controlled trial (PALACE 1). *J. Immunol. Res.* **2015**, 906349. [CrossRef] [PubMed]
57. Messamore, E.; Yao, J.K. Phospholipid, arachidonate and eicosanoid signaling in schizophrenia. *Oilseeds Fats Crops Lipids* **2016**, *23*, D112. [CrossRef]
58. Kiezel-Tsugunova, M.; Kendall, A.C.; Nicolaou, A. Fatty acids and related lipid mediators in the regulation of cutaneous inflammation. *Biochem. Soc. Trans.* **2018**, *46*, 119–129. [CrossRef] [PubMed]
59. Hwang, P.-A.; Hung, Y.-L.; Chien, S.-Y. Inhibitory activity of Sargassum hemiphyllum sulfated polysaccharide in arachidonic acid-induced animal models of inflammation. *J. Food Drug Anal.* **2015**, *23*, 49–56. [CrossRef] [PubMed]
60. Kawahara, K.; Hohjoh, H.; Inazumi, T.; Tsuchiya, S.; Sugimoto, Y. Prostaglandin E2-induced inflammation: Relevance of prostaglandin E receptors. *Biochim. Biophys. Acta Mol. Cell. Biol. Lipids* **2015**, *1851*, 414–421. [CrossRef]
61. Veras, H.N.H.; Araruna, M.K.A.; Costa, J.G.M.; Coutinho, H.D.M.; Kerntopf, M.R.; Botelho, M.A.; Menezes, I.R.A. Topical antiinflammatory activity of essential oil of *Lippia sidoides* Cham: Possible Mechanism of Action. *Phytother. Res.* **2013**, *27*, 179–185. [CrossRef]
62. Toda, K.; Tsukayama, I.; Nagasaki, Y.; Konoike, Y.; Tamenobu, A.; Ganeko, N.; Ito, H.; Kawakami, Y.; Takahashi, Y.; Miki, Y.; et al. Red-kerneled rice proanthocyanidin inhibits arachidonate 5-lipoxygenase and decreases psoriasis-like skin inflammation. *Arch. Biochem.* **2020**, 108307. [CrossRef]
63. Pincelli, C.; Schafer, P.H.; French, L.E.; Augustin, M.; Krueger, J.G. Mechanisms underlying the clinical effects of apremilast for psoriasis. *J. Drugs Dermatol.* **2018**, *17*, 835–840.
64. Da Silva, B.A.F.; da Costa, R.H.S.; Fernandes, C.N.; Leite, L.H.I.; Ribeiro-Filho, J.; Garcia, T.R.; Coutinho, H.D.M.; Wanderley, A.G.; de Menezes, I.R.A. HPLC profile and antiedematogenic activity of Ximenia americana L. (Olacaceae) in mice models of skin inflammation. *Food Chem. Toxicol.* **2018**, *119*, 199–205. [CrossRef]
65. Tang, S.-C.; Liao, P.-Y.; Hung, S.-J.; Ge, J.-S.; Chen, S.-M.; Lai, J.-C.; Hsiao, Y.-P.; Yang, J.-H. Topical application of glycolic acid suppresses the UVB induced IL-6, IL-8, MCP-1 and COX-2 inflammation by modulating NF-κB signaling pathway in keratinocytes and mice skin. *J. Dermatol. Sci.* **2017**, *86*, 238–248. [CrossRef] [PubMed]
66. De Vry, C.G.; Valdez, M.; Lazarov, M.; Muhr, E.; Buelow, R.; Fong, T.; Iyer, S. Topical application of a novel immunomodulatory peptide, RDP58, reduces skin inflammation in the phorbol ester-induced dermatitis model. *J. Invest Dermatol.* **2005**, *125*, 473–481. [CrossRef] [PubMed]
67. Schüler, R.; Brand, A.; Klebow, S.; Wild, J.; Veras, F.P.; Ullmann, E.; Roohani, S.; Kolbinger, F.; Kossmann, S.; Wohn, C.; et al. Antagonization of IL-17A attenuates skin inflammation and vascular dysfunction in mouse models of psoriasis. *J. Invest Dermatol.* **2019**, *139*, 638–647. [CrossRef] [PubMed]
68. Go, H.-N.; Lee, S.-H.; Cho, H.-J.; Ahn, J.-R.; Kang, M.-J.; Lee, S.-Y.; Hong, S.-J. Effects of chloromethylisothiazolinone/methylisothiazolinone (CMIT/MIT) on Th2/Th17-related immune modulation in an atopic dermatitis mouse model. *Sci. Rep.* **2020**, *10*, 4099. [CrossRef]
69. Lubrano, E.; Scriffignano, S.; Perrotta, F.M. TNF-alpha inhibitors for the six treatment targets of psoriatic arthritis. *Expert Rev. Clin. Immunol.* **2019**, *15*, 1303–1312. [CrossRef]
70. Mootoo, A.; Stylianou, E.; Arias, M.A.; Reljic, R. TNF-α in tuberculosis: A cytokine with a split personality. *Inflamm. Allergy Drug Targets* **2009**, *8*, 53–62. [CrossRef]
71. Chu, W.-M. Tumor necrosis factor. *Cancer Lett.* **2013**, *328*, 222–225. [CrossRef]
72. Liu, Y.; Yang, G.; Zhang, J.; Xing, K.; Dai, L.; Cheng, L.; Liu, J.; Deng, J.; Shi, G.; Li, C.; et al. Anti-TNF-α monoclonal antibody reverses psoriasis through dual inhibition of inflammation and angiogenesis. *Int. Immunopharmacol.* **2015**, *28*, 731–743. [CrossRef]
73. Lin, Z.-M.; Ma, M.; Li, H.; Qi, Q.; Liu, Y.-T.; Yan, Y.-X.; Shen, Y.-F.; Yang, X.-Q.; Zhu, F.-H.; He, S.-J.; et al. Topical administration of reversible SAHH inhibitor ameliorates imiquimod-induced psoriasis-like skin lesions in mice via suppression of TNF-α/IFN-γ-induced inflammatory response in keratinocytes and T cell-derived IL-17. *Pharmacol. Res.* **2018**, *129*, 443–452. [CrossRef]

74. Bianchi, L.; Del Duca, E.; Romanelli, M.; Saraceno, R.; Chimenti, S.; Chiricozzi, A. Pharmacodynamic assessment of apremilast for the treatment of moderate-to-severe plaque psoriasis. *Expert Opin. Drug Metab. Toxicol.* **2016**, *12*, 1121–1128. [CrossRef]
75. Ozawa, M.; Terui, T.; Tagami, H. Localization of IL-8 and Complement Components in Lesional Skin of Psoriasis vulgaris and Pustulosis palmaris et plantaris. *Dermatology* **2005**, *211*, 249–255. [CrossRef] [PubMed]
76. Kondo, S.; Kono, T.; Sauder, D.N.; McKenzie, R.C. IL-8 gene expression and production in human keratinocytes and their modulation by UVB. *J. Invest. Dermatol.* **1993**, *101*, 690–694. [CrossRef] [PubMed]
77. Bernardini, N.; Skroza, N.; Tolino, E.; Mambrin, A.; Anzalone, A.; Balduzzi, V.; Colapietra, D.; Marchesiello, A.; Michelini, S.; Proietti, I.; et al. IL-17 and its role in inflammatory, autoimmune, and oncological skin diseases: State of art. *Int. J. Dermatol.* **2020**, *59*, 406–411. [CrossRef] [PubMed]
78. Beringer, A.; Noack, M.; Miossec, P. IL-17 in chronic inflammation: From discovery to targeting. *Trends Mol. Med.* **2016**, *22*, 230–241. [CrossRef] [PubMed]
79. Medvedeva, I.V.; Stokes, M.E.; Eisinger, D.; LaBrie, S.T.; Ai, J.; Trotter, M.W.B.; Schafer, P.; Yang, R. Large-scale analyses of disease biomarkers and apremilast pharmacodynamic effects. *Sci. Rep.* **2020**, *10*, 605. [CrossRef]
80. Thangamani, S.; Younis, W.; Seleem, M.N. Repurposing ebselen for treatment of multidrug-resistant staphylococcal infections. *Sci. Rep.* **2015**, *5*, 11596. [CrossRef]
81. López-García, J.; Lehocký, M.; Humpolíček, P.; Sáha, P. HaCaT keratinocytes response on antimicrobial atelocollagen substrates: Extent of cytotoxicity, cell viability and proliferation. *J. Funct. Biomater.* **2014**, *5*, 43–57. [CrossRef]
82. Souto, E.B.; Zielinska, A.; Souto, S.B.; Durazzo, A.; Lucarini, M.; Santini, A.; Silva, A.M.; Atanasov, A.G.; Marques, C.; Andrade, L.N.; et al. (+)-Limonene 1,2-epoxide-loaded slns: Evaluation of drug release, antioxidant activity, and cytotoxicity in an HaCaT cell line. *Int. J. Mol. Sci.* **2020**, *21*, 1449. [CrossRef]
83. Villanueva-Martínez, A.; Hernández-Rizo, L.; Ganem-Rondero, A. Evaluating two nanocarrier systems for the transdermal delivery of sodium alendronate. *Int. J. Pharm.* **2020**, *582*, 119312. [CrossRef]
84. Alalaiwe, A.; Lin, C.-F.; Hsiao, C.-Y.; Chen, E.-L.; Lin, C.-Y.; Lien, W.-C.; Fang, J.-Y. Development of flavanone and its derivatives as topical agents against psoriasis: The prediction of therapeutic efficiency through skin permeation evaluation and cell-based assay. *Int. J. Pharm.* **2020**, *581*, 119256. [CrossRef]
85. Duplan, H.; Nocera, T. Hydratation cutanée et produits hydratants. *Ann. Dermatol. Venereol.* **2018**, *145*, 376–384. [CrossRef] [PubMed]
86. Tomita, Y.; Akiyama, M.; Shimizu, H. Stratum corneum hydration and flexibility are useful parameters to indicate clinical severity of congenital ichthyosis. *Exp. Dermatol.* **2005**, *14*, 619–624. [CrossRef] [PubMed]
87. Schario, M.; Tomova-Simitchieva, T.; Lichterfeld, A.; Herfert, H.; Dobos, G.; Lahmann, N.; Blume-Peytavi, U.; Kottner, J. Effects of two different fabrics on skin barrier function under real pressure conditions. *J. Tissue Viability* **2017**, *26*, 150–155. [CrossRef] [PubMed]
88. Zhang, Q.; Murawsky, M.; LaCount, T.; Kasting, G.B.; Li, S.K. Transepidermal water loss and skin conductance as barrier integrity tests. *Toxicol. In Vitro* **2018**, *51*, 129–135. [CrossRef]
89. Jansen van Rensburg, S.; Franken, A.; Du Plessis, J.L. Measurement of transepidermal water loss, stratum corneum hydration and skin surface pH in occupational settings: A review. *Skin Res. Technol.* **2019**, *25*, 595–605. [CrossRef]
90. Fujimura, T.; Shimotoyodome, Y.; Nishijima, T.; Sugata, K.; Taguchi, H.; Moriwaki, S. Changes in hydration of the stratum corneum are the most suitable indicator to evaluate the irritation of surfactants on the skin. *Skin Res. Technol.* **2017**, *23*, 97–103. [CrossRef]
91. Alvarado, H.L.; Abrego, G.; Garduño-Ramirez, M.L.; Clares, B.; García, M.L.; Calpena, A.C. Development and validation of a high-performance liquid chromatography method for the quantification of ursolic/oleanic acids mixture isolated from Plumeria obtusa. *J. Chromatogr. B* **2015**, *983–984*, 111–116. [CrossRef]
92. Pineros, I.; Slowing, K.; Serrano, D.R.; de Pablo, E.; Ballesteros, M.P. Analgesic and anti-inflammatory controlled-released injectable microemulsion: Pseudo-ternary phase diagrams, in vitro, ex vivo and in vivo evaluation. *Eur. J. Pharm. Sci.* **2017**, *101*, 220–227. [CrossRef]
93. Feng, H.; Kang, W.; Wu, H.; Li, Z.; Chen, J.; Zhou, Q.; Bai, B. Study on the relationship between emulsion stability and droplet dynamics of a spontaneous emulsion for chemical enhanced oil recovery. *J. Disper. Sci. Technol.* **2018**, *39*, 1214–1222. [CrossRef]

94. Sandig, A.G.; Campmany, A.C.C.; Campos, F.F.; Villena, M.J.M.; Naveros, B.C. Transdermal delivery of imipramine and doxepin from newly oil-in-water nanoemulsions for an analgesic and anti-allodynic activity: Development, characterization and in vivo evaluation. *Colloids Surf. B* **2013**, *103*, 558–565. [CrossRef]

Supplementary Materials

Table S1. Standards of APR to analyze the linearity.

Concentration (μg/ml)	Area (μV*sec)			Average Area (μV*sec)
	R1	R2	R3	
1.25	144612	147653	150885	147717 ± 2561
2.5	281224	294306	300770	292100 ± 8131
5	578459	590112	604541	591037 ± 10668
10	1166899	1171264	1247082	1195081 ± 36813
25	2862244	2913060	3017704	2931003 ± 64722
50	5784489	5906320	6015409	5902072 ± 94321
100	11368977	11312239	12010818	11564011 ± 316788
200	23137955	23624478	24041635	23601356 ± 369288
r^2	0.9999	0.9996	1.000	

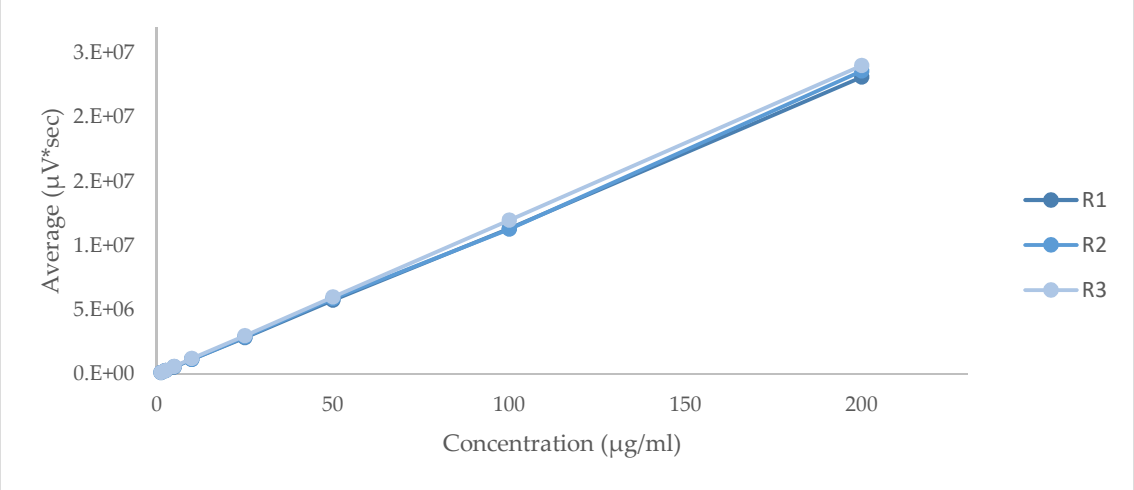

Figure S1. Linearity of the average of 3 calibrate curve. The test showed that deviation from linearity is not significant (p = 0.9068).

Table S2. Precision inter-day

Concentration (µg/ml)	Area (µV*sec)			Average (µV*sec)	SD	RSD%	Method Precision (%)
	Day 1	Day 2	Day 3				
1.25	144612	147653	150885	147717	3137	2.12	97.88
2.5	281224	294306	300770	292100	9958	3.41	96.59
5	578459	590112	604541	591037	13066	2.21	97.79
10	1166899	1171264	1247082	1195081	45086	3.77	96.23
25	2862244	2913060	3017704	2931003	79268	2.70	97.30
50	5784489	5906320	6015409	5902072	115519	1.96	98.04
100	11368977	11312239	12010818	11564011	387984	3.36	96.65
200	23137955	23624478	24041635	23601356	452284	1.92	98.08

SD = Deviation Standard; RSD = Relative Standard Deviation

Table S3. Accuracy of the analytical method.

Theoretical Concentration (µg/ml)	Real Concentration (µg/ml)			Average (µg/ml)	SD	Relative Error (%)	Method Accuracy (%)
	Day 1	Day 2	Day 3				
1.25	1.38	1.55	1.16	1.36	0.19	-8.36	108.36
2.5	2.56	2.80	2.41	2.59	0.19	-3.51	103.51
5	5.14	5.32	4.94	5.13	0.19	-2.57	102.57
10	10.24	10.27	10.29	10.26	0.02	-2.58	102.58
25	24.93	25.10	25.03	25.02	0.09	-0.08	100.08
50	50.25	50.59	49.98	50.28	0.31	-0.55	100.55
100	98.64	96.63	99.89	98.39	1.64	1.64	98.36
200	200.61	201.50	200.04	200.72	0.73	-0.36	100.36

SD = Deviation Standard; RE = Relative Error.

Table S4. Robustness of the analytical method: Variations of effect on the concentration *(v / v)* of the mobile phase.

Flux (ml/min)	Mobile Phase Concentration (v / v)	Average Retention Time (min)	SD
1	A: 60 B: 40	4.25	0.026
1	A: 70 B: 30	3.35	0.008
1	A: 80 B: 20	2.45	0.008

SD: Standard Deviation

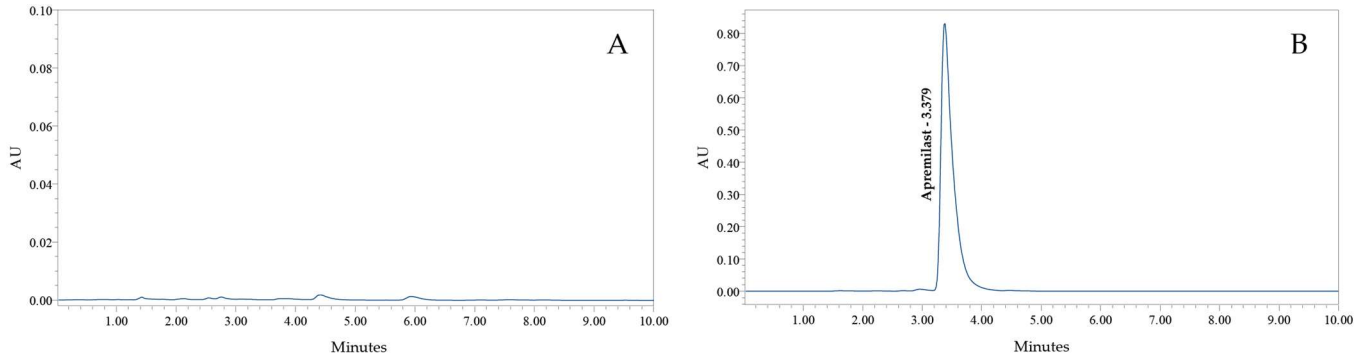

Peak Results								
Nº	Sample Name	Vial	Name	RT	Area (µV*sec)	Height	Amount	Unit
1	Blank control	3	Apremilast				Missing	mg/ml

Peak Results								
Nº	Sample Name	Vial	Name	RT	Area (µV*sec)	Height	Amount	Unit
11	100µg/ml_APR	18	Apremilast	3.379	11629185	830052	0.1023	mg/ml

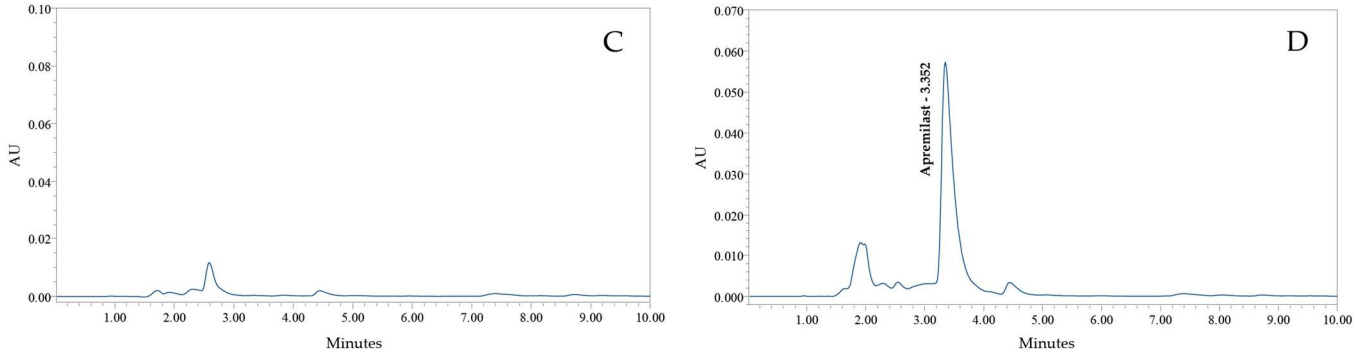

Peak Results								
Nº	Sample Name	Vial	Name	RT	Area (µV*sec)	Height	Amount	Unit
56	Blank skin	89	Apremilast				Missing	mg/ml

Peak Results								
Nº	Sample Name	Vial	Name	RT	Area (µV*sec)	Height	Amount	Unit
73	Qret_APR	25	Apremilast	3.352	773018	54764	0.0068	mg/ml

Figure S2. Apremilast chromatograms by HPLC. **(A)** Blank sample. **(B)** Apremilast Standard Sample 100 µg/mL. **(C)** Blank skin sample. **(D)** Apremilast extracted from human skin after the permeation study.

Table S5. Limit of detection (LOD) and limit of quantification (LOQ) of the analytical method.

	Average (µg/ml)	SD
LOD	1.13	1.04
LOQ	3.42	3.16

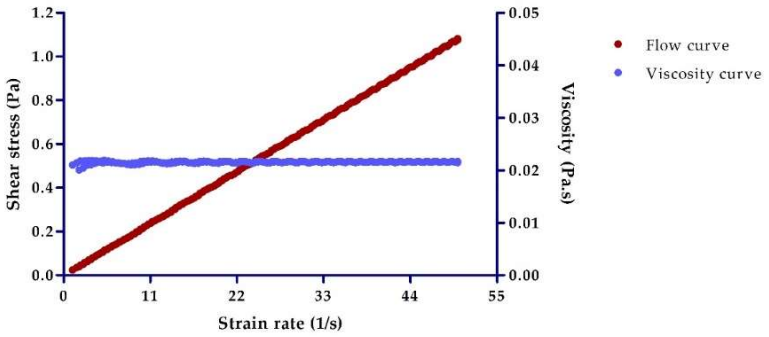

Figure S3. Rheogram of apremilast microemulsion (APR-ME) showing flow and viscosity curves at 25 °C.

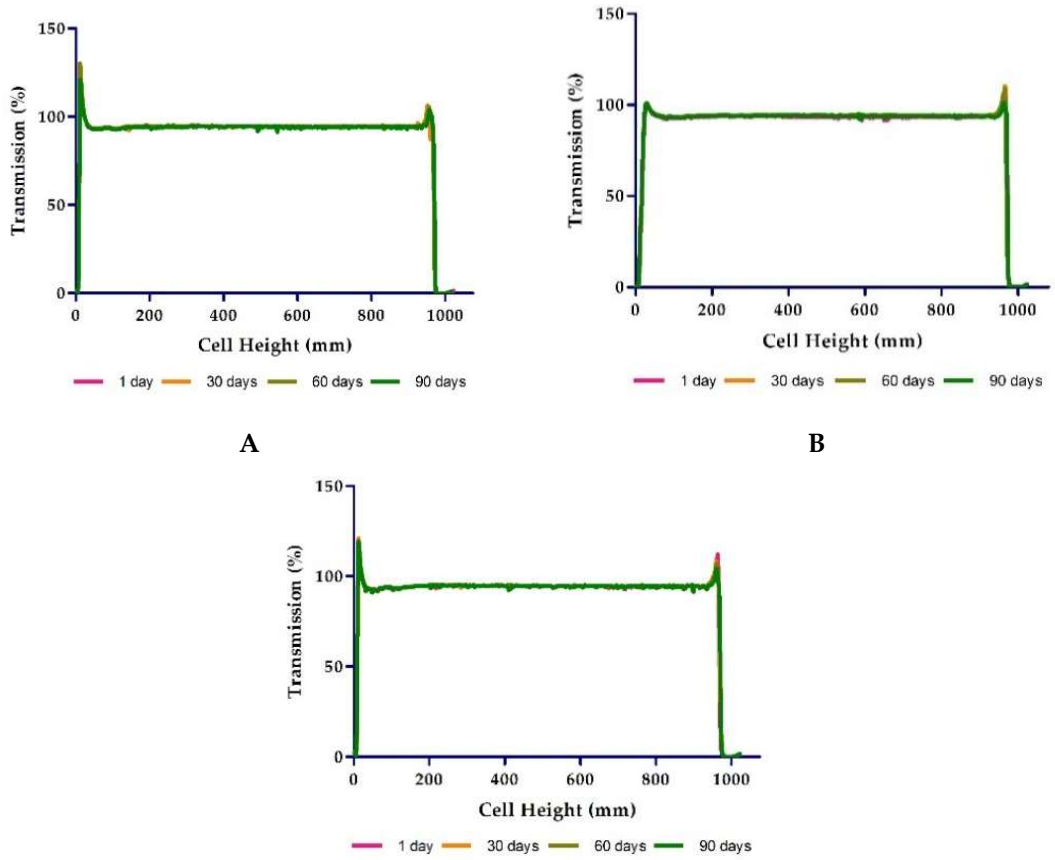

Figure S4. Transmission profiles of apremilast microemulsion after 1, 30, 60 and 90 days of production. **(A)** Storage 4 ± 1°C; **(B)** Storage 30 ± 2°C; and **(C)** Storage 40 ± 2°C.

3.2. Artículo 2

Journal	*Pharmaceutics*
Volume	*14*
Issue	*5*
Published date	7 May 2022
Section	*Physical Pharmacy and Formulation*
Special Issue	*New Formulation for Acute and Chronic Inflammatory Diseases*
ISSN:	1424-8247
Impact Factor:	5.863
DOI:	10.3390/pharmaceutics14051011

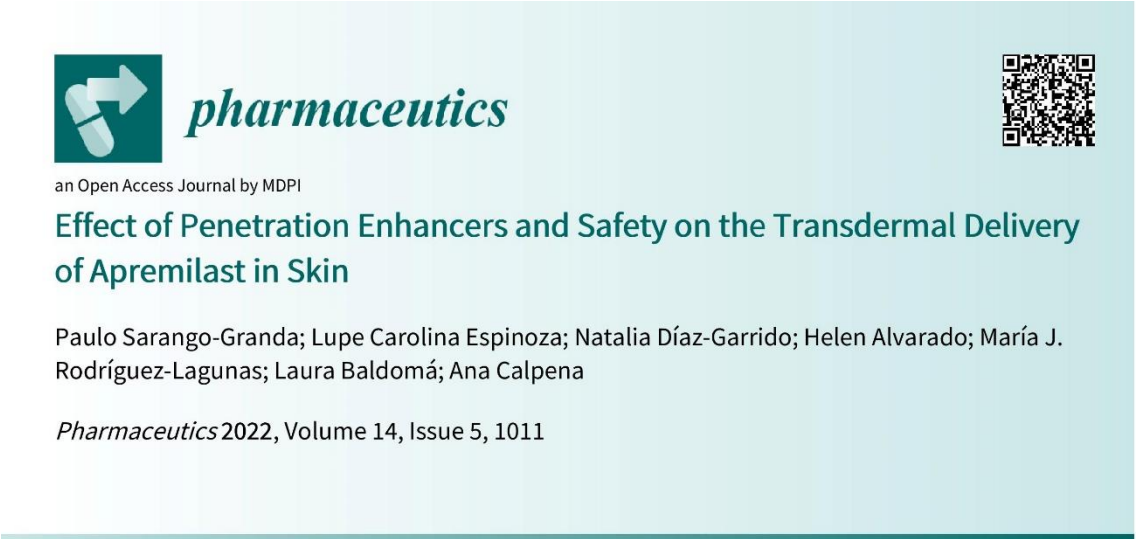

Afiliaciones:

[1] Department of Pharmacy, Pharmaceutical Technology and Physical Chemistry, Faculty of Pharmacy and Food Sciences, University of Barcelona, 08028 Barcelona, Spain.
[2] Institute of Nanoscience and Nanotechnology (IN2UB), University of Barcelona, 08028 Barcelona, Spain.
[3] Departamento de Química y Ciencias Exactas, Universidad Técnica Particular de Loja, Loja 1101608, Ecuador.
[4] Department of Biochemistry and Physiology, Faculty of Pharmacy and Food Sciences, University of Barcelona, 08028 Barcelona, Spain.
[5] Institute of Biomedicine of the University of Barcelona (IBUB), Sant Joan de Déu Research Institute, 08028 Barcelona, Spain.
[6] Nutrition and Food Safety Research Institute (INSA-UB), 08921 Santa Coloma de Gramenet, Spain.

pharmaceutics

MDPI

Article

Effect of Penetration Enhancers and Safety on the Transdermal Delivery of Apremilast in Skin

Paulo Sarango-Granda [1,2,3], Lupe Carolina Espinoza [2,3,*], Natalia Díaz-Garrido [4,5], Helen Alvarado [1], María J. Rodríguez-Lagunas [4,6], Laura Baldomá [4] and Ana Calpena [1,2]

1 Department of Pharmacy, Pharmaceutical Technology and Physical Chemistry, Faculty of Pharmacy and Food Sciences, University of Barcelona, 08028 Barcelona, Spain; paulogranda92@gmail.com (P.S.-G.); hl_alvarado@ub.edu (H.A.); anacalpena@ub.edu (A.C.)
2 Institute of Nanoscience and Nanotechnology (IN2UB), University of Barcelona, 08028 Barcelona, Spain
3 Departamento de Química, Universidad Técnica Particular de Loja, Loja 1101608, Ecuador
4 Department of Biochemistry and Physiology, Faculty of Pharmacy and Food Sciences, University of Barcelona, 08028 Barcelona, Spain; natalia.diaz.garrido@gmail.com (N.D.-G.); mjrodriguez@ub.edu (M.J.R.-L.); lbaldoma@ub.edu (L.B.)
5 Institute of Biomedicine of the University of Barcelona (IBUB), Sant Joan de Déu Research Institute, 08028 Barcelona, Spain
6 Nutrition and Food Safety Research Institute (INSA-UB), 08921 Santa Coloma de Gramenet, Spain
* Correspondence: lcespinoza@utpl.edu.ec; Tel.: +593-7-370-1-444

Abstract: The poor water solubility of apremilast (APR) is the main impediment to the penetration of the drug through the skin barrier. The objective of this study was to evaluate the permeability of APR in different solutions enriched with penetration promoters in ex vivo samples of human skin, and additionally assess its tolerance in vivo. To this end, APR solutions with 5% promoter were developed, and the drug's ability to penetrate human abdominal skin samples was evaluated; the coefficients of permeability, cumulated amounts permeated, and flow were some of the parameters evaluated; likewise, the in vitro and in vivo tolerance of the solutions was evaluated. The results obtained showed that the solutions containing squalene as a promoter improved the penetration of APR compared to the other promoters evaluated; in the same way, on an in vitro scale in HaCaT cells, the promoters were not toxic, finding a cell viability greater than 80% at the different dilutions evaluated. In the in vivo tests carried out with the solution that presented the best results (APR-Squalene solution), it was observed that it does not cause irritation or erythema on the skin after its colorimetric and histological evaluation of the dorsal region of rats after its application. Squalene becomes an excellent candidate to improve the permeability of the drug in the case of the development of a topical formulation; in addition, it was confirmed that this penetration enhancer is neither toxic nor irritating when in contact with the skin in in vivo tests.

Keywords: apremilast; squalene; skin; promoter

Citation: Sarango-Granda, P.; Espinoza, L.C.; Díaz-Garrido, N.; Alvarado, H.; Rodríguez-Lagunas, M.J.; Baldomá, L.; Calpena, A. Effect of Penetration Enhancers and Safety on the Transdermal Delivery of Apremilast in Skin. *Pharmaceutics* **2022**, *14*, 1011. https://doi.org/10.3390/pharmaceutics14051011

Academic Editors: Jianqing Gao and Bozena B. Michniak-Kohn

Received: 14 March 2022
Accepted: 27 April 2022
Published: 7 May 2022

1. Introduction

The transdermal drug administration consists of the application of a pharmaceutical product on the skin; the drug penetrates through the epidermis and the dermis and, in many cases, a dermal microcirculation can occur [1]. Transdermal administration provides a non-invasive alternative (unlike the parenteral route), minimizes the risk of toxic side effects, and avoids pre-systemic metabolism (oral route), improving bioavailability [2]. Pharmaceutical products, when administered to the skin, and upon contact and penetration through its layers, encounter dendritic cells (epidermis and dermis) that play a crucial role in immune responses [3]. There are some strategies to facilitate and enhance transdermal drug permeation including the use of penetration enhancers as well as laser and light devices in fractional mode [4].

The skin represents 16% of the total body mass (in an average person) and fulfills a protective barrier function. The skin allows the body to protect itself from the external environment and water loss [5,6]. The skin is divided into three sections, the epidermis, dermis, and hypodermis [7]. The possible routes of drug penetration through these layers of the skin are known as transepidermal and transappendageal routes [8]. The transepidermal route consists of the passage of the drug through the stratum corneum (a multicellular layer that is subdivided into several layers); this type of penetration can be intracellular (through corneocytes, keratinocytes, the transport of hydrophilic compounds prevails) or intercellular (transport of lipid compounds through intercellular spaces). The transappendegean route, on the other hand, consists of the passage of molecules through the hair follicles and sweat glands [9,10]

Penetration enhancers are substances that facilitate the transport of the drug through the skin; their properties include that they are mostly colorless and odorless substances, pharmacologically inert, specific in their mode of action, physically and chemically stable, non-toxic, non-irritating, non-allergenic, and have a reversible action [11]. Penetration enhancers act primarily on the stratum corneum and may influence drug diffusion through it or change partitioning in the stratum corneum; the most common penetration enhancers include fatty acids, alkanes, esters, terpenes, cyclodextrins, surfactants, and azone, among others [12,13].

Apremilast (APR) is a selective inhibitor of phosphodiesterase IV. The mechanism of action of this drug consists of modulating a series of proinflammatory and anti-inflammatory mediators (for example: TNFα, IL-23, IL-10, and IL-17), this modulation is achieved by increasing the levels of cyclic adenosine monophosphate (cAMP) intracellular [14]. APR is effective for the treatment of psoriasis, an autoimmune and chronic disease that is characterized by thick patches of inflamed, scaly skin due to an excessive proliferation of skin cells whose treatment is based on control of symptoms using phototherapy, and systemic and topical therapies with different drugs including corticosteroids, vitamin D3 analogues, methotrexate, acitretin, cyclosporine, and biological-targeted agents such as ustekinumab, secukinumab, and ixekizumab [15]. APR administration is currently approved, in the form of oral tablets of 10, 20, and 30 mg, manufactured and marketed by the Celgene Corporation under the trade name of Otezla, indicated for patients with psoriatic arthritis, and moderate to severe psoriasis, and patients with Behcet's syndrome [16,17]. The effectiveness of this drug is limited by its side effects such as diarrhea, nausea, depression, and weight loss [18]. For this reason, the development of alternative administration forms, such as topical formulations, are attractive for local anti-inflammatory therapy; some research has covered this field with the development of nanocarriers incorporated into gels in some cases to improve the administration and bioavailability of APR [19–23].

The poor water solubility of APR is the main impediment to the penetration of the drug through the skin barrier (stratum corneum). Therefore, the objective of this study is based on evaluating the permeability of APR contained in a solution with different penetration promoters in ex vivo samples of human skin, and at the same time to evaluate their tolerance in vivo.

2. Materials and Methods

2.1. Materials

APR (purity: 99.6%; MW: 460.5 g/mol) was acquired from Wuhan Senwayer Century Chemical (Wuhan, China). Gattefossé (Barcelona, Spain) supplied Transcutol® P [Diethylene glycol monoethyl ether]. The permeation promoters Azone® [1-dodecylazacycloheptan-2-one] was supplied by Durham Pharmaceuticals (Durham, UK). Carene [3-Carene], Decanol [1-Decanol], Limonene [(S)-4-Isopropenyl-1-methyl cyclohexene], Menthone [(2S,5R)-2-Isopropyl-5-methyl cyclohexanone], Nonane [*n*-Nonane], Pinene [(+)-α-Pinene], and Squalene [2,6,10,15,19,23-Hexamethyltetracosane] were purchased from Sigma Aldrich (Madrid, Spain). Reagents for histological procedures were purchased from Sigma and Thermo Fisher Scientific (Barcelona, Spain). Reagents for cellular assays, HaCaT cell lines,

and 3-[4,5-Dimethylthiazol-2-yl]-2,5- diphenyltetrazolium bromide (MTT) cell-proliferation assay were obtained from Gibco (Cacavelos, Portugal), Cell Line Services (Eppelheim, Germany), and Sigma (Barcelona, Spain), respectively. Ultrapure water was obtained from Water Millipore MilliQ purification system (Millipore Corporation, Burlington, VT, USA), and all the other chemical reagents used were analytical grade.

2.2. Validation of Analytical Method

An analytical method was validated by high performance liquid chromatography (HPLC) for the identification and quantification of APR. The HPLC system is detailed in previous studies [21].

A 200 µg/mL stock solution was prepared. Different calibration curves were prepared from the stock solution in two ranges and five concentrations of each. The injection volume for the low range was 50 µL and the high range was 20 µL:

Low range: 0.156, 0.313, 0.625, 1.25, 2.5 and 5 µg/mL.

High range: 5, 10, 20, 50, 75, and 100 µg/mL.

Data was collected and processed using Empower 3 software (Waters, Milford, CT, USA). Method validation was carried out in accordance with the International Conference on Harmonization (ICH) Q2A and ICH Q2B Guidelines [24]:

Linearity

The linearity of five calibration curves at two ranges, each with six concentration levels, was evaluated. The correlation coefficient (r^2) obtained after the least squares linear regression analysis of the calibration lines was evaluated; in addition, the linearity ratios were evaluated using a one-way analysis of variance (ANOVA) test comparing the concentration of the standards. In relation to the areas obtained from them, this statistical treatment was carried out using the Graph Pad Prism® 5.0 software.

Accuracy and Precision

Five calibration curves were performed on different days at two concentration levels: 0.156–5 µg/mL and 5–100 µg/mL. Accuracy was expressed as the percentage of relative error (%RE) (Equation (1)). Precision was defined as the relative standard deviation (*%RSD*) or correlation coefficient:

$$\%\mathrm{RE} = \frac{C_0 - C_n}{C_n} \quad (1)$$

where, C_0 is the observed concentration; C_n is the nominal concentration and %RE represents the mean percentage deviation (% relative error).

Specificity

The specificity of the method was evaluated by the absence of interference in the retention time of the analyte. Volumes of 20–50 µL were injected and the chromatographic profiles were analyzed at a wavelength of 230 nm. Five different samples were evaluated: (i) mobile phase blank, (ii) APR standard, (iii) skin blank as control, (iv) APR sample released through the skin, and (v) APR sample retained in skin.

Sensitivity

Sensitivity was measured by determining the limits of detection (LOD) and quantification (LOQ). The LOD and LOQ were measured as a function of the standard deviation of the response and the slope of the calibration curve. LOD and LOQ were calculated by:

$$\mathrm{LOD} = \left[\frac{(3.3\ s)}{p}\right] \quad (2)$$

$$\mathrm{LOD} = \left[\frac{(10\ s)}{p}\right] \quad (3)$$

where, s is the standard deviation of the Y-intercept, and p is the slope of the calibration curve.

2.3. Apremilast Solution Preparation

APR solution was prepared by dissolving APR in Transcutol® P: water (60:40 *v*/*v*) and the addition of 5% *v*/*v* penetration enhancer (Table 1). A solution with a concentration of 1.5 mg/mL was obtained.

Table 1. Permeation enhancer used in this study.

Molecular Formula	Molecular Mass	Permeation Enhancer Substance	CAS Register Number
$C_{18}H_{35}NO$	281.5 g/mol	Azone®	59227-89-3
$C_{10}H_{16}$	136.2 g/mol	Carene	13466-78-9
$C_{10}H_{16}$	136.24 g/mol	Limonene	5989-27-5
$C_{10}H_{18}O$	154.25 g/mol	Menthone	14073-97-3
C_9H_{20}	128.25 g/mol	Nonane	111-84-2
$C_{10}H_{16}$	136.23 g/mol	Alpha-Pinene	80-56-8
$C_{30}H_{62}$	422.8 g/mol	Squalene	111-01-3

2.4. Ex Vivo Skin Permeation Test

The permeation of the drug through the skin was determined using the Franz diffusion technique [25]. Franz diffusion cells (Hanson Research, Chatsworth, CA, USA; Crown Glass Company, New Jersey, NJ, USA), with a diffusion area of 0.64 cm^2 and receptor compartment of 6 mL, were used. Samples of abdominal human skin (Hospital de Barcelona, SCIAS, Barcelona, Spain) were used for this experiment in accordance with the Ethics Committee of the Hospital de Barcelona (17 January 2020). Human skin was dermatomized to 400 µm thickness with an Aesculap GA 630 dermatome (Aesculap, Tuttligen, Germany). The skin was equilibrated for 30 min and the integrity of the skin was evaluated based on its TEWL using Tewameter TM 300 (Courage & Khazaka Electronics GmbH, Cologne, Germany); those that met an acceptance criterion of TEWL less than 10 g m^{-2} h^{-1} were used [26]. The receptor medium consisted of Transcutol® P: Water (60:40 *v*/*v*) in order to maintain *sink* conditions [27]. The assay was carried out at controlled temperature of 32 ± 0.5 °C and magnetic stirring of 500 r.p.m. Aliquots of 500 µL (APR-solutions 1.5 mg/mL) were added to the donor compartment of each cell. APR solution without promoter was used as a control (No promotor). Then, 200 µL aliquots were removed from the receptor compartment and replaced by the same volume of medium at different time intervals including 0 (pre sample time point), 14, 17, 20, 23, and 24 h. The samples obtained were quantified by HPLC as described in Section 2.2. Table 2 details the experimental conditions of the ex vivo permeation test. All solutions were made with skin from the same donor in triplicate, in this way an attempt is made to reduce the interindividual variability of the response due to biological differences.

Table 2. Experimental conditions for Ex vivo skin permeation test.

Condition	Description
Receptor fluid:	Transcutol® P: Water (60:40 *v*/*v*)
Cell volume:	6 mL
Diffusion area:	0.64 cm^2
Membrane:	Human skin
Thickness:	400 µm
Replicates:	3 replicates
Temperature:	32 ± 0.5 °C
Stirring:	500 r.p.m.
Dose:	500 µL (1.5 mg/mL)
Sample volume:	200 µL
Sampling times:	0 (pre-sample time point), 14, 17, 20, 23 and 24 h

2.5. Biopharmaceutical Parameter Data Analysis

The amount of drug permeated were determined by HPLC (Section 2.2). The permeation parameter such as: flux [J_{ss} (μg/h^{-1}/cm^{-2})] (Equation (4)), permeability coefficients [K_p (cm^2/h^{-1})] (Equation (5)), and cumulative permeated amount at 24 h [*Cum AP 24 h* (μg)] in skin were calculated per unit area as a function of the graph determined by the time of the test. The slope of linear portion was determinated using linear least-squares regression model with GraphPad Prism® (GraphPad Software Inc. version 5.0, San Diego, CA, USA) Software.

$$J_{ss} = \frac{Q_t}{A \cdot t} \quad (4)$$

where, Q_t is the amount of drug that passed through the skin and was concentrated in the receptor compartment (μg); A is the area of the cell-cap for diffusion (cm^2); and t is the time of the assay (h).

$$K_p = \frac{J_{ss}}{C_0} \quad (5)$$

where, J_{ss} is the flux calculated at the steady test and C_0 is the initial concentration of drug administer in the donor compartment.

The theoretical plasma concentration in human steady-state [C_{ss} (ng/mL)] of the drug was used to predict the concentration of APR at the systemic level in a hypothetical surface of 25 cm^2, it was obtained by Equation (6):

$$C_{ss} = J_{ss} \cdot \frac{A}{Cl_p} \quad (6)$$

where, A is the hypothetical area of application and Cl_p is the plasmatic clearance. The hypothetical area of application was 25 cm^2. The plasmatic clearance value was 8.7 L/h [28].

2.6. Amount of Drug Retained in the Skin

The APR amount retained in the skin (Qret (μg/g skin/cm^2)) was extracted in 1 mL of ACN by ultrasound water-bath technique. The skin samples were cleaned with gauze soaked in 0.05% dodecyl sulfate solution and washed with distilled water. The extract obtained was filtered and taken for analysis (Section 2.2).

2.7. In Vitro Skin Tolerance Study

To evaluate the effect of the different promoters that make up each APR solution on cell viability, the MTT assay was used in immortalized keratinocytes cell line HaCaT.

The cells were grown in Dubelcco's Modified Eagle's Medium (DMEM) -high glu-cose containing 25 mM HEPES, 1% non-essential amino acids, 100 U/mL penicillin, 100 g/mL streptomycin, and 10% heat inactivated Fetal Bovine Serum (FBS). Briefly, HaCaT cells were adjusted at 2 × 10^5 cell/mL and seeded in 96-well plate and incubated by 48 h at 37 °C under 5% CO^2 atmosphere until its adhesion. The experiments were performed with 80–90% confluency. Cells were incubated at different dilutions of the APR-solutions, these dilutions were from 1/50 to 1/2000 for 24 h. Untreated control cells were processed in parallel for comparison. Then, HaCaT cells were washed with PBS, incubated with MTT (2.5 mg/mL) for 2 h at 37 °C and processed as described previously [21].

Absorbance was measured at 570 nm in a microplate photometer Varioskan TM LUX (Thermo Scientific, Waltham, MS, USA). The percentage of cell survival relative to untreated control cells was calculated using the following equation:

$$\%MTT = \frac{Absorbance\ of\ cells\ treated\ with\ compounds}{Absorbance\ of\ control\ cells\ without\ compounds} \cdot 100 \quad (7)$$

2.8. In Vivo Skin Tolerance Study

The skin irritation potential of apremilast squalene solution was determined by a skin irritation test in rats [29]. This test was carried out with the approval of the Ethics

Committee of the University of Barcelona and the Bellvitge Establishment, Barcelona, Spain (number 387/18, 26 November 2018).

Sprague Dawel rats (600–700 g) (n = 12) divided in three groups (n = 4) in a room with controlled temperature and humidity with food and water ad libitum, were used. The first group was treated with APR solution enriched with squalene (APR-Squalene solution), the second group was treated only with squalene solution without drug (Blank-Squalene solution), and the third group correspond to the positive control (Treatment with 0.8 mL of Xylol). The rats were shaved in the dorsal area 24 h before starting the test. Three areas were drawn in the dorsal region of the animal.

2.8.1. Biomechanical Skin Properties Evaluation

Stratum corneum hydration (SCH) was measured in the basal state and ten minutes after the application of APR-Squalene and Blank-Squalene solutions in the treated area using a CM-825 Corneometer (Courage & Khazaka Electronics GmbH, Köln, Germany).

2.8.2. Colorimetric Parameters

The possible changes at the skin level after the application of APR-Squalene solution and Blank-Squalene solution were evaluated through the color differences in the skin of the rat dorsal region with respect to the basal color, this assay was performed according to a study by Limon et al., 2017 [30] modified.

Skin color detection was performed on the dorsal area of the rats, using an MPA5 Multiprobe adapter with CL400 skin colorimeter probe from Courage + Khazaka electronic GmbH, Köln, Germany. The measuring probe on contact with the skin emitted a white LED light that homogeneously illuminated the area where it was applied; the light scattered on the skin is detected by the probe and expressed as light intensity: R, red; G, green; and B, white, on a numerical scale from 0 to 255 each.

A first measurement (basal value) was performed and then the addition of Xylol and APR-Squalene solution (or Blank-Squalene solution) was performed as indicated in Section 2.5.

The color determinations were performed 10 min after the application of the various solutions. The colors found were reproduced with the Microsoft Excel program from the RGB codes.

The treatment of the RGB color data obtained A (R_1, G_1, B_1) and B (R_2, G_2, B_2); the difference was obtained by calculating the linear distance in space between the two points and subsequently evaluating the distance; the following geometric equation was used for the linear distance:

$$\left|\vec{AB}\right| = \sqrt{(R_2 - R_1)^2 + (G_2 - G_1)^2 + (B_2 - B_1)^2} \quad (8)$$

From the results of the linear distance, the direction of the distance was determined through the determination of the general difference of the light intensity, using the following equation:

$$\Delta_{intensity} = (R_2 - R_1) + (G_2 - G_1) + (B_2 - B_1) \quad (9)$$

A negative result corresponds to a darker coloration, which is indicative of erythema and was assigned a value (+1), and a positive result corresponds to a lighter coloration, which indicates less erythema and was assigned a value (−1).

Finally, the difference between the two colors was obtained by multiplying the linear distance by the direction of the distance; the mean values obtained initially (basal) and those obtained after the induction of vasodilatation (application of xylol) were calculated and considered as 0% and 100%, respectively.

Consequently, the values obtained from the samples were calculated with respect to those obtained with 100% and in this way the sequence of the different stages of evolution of the erythema was traced.

2.8.3. Histological Analysis

Rat skin biopsies were stored in cassettes for 24 h in 4% formaldehyde, the cassettes were washed by immersion in PBS (3 washes at 1 h intervals) and stored in 96% ethanol.

The samples were fixed in paraffin; sections of 6-µm thickness were stained with hematoxylin and eosin.

The samples were observed through a suitable Olympus BX41 microscope with an Olympus XC50 camera.

3. Results

3.1. Validation of Analythical Method

The conditions such as linearity, accuracy, precision, specificity, and sensitivity show that the method is specific for the detection and quantification of APR.

Linearity was evaluated from five calibration curves at two concentration levels ranging from 0.156–5 µg/mL and 5–100 µg/mL. Tables 3 and 4 show the areas obtained from each standard concentration. The r2 values of each of the calibration lines were >0.999. The graphic representation of mean values are shown in Figure 1. The statistical analysis of variance (ANOVA) showed that there were no statistically significant differences between the response areas obtained ($p = 0.06$ for low range and $p = 0.39$ for high range.

Table 3. Standard APR curve and respective area response factor. Low range.

Concentration (µg/mL)	Ratio 1	Ratio 2	Ratio 3	Ratio 4	Ratio 5
0.156	252,307.69	269,166.67	249,397.44	256,782.05	242,217.95
0.313	260,434.50	262,038.34	256,102.24	249,444.09	259,776.36
0.625	264,326.40	258,344.00	253,980.80	256,646.40	260,494.40
1.25	265,984.00	263,853.60	257,673.60	260,917.60	266,177.60
2.5	268,948.00	266,495.20	261,592.80	261,648.80	264,435.20
5	254,123.20	265,660.60	263,674.80	260,534.60	264,838.60

Table 4. Standard APR curve and respective area response factor. High range.

Concentration (µg/mL)	Ratio 1	Ratio 2	Ratio 3	Ratio 4	Ratio 5
5	109,557.800	74,592.400	82,219.400	99,394.400	84,412.600
10	106,052.700	73,916.800	93,962.200	93,504.300	85,729.500
25	107,647.960	86,377.760	91,944.640	100,525.680	97,117.120
50	103,422.940	87,307.680	105,285.220	90,515.760	95,526.080
75	104,525.933	95,189.893	87,206.813	100,035.547	103,939.733
100	104,007.780	93,685.270	104,641.200	107,957.790	97,844.260

The accuracy and precision of the method were obtained through the analysis of samples with an APR standard concentration of 0.156–5 µg/mL and 5–100 µg/mL. The results are expressed as %RE and %RSD, for accuracy and precision, respectively. The data are reported in Tables 5 and 6. These results show good precision with 11.93% and 13.28 for low and high range, respectively. The accuracy of the method was 2.54% and −12.21% for low and high range, respectively, for lowest standard concentration.

The analytical method was considered specific because it demonstrated that there is no interference in the identification and retention time of APR (Figure 2). The retention time of APR was 3.3 min.

(**a**)

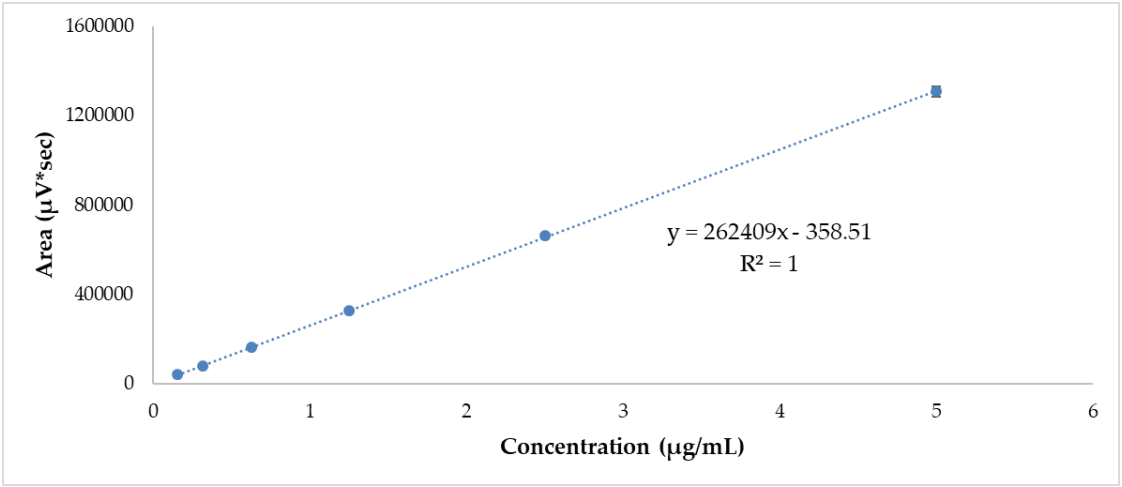

(**b**)

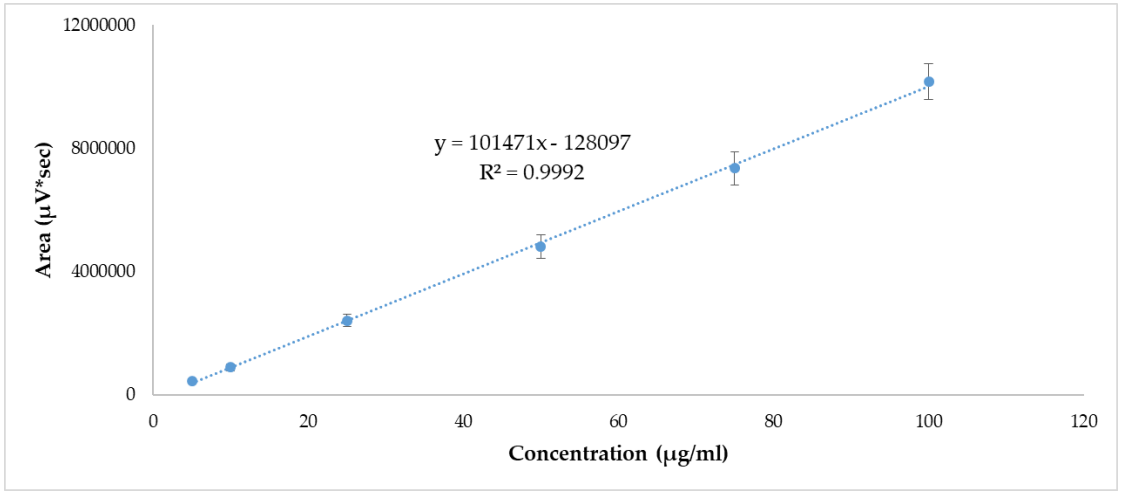

Figure 1. APR standard calibration curves. (**a**) Low range mean values, 0.156–5 µg/mL. (**b**) High range mean values, 5–100 µg/mL. Results are expressed as mean ± SD (*n* = 5).

Table 5. Accuracy and precision inter-day data for APR standard solutions. Low range.

Theoretical Conc. (µg/mL)	Calculated Conc. (µg/mL)	%RE	%RSD
0.156	0.15 ± 0.02	2.52	11.93
0.313	0.31 ± 0.01	1.49	4.38
0.625	0.62 ± 0.00	1.18	0.58
1.25	1.25 ± 0.01	−0.31	1.04
2.5	2.52 ± 0.05	−0.92	1.79
5	4.99 ± 0.02	0.22	0.47

Table 6. Accuracy and precision inter-day data for APR standard solutions. High range.

Theoretical Conc. (µg/mL)	Calculated Conc. (µg/mL)	%RE	%RSD
5	5.70 ± 0.76	−12.21	13.28
10	10.19 ± 0.60	−1.82	5.89
25	25.079 ± 0.66	−0.31	2.64
50	48.79 ± 3.17	2.47	6.50
75	73.86 ± 4.78	1.54	6.47
100	101.38 ± 2.90	−1.36	2.86

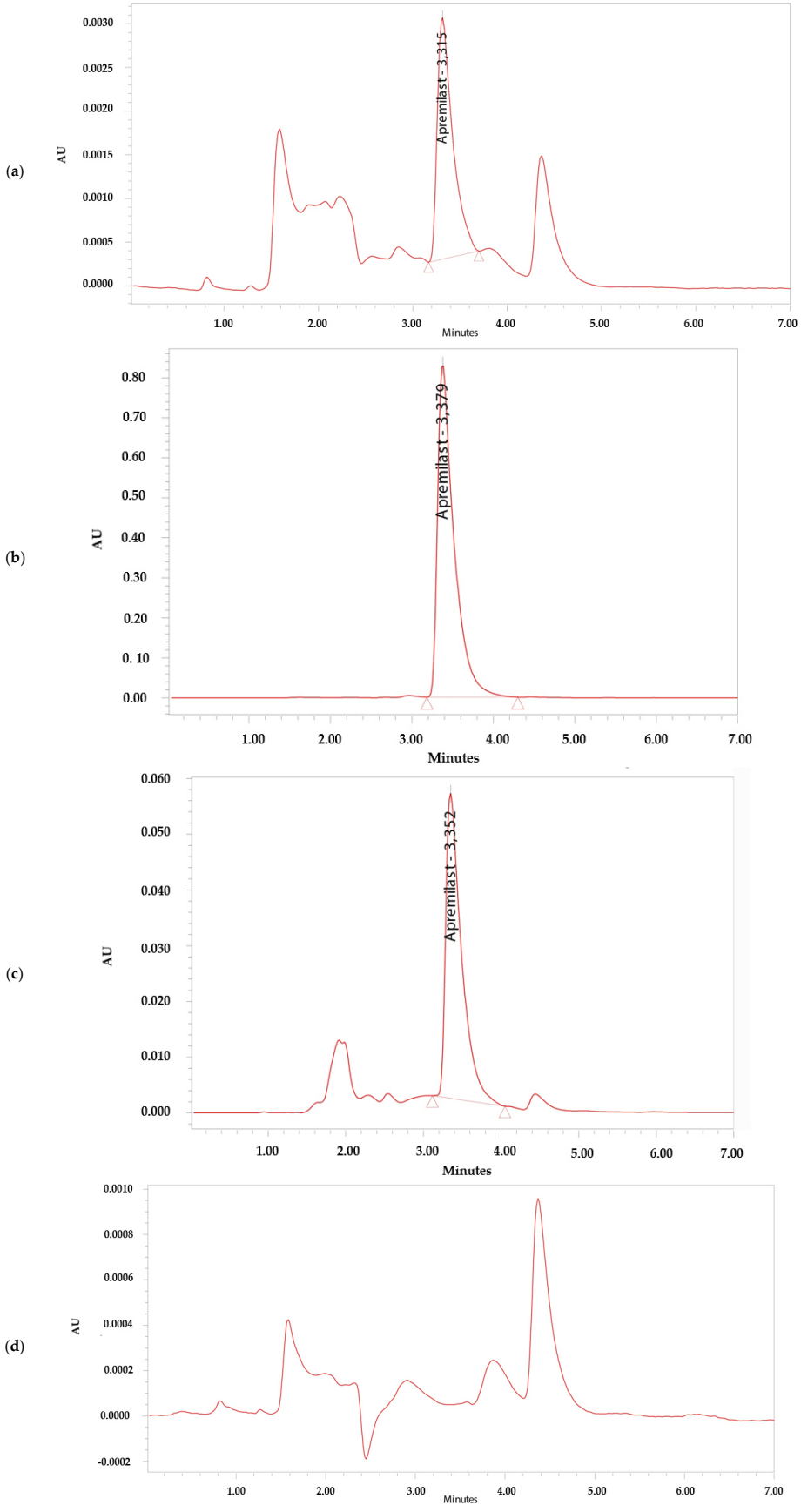

Figure 2. Chromatograms. (**a**) Apremilast standard 0.156 µg/mL. (**b**) Apremilast standard 100 µg/mL. (**c**) Apremilast extracted from human skin after the permeation study. (**d**) Blank sample.

The LOD and LOQ were calculated using the response standard deviation and the slope of the calibration curve of 0.156–5 µg/mL and 5–100 µg/mL. From the flow and the Y-intersection of the five straight lines, the LOD for APR was established at 0.04 ± 0.05 µg/mL for low range and 5.70 ± 4.25 µg/mL for high range; the LOQ for APR was established at 0.11 ± 0.14 for low range and 17.28 ± 12.87 for high range. The method is sensitive enough for the drug determination.

3.2. Ex Vivo Skin Permeation Studies

The drug permeation was carried out in triplicate over a 24 h period using skin samples with normal TEWL values (10 g m^{-2} h^{-1}) demonstrating skin integrity. The solutions showed slopes greater than 0.9, except the Menthone, which had a result of 0.86 in its linear section.

The permeation profile and retained amount of APR are detailed in the Figure 3 and Table 7 shows the permeation parameters such as flux (J_{ss}, µg/h^{-1}/cm^{-2}), permeability coefficient (K_p, cm^2/h^{-1}), cumulative permeated amount 24 h (*Cum AP 24 h*, µg) and theoretical plasma concentration in human steady-state (C_{ss}, ng/mL) of APR using various penetration enhancers.

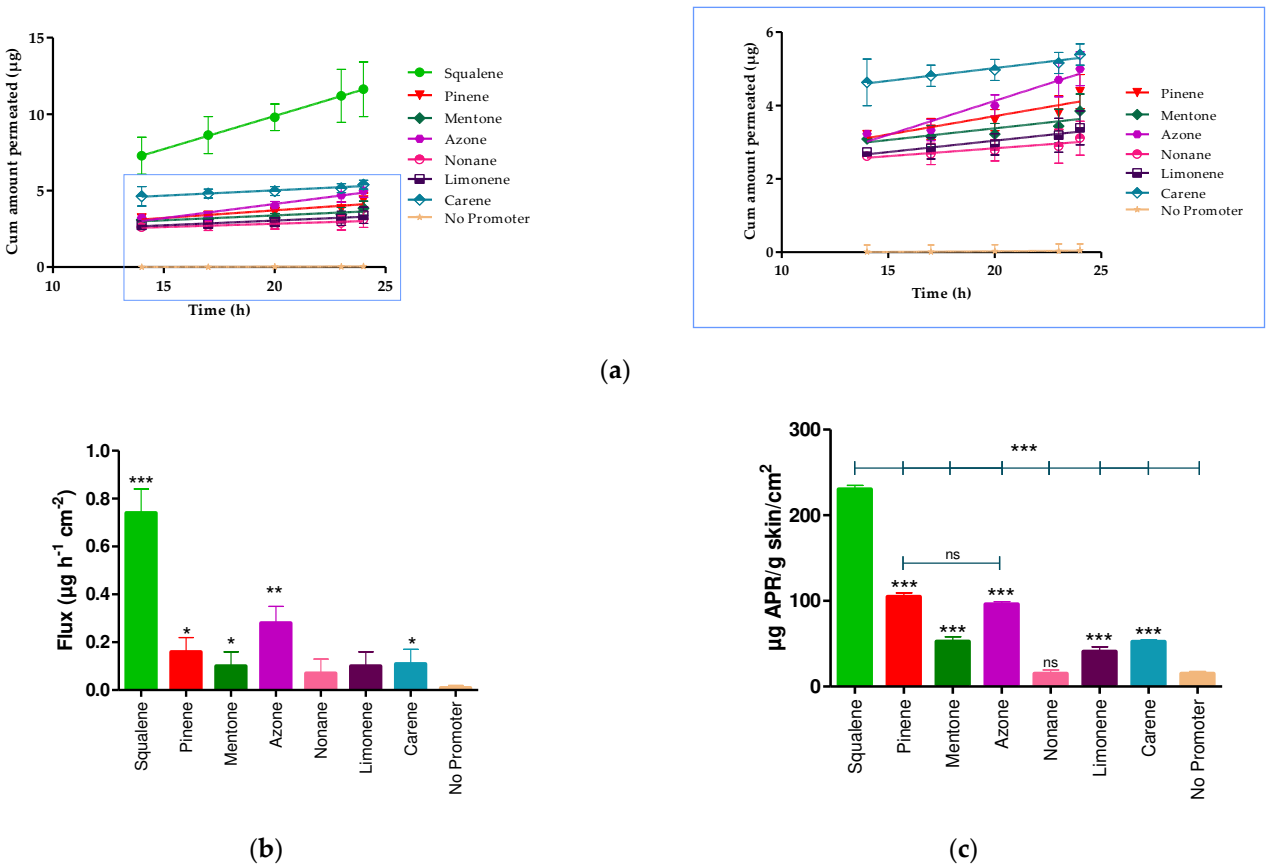

Figure 3. APR permeation profile. (**a**) Mean cumulative amount APR permeated. (**b**) APR-solutions flux. (**c**) APR retained amount in skin. Results are expressed as mean ± SD (n = 3). Statistically significant difference between solutions vs. No promoter: * = $p < 0.05$; ** = $p < 0.01$; *** = $p < 0.0001$.

The *Kp* is calculated from the flux dividing by the initial concentration of drug (1.5 mg/mL). After 24 h of assay, the amount of permeated drug (*Cum AP 24 h*) was 18.17 ± 3.10 µg for squalene. Statistical differences were found between the flux presented by squalene, pinene, mentone, azone, and carene compared to the APR solution without penetration enhancer (No promoter), whereas there were no statistically significant differences between nonane, and limonene compared to the solution without promoter.

Table 7. Biopharmaceutical parameters of Apremilast-solutions with and without penetration enhancer.

n = 3	J_{ss} (μg h^{-1} cm^{-2})	K_p (cm^2 h^{-1})	*Cum AP 24* h (μg)	C_{ss} (ng/mL)	Q_{ret} (μg/g skin/cm^2)
Azone®	0.28 ± 0.07 [e,g,h]	1.88×10^{-4} [e,g,h]	8.15 ± 0.75 [h]	0.81 ± 0.01 [a,c,e,h]	96.05 ± 3.10 [b,c,e,h]
Carene	0.11 ± 0.06 [g,h]	7.21×10^{-5} [g,h]	8.41 ± 0.50 [h]	0.31 ± 0.05 [h]	52.27 ± 2.10 [h]
Limonene	0.10 ± 0.06 [g]	6.49×10^{-5} [g]	5.30 ± 0.92 [h]	0.28 ± 0.03 [h]	40.91 ± 5.50 [h]
Menthone	0.10 ± 0.06 [g]	6.67×10^{-5} [g]	6.01 ± 0.80 [h]	0.28 ± 0.05 [a,e,h]	52.61 ± 5.60 [a,e,h]
Nonane	0.07 ± 0.06 [g]	4.48×10^{-5} [g]	4.85 ± 0.90 [h]	0.19 ± 0.02 [b,c,h]	15.13 ± 4.20 [b,c]
Pinene	0.16 ± 0.06 [g,h]	1.04×10^{-4} [g,h]	6.84 ± 0.80 [h]	0.45 ± 0.02 [d,a,e,c,b,h]	104.99 ± 4.30 [b,c,d,e,h]
Squalene	0.74 ± 0.10 [a,b,c,d,e,f,h]	4.93×10^{-4} [a,b,c,d,e,f,h]	18.17 ± 3.10 [a,b,c,d,e,f,h]	2.13 ± 0.02 [a,b,c,d,e,f,h]	230.40 ± 4.50 [a,b,c,d,e,f,h]
No promoter	0.01 ± 0.01	3.8×10^{-6}	0.08 ± 0.30	0.02 ± 0.01	15.14 ± 2.40

[a] Azone; [b] Carene; [c] Limonene; [d] Menthone; [e] Nonane; [f] Pinene; [g] Squalene; [h] No promoter. Results are expressed by mean ± SD ($n = 3$). One-way Analysis of Variance (ANOVA) with Tukey's Multiple Comparison Test were performed to assess the statistical significance between groups at ($p < 0.05$). *Underline value:* Promoter enhancer that presents a greater retained amount of drug in the skin.

The APR retained amount was more evident in the presence of squalene, pinene, and azone (Figure 3c) where squalene presented a greater amount retained (230.40 ± 4.50 μg/g skin/cm^2), showing statistically significant differences with pinene (104.99 ± 4.30 μg/g skin/cm^2) and azone (96.05 ± 3.10 μg/g skin/cm^2).

3.3. In Vitro Tolerance Studies or Cell Viability Studies

The toxicity of the seven permeation promoters used in this study was evaluated in skin cells (HaCaT cells) by the MTT assay. The results of treatment of HaCaT cells treated with different dilutions of the permeation promoters are shown in Figure 4.

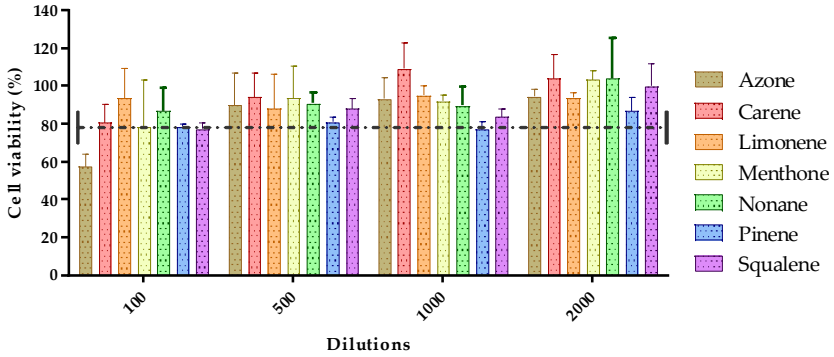

Figure 4. Effect of permeation promoters at different dilutions on the viability of HaCaT keratinocyte cells in vitro.

Most of the permeation promoters tested were found not to induce cytotoxicity in the cells, except for azone which, at 1/100 dilution (highest concentration tested), induced cytotoxicity. The results suggested that the promoters evaluated do not generate skin irritation, but caution should be exercised with the use of azone; likewise, no correlation was found between the results obtained for skin cell toxicity with reference to its effect on drug penetration through the skin.

3.4. In Vivo Skin Tolerance Study

3.4.1. Biomechanical Skin Properties Evaluation

Hydration in the stratum corneum was evaluated after the application of the two solutions (APR-Squalene solution and Blank-Squalene solution).

Topical application of these solutions on the skin significantly increased hydration in stratum corneum. These results were predictable, taking into account that the solutions are mostly made up of water and Transcutol.

These results suggest that the solutions with Squalene do not cause damage or irritation in the skin barrier (Figure 5).

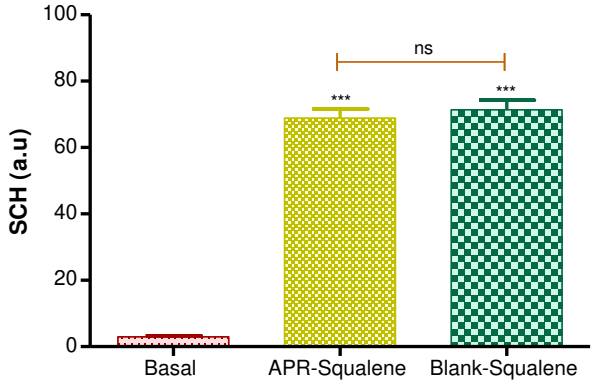

Figure 5. Stratum corneum hydration. p value: *** = $p < 0.0001$; ns = no significance.

3.4.2. Colorimetric Parameters

The irritation potential of a solution containing APR and Squalene in its composition was evaluated. The irritation was measured through the color differences that appeared after the application of the solutions on the back of the rats' skin.

The results were obtained as light intensity on a numerical scale for RGB and finally calculated with respect to the baseline value and expressed as % erythema.

Table 8 shows the values obtained from the colorimetric study for APR-Squalene solution and Blank-Squalene solution. It was evidenced that the APR-Squalene (4% erythema) and Blank-Squalene (3% erythema) solutions has not caused irritation after contact with the skin in comparison with the positive control (100% erythema).

Table 8. Skin color measurements expressed in RGB code of APR-Squalene and Blank-Squalene solutions. Measurements were made in the established quadrants of the dorsal area of the animal. RGB values represent median (min-max). ANOVA p value ≤ 0.0001 compared solutions vs. C+.

Group	RGB Value			Difference			Squares			Sum Square	Square Root of Sum	Normalized Dose	%Erythema
	R	G	B	dR	dG	dB	dR	dG	dB				
Basal	195 (195–196)	174 (174–175)	181 (180–181)	0.0	0.0	0.0	0.0	0.0	0.0	0.0	0.0	0.0	0%
C+	183 (182–183)	144 (144–144)	157 (157–158)	−12.0	−30.0	−24.0	144.0	900.0	576.0	1620.0	40.3	8.1	100%
APR-Squalene	195 (194–195)	173 (170–174)	180 (179–181)	0.0	−1.0	−1.0	0.0	1.0	1.0	2.0	1.4	0.3	4%
Blank-Squalene	193 (193–194)	161 (161–163)	166 (166–166)	−1.0	0.0	0.0	1.0	0.0	0.0	1.0	1.0	0.2	3%

To corroborate this information, an ANOVA was performed with the RGB values, and it was shown that the APR-Squalene and Blank-Squalene solutions presented statistically significant differences with a p value <0.0001, when compared with the positive control (Application of xylol as a skin irritant); on the other hand, it was evidenced that after the application of the solution on irritated skin it does not enhance the irritation.

RGB colors were reproduced in a Microsoft Excel program. Skin redness was presented as a sign of irritation as shown in Figure 6 where the color reproduction marks greater redness after contact with xylol (C+) when it is compared to the RGB reproductions of the other groups. It is corroborated with the results showed in Table 8, which indicated with that the squalene and the combination of Squalene and APR are not irritating at the concentrations tested.

The results of the histological sections of the skin samples (Figure 7) showed tissue damage in those samples where xylol was applied, on the other hand, the samples where the solutions were applied do not show any damage.

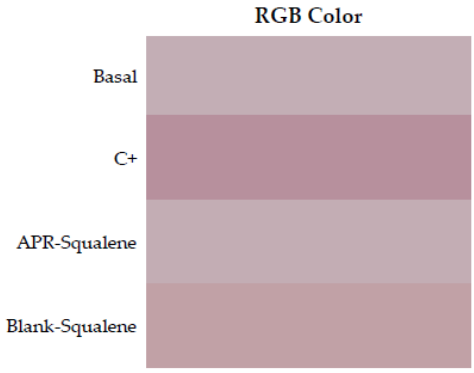

Figure 6. Erythema shown as skin color sequence section, using APR-Squalene solution and Blank-Squalene solution. Colors are reproduced from the Median values of RGB codes.

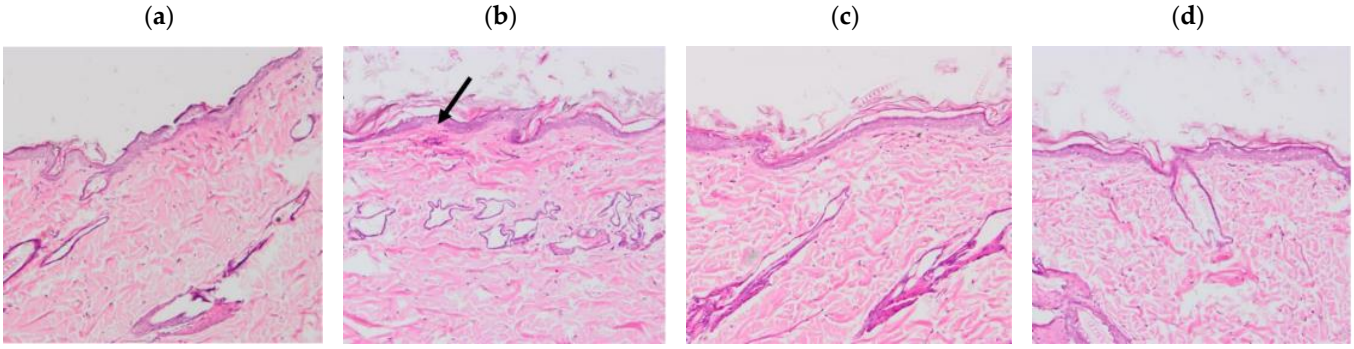

Figure 7. Histological sections of the dorsal area of rats (100× magnification). Arrows indicate signs of tissue damage. (**a**) Basal, (**b**) Xylol (C+), (**c**) APR-Squalene, (**d**) Blank-Squalene.

4. Discussion

Unlike previous studies, the method was validated in a range of 0.156–5 µg/mL and verified from 5–100 µg/mL [21]. During ex vivo drug penetration studies, the components that make up the skin and excipients present in the formulations are released into the receiving fluid together with the active ingredient, so the matrix was evaluated to ensure correct identification and quantification of the drug.

Numerous methodologies have been described for the detection and quantification of APR [31–33]. However, the methodology described in this article was developed in a simple, easy way, with fewer chemical reagents and low cost, compared to the proposals of other authors [34,35]. In addition, a method under isocratic conditions is proposed, with a sample analysis time of 7 min and an APR retention time of 3.3 min. The objective of validating an analytical method is to demonstrate that it is adequate for the purpose for which it will be used; therefore, the analytical method of this study has been validated considering the implications that its use entails. The parameters of linearity, precision, accuracy, sensitivity, and selectivity have been determined according to the Harmonization Guidelines of the International Conference (ICH) [36] in the ranges of 0.156–5 µg/mL and 5–100 µg/mL, for the detection and quantification of APR from samples obtained from ex vivo permeation studies, using human skin as a matrix.

APR is insoluble in water [37] and most of the techniques described for the identification of active ingredients in complex samples require pretreatment. The receptor fluid used for in vitro permeation techniques consisted in transcutol:water solutions. Transcutol is commonly used in dermal formulations. Moreover, previous studies have reported the high solubilizing capacity of Transcutol for APR (Cs < 2.51~2.69 mg/mL) [21,38], and its use as part of the receptor fluid to guarantee the *sink* condition in the in vitro release and permeation studies [39].

The permeation of the drug through the skin was determined with the Franz Cell Diffusion technique and the membrane used was dermatomized human abdominal skin. The promoters evaluated have been extensively studied and were selected because there is research that has reported that these promoters increase drug penetration without having other pharmacological activities in the body. Moreover, they are non-toxic, non-irritating, non-allergenic, unidirectional, and compatible with drugs and excipients of dermal formulations, in addition to being cosmetologically acceptable [40,41]. However, despite its good performance in improving the skin permeability of drugs, there are still substances used as penetration enhancers that can cause skin irritation or, in some cases, skin toxicity in vitro in HACAT cells [42]. Azone, which was patented in 1976, is the first compound designed specifically as a penetration enhancer. It interacts with the structural lipids that make up the stratum corneum, thus allowing the passage of the drug, as well as acting by denaturing proteins and modifying the coefficient of diffusion of the drug favoring permeation through the skin [43,44]. The terpenes used in this study, such as Carene, Limonene, Mentona, Nonane, Alpha-pinene, and squalene, are organic compounds and laboratory designed that attract great interest. Terpenes are generally considered to be less toxic and have a potential of low irritation compared to other substances such as surfactants and other synthetic penetration enhancers [45]. Terpenes are a class of clinically acceptable and relatively safe permeation enhancers for hydrophilic and lipophilic drugs [40]. Terpenes are of natural origin and are generally considered "*safe*" by the US Federal Drug Administration, which allow them to offer advantages over other enhancers including alcohols, fatty acids, sulfoxides, and azone [46]. In this study, squalene was the most effective promoter in improving the permeability of APR through human abdominal skin. The squalenic acid chain confers high hydrophobicity for skin penetration of hydrophobic drugs, such as APR [47]. Squalene reduces the oxidative damage of free radicals in the skin; in addition, this promoter is present in a percent of around 13% in sebum which is produced by the sebaceous glands that correspond to small glands present in the skin that secrete sebum in hair follicles to lubricate skin and hair in animals [48]. Squalene is considered a great emollient in nature; it is quickly and efficiently absorbed into the skin [49]. Therefore, these results suggest that the incorporation of squalene in dermal formulations could be used as a strategy to improve the permeation of APR through the stratum corneum and their retention within the skin providing topical therapeutic alternatives with reduced side effects for the local treatment of psoriasis.

Squalene and the other penetration promoters evaluated in this study were non-toxic substances according to the results obtained for cell viability in HACAT keratinocyte cells. According to several studies, penetration promoters must be non-toxic or irritating substances, the absorption must be immediate and unidirectional [50,51]. In addition, after removing the material from the membrane, the tissue should immediately recover its barrier properties and the promoter should be compatible with the drug and pharmaceutical excipients [52].

For the in vivo tolerance test through animal models, APR solutions were used together with 5% squalene, as a penetration promoter. The evaluated colorimetric parameters showed that the squalene solutions (with and without drug) are neither irritant nor toxic when in contact with the back of the animal's skin in comparison with the positive control and that was corroborated with histological tests. The histological results showed tissue damage after the application of xylol; however, this was not evidenced with the solutions evaluated. Consistent and reproducible color assessment is one of the most useful techniques in dermatology. Devices used for this purpose can quantify color, erythema, and tan in various skin types; the devices contain a spectrophotometer that analyzes the spectral characteristics of a color [53]. This technique is currently used due to its non-invasive nature and allows the characterization of injured skin from non-injured skin in patients with skin involvement; it is also used to evaluate the efficacy of drugs on skin pigmentation [54].

5. Conclusions

Squalene presented better results as an enhancer of the penetration of apremilast through the stratum corneum of a human abdominal skin sample, making it an excellent candidate to improve the permeability of the drug in the case of the development of a topical formulation. It was confirmed that squalene is a non-irritating, non-toxic, and non-allergenic substance that did not cause changes like irritation or erythema when in contact with the skin in experimental studies with animals.

Author Contributions: P.S.-G. carried out all the experiments, analyzed the data/results, and wrote the manuscript; L.C.E. analyzed the data/results, ensured that the goals of the study were met, and review and edited the manuscript; N.D.-G. and L.B. realized cell studies; M.J.R.-L. carried out the histological studies. H.A. analytical validation development; and A.C. developed the biopharmaceutical studies, designed protocol for the entire study, and analyzed the data/results. All authors have read and agreed to the published version of the manuscript.

Funding: This research received no external funding.

Institutional Review Board Statement: The animal study protocol was approved by the Ethics Committee of the University of Barcelona and the Bellvitge Establishment, Barcelona, Spain (number 387/18, 26 November 2018).

Informed Consent Statement: Not applicable.

Data Availability Statement: Data are contained within the article.

Acknowledgments: P.S.-G and L.C.E. thanks the support of the Universidad Técnica Particular de Loja, Ecuador and Gattefossé España S.A.

Conflicts of Interest: The authors declare no conflict of interest.

References

1. Zaid Alkilani, A.; McCrudden, M.T.C.; Donnelly, R.F. Transdermal drug delivery: Innovative pharmaceutical developments based on disruption of the barrier properties of the stratum corneum. *Pharmaceutics* **2015**, *7*, 438–470. [CrossRef] [PubMed]
2. Prausnitz, M.R.; Langer, R. Transdermal drug delivery. *Nat. Biotechnol.* **2008**, *26*, 1261–1268. [CrossRef] [PubMed]
3. Clausen, B.E.; Stoitzner, P. Functional specialization of skin dendritic cell subsets in regulating T Cell responses. *Front. Immunol.* **2015**, *6*, 534. [CrossRef] [PubMed]
4. Lodi, G.; Sannino, M.; Caterino, P.; Cannarozzo, G.; Bennardo, L.; Nisticò, S.P. Fractional CO_2 laser-assisted topical rifamycin drug delivery in the treatment of pediatric cutaneous leishmaniasis. *Pediatric. Dermatol.* **2021**, *38*, 717–720. [CrossRef] [PubMed]
5. Kligman, A.M. What is the 'true' function of skin? *Exp. Dermatol.* **2002**, *11*, 159–187. [CrossRef]
6. Wilhelm, K.-P.; Cua, A.B.; Maibach, H.I. Skin aging: Effect on transepidermal water loss, stratum corneum hydration, skin surface ph, and casual sebum content. *Arch. Dermatol.* **1991**, *127*, 1806–1809. [CrossRef]
7. Yousef, H.; Alhajj, M.; Sharma, S. Anatomy, skin (integument), epidermis. In *StatPearls*; StatPearls Publishing: Treasure Island, FL, USA, 2022.
8. Javadzadeh, Y.; Azharshekoufeh Bahari, L. Chapter 8—Therapeutic nanostructures for dermal and transdermal drug delivery. In *Nano- and Microscale Drug Delivery Systems*; Grumezescu, A.M., Ed.; Elsevier: Amsterdam, The Netherlands, 2017; pp. 131–146. ISBN 978-0-323-52727-9.
9. Naik, A.; Kalia, Y.N.; Guy, R.H. Transdermal drug delivery: Overcoming the skin's barrier function. *Pharm. Sci. Technol. Today* **2000**, *3*, 318–326. [CrossRef]
10. Hueber, F.; Wepierre, J.; Schaefer, H. Role of transepidermal and transfollicular routes in percutaneous absorption of hydrocortisone and testosterone: In vivo study in the hairless rat. *Skin Pharmacol.* **1992**, *5*, 99–107. [CrossRef]
11. Charoo, N.A.; Shamsher, A.A.A.; Kohli, K.; Pillai, K.; Rahman, Z. Improvement in bioavailability of transdermally applied flurbiprofen using tulsi (ocimum sanctum) and turpentine oil. *Colloids Surf. B Biointerfaces* **2008**, *65*, 300–307. [CrossRef]
12. Walker, R.B.; Smith, E.W. The role of percutaneous penetration enhancers. *Adv. Drug Deliv. Rev.* **1996**, *18*, 295–301. [CrossRef]
13. Foldvari, M. Non-invasive administration of drugs through the skin: Challenges in delivery system design. *Pharm. Sci. Technol. Today* **2000**, *3*, 417–425. [CrossRef]
14. Parmar, P.K.; Bansal, A.K. Novel nanocrystal-based formulations of apremilast for improved topical delivery. *Drug Deliv. Transl. Res.* **2020**, *11*, 966–983. [CrossRef] [PubMed]
15. Guo, J.-W.; Cheng, Y.-P.; Liu, C.-Y.; Thong, H.-Y.; Huang, C.-J.; Lo, Y.; Wu, C.-Y.; Jee, S.-H. Salvianolic acid B in microemulsion formulation provided sufficient hydration for dry skin and ameliorated the severity of imiquimod-induced psoriasis-like dermatitis in mice. *Pharmaceutics* **2020**, *12*, 457. [CrossRef] [PubMed]

16. Fala, L. Otezla (apremilast), an oral PDE-4 inhibitor, receives FDA approval for the treatment of patients with active psoriatic arthritis and plaque psoriasis. *Am. Health Drug Benefits* **2015**, *8*, 105–110. [PubMed]
17. FDA Approves OTEZLA® (apremilast) for the Treatment of Oral Ulcers Associated with Behçet's Disease. Available online: https://ir.celgene.com/press-releases-archive/press-release-details/2019/FDA-Approves-OTEZLA-apremilast-for-the-Treatment-of-Oral-Ulcers-Associated-with-Behets-Disease/default.aspx (accessed on 13 February 2022).
18. Langley, A.; Beecker, J. Management of common side effects of apremilast. *J. Cutan. Med. Surg.* **2018**, *22*, 415–421. [CrossRef] [PubMed]
19. Rapalli, V.K.; Sharma, S.; Roy, A.; Singhvi, G. Design and dermatokinetic evaluation of apremilast loaded nanostructured lipid carriers embedded gel for topical delivery: A potential approach for improved permeation and prolong skin deposition. *Colloids Surf. B Biointerfaces* **2021**, *206*, 111945. [CrossRef] [PubMed]
20. Rapalli, V.K.; Sharma, S.; Roy, A.; Alexander, A.; Singhvi, G. Solid lipid nanocarriers embedded hydrogel for topical delivery of apremilast: In-vitro, ex-vivo, dermatopharmacokinetic and anti-psoriatic evaluation. *J. Drug Deliv. Sci. Technol.* **2021**, *63*, 102442. [CrossRef]
21. Sarango-Granda, P.; Silva-Abreu, M.; Calpena, A.C.; Halbaut, L.; Fábrega, M.-J.; Rodríguez-Lagunas, M.J.; Díaz-Garrido, N.; Badia, J.; Espinoza, L.C. Apremilast microemulsion as topical therapy for local inflammation: Design, characterization and efficacy evaluation. *Pharmaceuticals* **2020**, *13*, 484. [CrossRef] [PubMed]
22. Mulleria, S.S.; Marina, K.; Ghetia, S.M. Formulation, optimization and in vitro evaluation of apremilast nanoemulgel for topical delivery. *Int. J. Pharm. Investig.* **2021**, *11*, 230–237. [CrossRef]
23. Sindhoor, S.M.; Koland, M. Topical delivery of apremilast loaded nanostructured lipid carrier based hydrogel for psoriasis therapy. *J. Pharm. Res. Int.* **2021**, *33*, 7–20. [CrossRef]
24. ICH: Quality Guidelines. Available online: https://www.ich.org/page/quality-guidelines (accessed on 14 February 2022).
25. Zsikó, S.; Csányi, E.; Kovács, A.; Budai-Szűcs, M.; Gácsi, A.; Berkó, S. Methods to evaluate skin penetration in vitro. *Sci. Pharm.* **2019**, *87*, 19. [CrossRef]
26. Guth, K.; Schäfer-Korting, M.; Fabian, E.; Landsiedel, R.; van Ravenzwaay, B. Suitability of skin integrity tests for dermal absorption studies in vitro. *Toxicol. Vitr.* **2015**, *29*, 113–123. [CrossRef] [PubMed]
27. Espinoza, L.C.; Silva-Abreu, M.; Calpena, A.C.; Rodríguez-Lagunas, M.J.; Fábrega, M.-J.; Garduño-Ramírez, M.L.; Clares, B. Nanoemulsion strategy of pioglitazone for the treatment of skin inflammatory diseases. *Nanomed. Nanotechnol. Biol. Med.* **2019**, *19*, 115–125. [CrossRef] [PubMed]
28. Liu, Y.; Zhou, S.; Nissel, J.; Wu, A.; Lau, H.; Palmisano, M. The pharmacokinetic effect of coadministration of apremilast and methotrexate in individuals with rheumatoid arthritis and psoriatic arthritis. *Clin. Pharmacol. Drug Dev.* **2014**, *3*, 456–465. [CrossRef]
29. Sekizawa, J.; Yasuhara, K.; Suyama, Y.; Yamanaka, S.; Tobe, M.; Nishimura, M. A simple method for screening assessment of skin and eye irritation. *J. Toxicol. Sci.* **1994**, *19*, 25–35. [CrossRef] [PubMed]
30. Limón, D.; Jiménez-Newman, C.; Rodrigues, M.; González-Campo, A.; Amabilino, D.B.; Calpena, A.C.; Pérez-García, L. Cationic supramolecular hydrogels for overcoming the skin barrier in drug delivery. *ChemistryOpen* **2017**, *6*, 585–598. [CrossRef]
31. Xiong, K.; Ma, X.; Cao, N.; Liu, L.; Sun, L.; Zou, Q.; Wei, P. Identification, characterization and HPLC quantification of impurities in apremilast. *Anal. Methods* **2016**, *8*, 1889–1897. [CrossRef]
32. Landge, S.B.; Dahale, S.B.; Jadhav, S.A.; Solanki, P.V.; Bembalkar, S.R.; Mathad, V.T. Development and Validation of stability indicating rapid RP-LC method for determination of process and degradation related impurities of apremilast, an anti-inflammatory drug. *AJAC* **2017**, *08*, 380–394. [CrossRef]
33. Panchumarthy, R.; Sulthana, S.; Harsha Sri, K. *Development and Validation of a Stability-Indicating Reversed Phase Hplc Method for Determination of Apremilast in Bulk and Pharmaceutical Dosage Form*; Scholars Research Library: Uxbridge, UK, 2020.
34. Kulkarni, P.; Deshpande, A. Analytical methods for determination of apremilast from bulk, dosage form and biological fluids: A critical review. *Crit. Rev. Anal. Chem.* **2020**, *51*, 258–267. [CrossRef]
35. Patel, N.; Patel, S.; Surati, J.; Akbari, A.; Shah, D. Apremilast—A review of analytical methods developed for API with its impurities, pharmaceutical formulations and biological matrices. *Int. J. Pharm. Res. Appl.* **2021**, *6*, 735–755.
36. European Medicines Agency ICH Q2 (R1) Validation of Analytical Procedures: Text and Methodology. Available online: https://www.ema.europa.eu/en/ich-q2-r1-validation-analytical-procedures-text-methodology (accessed on 15 July 2020).
37. Madan, J.R.; Khobaragade, S.; Dua, K.; Awasthi, R. Formulation, optimization, and in vitro evaluation of nanostructured lipid carriers for topical delivery of apremilast. *Dermatol. Ther.* **2020**, *33*, e13370. [CrossRef] [PubMed]
38. Shakeel, F.; Haq, N.; Alanazi, F.K.; Alsarra, I.A. Solubility and thermodynamics of apremilast in different mono solvents: Determination, correlation and molecular interactions. *Int. J. Pharm.* **2017**, *523*, 410–417. [CrossRef] [PubMed]
39. Osborne, D.W.; Musakhanian, J. Skin penetration and permeation properties of transcutol®—Neat or diluted mixtures. *AAPS PharmSciTech* **2018**, *19*, 3512–3533. [CrossRef]
40. Amin, S.; Kohli, K.; Khar, R.K.; Mir, S.R.; Pillai, K.K. Mechanism of in vitro percutaneous absorption enhancement of carvedilol by penetration enhancers. *Pharm. Dev. Technol.* **2008**, *13*, 533–539. [CrossRef] [PubMed]
41. Kováčik, A.; Kopečná, M.; Vávrová, K. Permeation enhancers in transdermal drug delivery: Benefits and limitations. *Expert Opin. Drug Deliv.* **2020**, *17*, 145–155. [CrossRef] [PubMed]

42. Chen, J.; Jiang, Q.-D.; Wu, Y.-M.; Liu, P.; Yao, J.-H.; Lu, Q.; Zhang, H.; Duan, J.-A. Potential of essential oils as penetration enhancers for transdermal administration of ibuprofen to treat dysmenorrhoea. *Molecules* **2015**, *20*, 18219–18236. [CrossRef] [PubMed]
43. Hadgraft, J.; Peck, J.; Williams, D.G.; Pugh, W.J.; Allan, G. Mechanisms of action of skin penetration enhancers/retarders: Azone and analogues. *Int. J. Pharm.* **1996**, *141*, 17–25. [CrossRef]
44. Haq, A.; Michniak-Kohn, B. Effects of solvents and penetration enhancers on transdermal delivery of thymoquinone: Permeability and skin deposition study. *Drug Deliv.* **2018**, *25*, 1943–1949. [CrossRef]
45. Sapra, B.; Jain, S.; Tiwary, A.; Sapra, B.; Jain, S.; Tiwary, A.K. Percutaneous permeation enhancement by terpenes: Mechanistic view. *AAPS J.* **2008**, *10*, 120–132. [CrossRef]
46. Fox, L.T.; Gerber, M.; Plessis, J.D.; Hamman, J.H. Transdermal drug delivery enhancement by compounds of natural origin. *Molecules* **2011**, *16*, 10507–10540. [CrossRef]
47. Gref, R.; Deloménie, C.; Maksimenko, A.; Gouadon, E.; Percoco, G.; Lati, E.; Desmaële, D.; Zouhiri, F.; Couvreur, P. Vitamin C–squalene bioconjugate promotes epidermal thickening and collagen production in human skin. *Sci. Rep.* **2020**, *10*, 16883. [CrossRef] [PubMed]
48. Pragst, F.; Auwärter, V.; Kießling, B.; Dyes, C. Wipe-test and patch-test for alcohol misuse based on the concentration ratio of fatty acid ethyl esters and squalene CFAEE/CSQ in skin surface lipids. *Forensic Sci. Int.* **2004**, *143*, 77–86. [CrossRef] [PubMed]
49. Huang, Z.-R.; Lin, Y.-K.; Fang, J.-Y. Biological and pharmacological activities of squalene and related compounds: Potential uses in cosmetic dermatology. *Molecules* **2009**, *14*, 540–554. [CrossRef] [PubMed]
50. Herman, A.; Herman, A.P. Essential oils and their constituents as skin penetration enhancer for transdermal drug delivery: A review. *J. Pharm. Pharmacol.* **2015**, *67*, 473–485. [CrossRef] [PubMed]
51. Chapter 5—Chemical permeation enhancers. In *Transdermal Drug Delivery*; Ita, K. (Ed.) Academic Press: Cambridge, MA, USA, 2020; pp. 63–96. ISBN 978-0-12-822550-9.
52. Junginger, H.E.; Verhoef, J.C. Macromolecules as safe penetration enhancers for hydrophilic drugs—A fiction? *Pharm. Sci. Technol. Today* **1998**, *1*, 370–376. [CrossRef]
53. Ly, B.C.K.; Dyer, E.B.; Feig, J.L.; Chien, A.L.; Del Bino, S. Research techniques made simple: Cutaneous colorimetry: A reliable technique for objective skin color measurement. *J. Investig. Dermatol.* **2020**, *140*, 3–12.e1. [CrossRef]
54. Nam, G.W.; Baek, J.H.; Koh, J.S.; Hwang, J.-K. The seasonal variation in skin hydration, sebum, scaliness, brightness and elasticity in Korean females. *Skin Res. Technol.* **2015**, *21*, 1–8. [CrossRef]

CAPÍTULO 4

DISCUSIÓN

Las enfermedades inflamatorias de la piel afectan a numerosos pacientes en todo el mundo (173), no sólo desde el punto de vista fisiológico, sino también psicológico y socioeconómico (174,175). La APR es un fármaco oral aprobado por la FDA para el tratamiento de pacientes adultos con artritis psoriásica activa, pacientes adultos con psoriasis en placas de moderada a grave que son candidatos a fototerapia o terapia sistémica, y pacientes adultos con úlceras orales asociadas a la enfermedad de Behçet (176,177). En este estudio se evaluó la aplicación tópica de APR como tratamiento alternativo para la inflamación local de la piel. Se realizó la validación del método analítico con el fin de obtener un método fiable para la cuantificación del fármaco. Los resultados mostraron el cumplimiento de las directrices de la ICH, exhibiendo una buena linealidad en un rango de 1.25 a 200 μg/mL (r^2 = 0.999) además de tener una precisión, exactitud y robustez aceptables (178). Los resultados detallados se muestran en los Materiales Suplementarios del artículo 1. APR está categorizada como un fármaco de clase IV, según el Sistema de Clasificación Biofarmacéutica (BCS), debido a su baja solubilidad y baja permeabilidad (179). Por lo tanto, este estudio incorporó APR en una ME como estrategia para mejorar la solubilidad y permeabilidad del fármaco.

La formulación se desarrolló utilizando los excipientes que mostraron la mayor capacidad de solubilización para el fármaco: Plurol® oleique CC497, Labrasol® y Transcutol® P. La búsqueda de los componentes más adecuados con respecto a la solubilidad del fármaco es un paso crítico en el desarrollo de una ME para garantizar su estabilidad y una elevada capacidad de carga de fármaco (180,181). Labrasol® es un tensioactivo aceite/agua no iónica que se caracteriza por su baja irritabilidad para la piel y que se utiliza habitualmente con Plurol® oleique en formulaciones dérmicas (182). Se seleccionó Transcutol® P como cotensioactivo debido a su capacidad para solubilizar APR con propiedades no tóxicas y biocompatibles con la piel (183).

El diagrama de fase pseudo-ternario con una mezcla de surfactante-cosurfactante (S_{mix}) en la proporción 2:1 (*p:p*) mostró una mayor región ME, y por lo tanto se utilizó para la incorporación del fármaco. La APR-ME (1.5 mg/mL) se preparó por el método de titulación, en el que se produce una emulsificación espontánea por un proceso de baja energía (184). La formulación final era homogénea y transparente, con un pH ligeramente ácido, que es biocompatible con la piel y, por tanto, sugiere que la APR-ME no tiene un efecto irritante (185). La caracterización física mediante DLS y TEM mostró la presencia de gotas de tamaño nanométrico y forma esférica distribuidas uniformemente. La microemulsión presentó características isotrópicas (186) tras su evaluación con un microscopio de luz polarizada. El comportamiento reológico de las formulaciones dérmicas influye en las propiedades de administración, tales como las características sensoriales, la extensión y la dosificación (187,188).

En los sistemas ME, la evaluación de las propiedades reológicas proporciona información sobre la constitución estructural, así como sobre las interacciones entre las gotas (189,190). El comportamiento reológico de APR-ME se determinó a partir de la relación entre la tensión de cizallamiento y la velocidad de cizallamiento (curva de flujo), que fue lineal, mientras que la viscosidad se mantuvo constante. Este resultado fue apoyado por la modelización matemática que confirmó el comportamiento newtoniano que es típico para este tipo de formulación y que, por tanto, ofrece la posibilidad de ser administrado fácilmente por pulverización.

Los perfiles de transmisión obtenidos mediante el análisis de dispersión de luz múltiple permitieron evaluar y demostrar la estabilidad física de APR-ME durante un período de 90 días, ya que no se detectaron señales de cremosidad, sedimentación, floculación o coalescencia. La evaluación adicional de los parámetros físicos, incluyendo el tamaño de las gotas, la PDI y el pH, confirmó la alta estabilidad física de la formulación. APR-ME también mostró estabilidad química, ya que hubo cambios insustanciales en el contenido cuantificado del fármaco después de 90 días a diferentes temperaturas, lo que demuestra la alta compatibilidad de los componentes con el fármaco.

En las formulaciones dérmicas, los estudios de liberación y permeabilidad del fármaco son herramientas útiles para predecir la biodisponibilidad del mismo y, en consecuencia, determinar su eficacia (191,192). En este trabajo, la APR se liberó de la ME siguiendo un modelo de primer orden (cinética de Fick) en el que la tasa de liberación es directamente proporcional a la concentración del fármaco restante. Así, se observa el cumplimiento de la ley de Fick, que establece que la tasa de difusión a través de una membrana es directamente proporcional al gradiente de concentración de la sustancia a ambos lados (193). Este resultado confirmó que la formulación puede liberar el fármaco incorporado y, por tanto, no limita la permeación del fármaco a través de la piel. Los estudios de permeación *ex vivo* utilizando piel humana y en condiciones adecuadas se utilizan con éxito para predecir el comportamiento in vivo de las formulaciones tópicas (194,195). Los resultados de este ensayo revelaron que la APR-ME podría utilizarse como un tratamiento local eficaz para la inflamación de la piel, ya que el fármaco fue capaz de atravesar el estrato corneo y quedar retenido en la piel (479,35 μg APR/g piel/cm^2) sin alcanzar el compartimento receptor. Estos resultados sugieren que es posible alcanzar una concentración adecuada del fármaco en la zona diana y evitar al mismo tiempo los efectos adversos sistémicos. En cuanto a la eficacia terapéutica, tanto en las pruebas *in vitro* como *in vivo* APR-ME demostró potencial antiinflamatorio tras su aplicación. Los estudios de eficacia *in vitro* con la línea celular HaCaT corroboraron la actividad del fármaco sobre la expresión de interleucinas proinflamatorias previamente reportadas, como la IL-6 y la IL-8 (196). Los efectos inhibidores de APR-ME sobre la producción de mediadores inflamatorios fueron acompañados por disminuciones dependientes de la concentración en los niveles de expresión de ARNm y proteínas de IL-6 e IL-8. Además, se realizaron estudios de eficacia *in vivo* utilizando ácido aracquidónico para inducir la inflamación en el oído de los ratones. El ácido araquidónico es un ácido graso esencial insaturado de cadena larga que se forma a partir de la síntesis del ácido linoleico en la dieta, y se considera uno de los precursores de las prostaglandinas, los tromboxanos y los leucotrienos (197,198). Las investigaciones apoyan el uso del ácido araquidónico para la inducción de procesos inflamatorios porque es un componente intrínseco de la respuesta inflamatoria, que posteriormente puede utilizarse en modelos de edema de oreja de ratón para evaluar el potencial antiinflamatorio de los fármacos (199–202). La

APR, al ser un inhibidor de la fosfodiesterasa 4, eleva los niveles intracelulares de AMPc, que a su vez interviene en la regulación de la respuesta inflamatoria modulando la expresión de TNF e IL-17 (203). El proceso inflamatorio de la piel favorece la sequedad cutánea, induce la infiltración de células inflamatorias, aumenta el engrosamiento de la piel y estimula los receptores de membrana de los queratinocitos, lo que favorece la liberación de diversos mediadores inflamatorios como el TNFα, IL-8, IL-1, IL-6 y IL-12 (204,205). En nuestro estudio, los resultados del SCH mostraron que el contenido de agua del estrato corneo no se alteró con la aplicación tópica de ácido araquidónico; sin embargo, se observó un efecto hidratante en los ratones tratados con APR-ME. No obstante, el ácido araquidónico indujo un aumento del grosor de la piel, lo que es indicativo de edema, hiperplasia e intensificación de la permeabilidad vascular (206). Este efecto fue corroborado por estudios histológicos que mostraron la presencia de edema e infiltrado leucocitario en el control positivo. La eficacia terapéutica de la formulación en el tratamiento de estos síntomas se confirmó en este estudio, ya que se produjo una reducción del grosor de la piel, así como en la infiltración de células inflamatorias tras la administración tópica de APR-ME. En cuanto a los mecanismos inmunológicos implicados en el proceso inflamatorio local inducido por el ácido araquidónico, se observó un aumento de la expresión de las citoquinas proinflamatorias IL-8, IL-17A y TNF en comparación con el grupo de control negativo. El tratamiento tópico con APR-ME en la zona inflamada redujo significativamente la expresión de estas citocinas. El papel de la IL-8, IL-17A y TNFα en la inflamación de la piel se ha descrito ampliamente en estudios anteriores (207–209). El TNFα es un agente multifuncional que estimula la fase aguda de una reacción inflamatoria y es secretado por diferentes tipos de células, como monocitos, macrófagos, células de Langerhans y microglía (210,211). Esta citocina es uno de los marcadores tempranos más abundantes y se considera un *"regulador maestro"* en los procesos inflamatorios porque puede desencadenar expresiones locales de otras citocinas proinflamatorias como la IL-1, IL-6 e IL-8 (171,212,213). La IL-8 es una quimiocina inflamatoria producida por diversas células, como monocitos, fibroblastos, células endoteliales, queratinocitos y condrocitos (214). El papel de la IL-8 en la inflamación y en las enfermedades inflamatorias de la piel ha sido confirmado por modelos experimentales que mostraron una expresión constitutiva del

ARNm de la IL-8 en queratinocitos normales cultivados junto con un rápido aumento de su nivel cuando se somete a un estímulo, como la irradiación (215). Por último, la IL-17 desempeña un papel importante en la regulación de los sistemas inmunitarios innato y adaptativo. Sin embargo, su sobreexpresión está implicada en varias enfermedades inflamatorias y autoinmunes, como la dermatitis y la psoriasis (216–218). En resumen, los estudios de eficacia realizados en este trabajo confirmaron (i) el efecto terapéutico de la RAP en un modelo in vitro en líneas celulares HaCaT; (ii) la ausencia de citotoxicidad aparente (viabilidad celular de la APR-ME en concentraciones a partir de 6 μg/mL; (iii) el potencial terapéutico de la APR-ME que se evidenció por la disminución de la expresión de las citocinas IL-8, IL-17A y TNFα; reducción de la infiltración de células inflamatorias, así como del edema y el enrojecimiento; y (iv) efecto hidratante en la zona afectada gracias a la composición de la formulación a base de aceites y tensioactivos.
Por último, se realizó el estudio de tolerancia *in vivo*, en el que se analizaron las propiedades bioquímicas de la piel en voluntarios sanos. El TEWL y el SCH se han utilizado en dermatología para detectar posibles efectos irritantes de las formulaciones tópicas (219–221). Los niveles normales de hidratación mantienen la flexibilidad del estrato corneo y sus características viscoelásticas, además de facilitar las reacciones enzimáticas implicadas en la maduración de los corneocitos (222,223). La desestabilización o el daño de la superficie de la piel por la exposición a agentes físicos o agentes químicos puede provocar cambios en la TEWL y la SCH (224,225). En este estudio, la evaluación de estos parámetros confirmó que la APR-ME no altera la función sebácea ni compromete la integridad de la barrera cutánea. Por el contrario, la mejora de los niveles de hidratación se evidenció mediante una reducción significativa de TEWL junto con un aumento de SCH tras la aplicación tópica de APR-ME, probablemente debido al efecto hidratante de la formulación.

A diferencia de una primera validación realizada, el método se validó aumentando el rango de 0.156-5 μg/mL y se verificó de 5-100 μg/mL. Durante los estudios de penetración de fármacos *ex vivo*, los componentes que conforman la piel y los excipientes presentes en las formulaciones se liberan en el fluido receptor junto con el principio activo, por lo que se evaluó la matriz para asegurar la correcta identificación y

cuantificación del fármaco. Sin embargo, la metodología descrita en el segundo artículo se desarrolló de forma sencilla, fácil, con menos reactivos químicos y de bajo coste, en comparación con las propuestas de otros autores. Además, se propone un método en condiciones isocráticas, con un tiempo de análisis de la muestra de 7 min y un tiempo de retención de la APR de 3.3 min. Tal y como se mencionó anteriormente, el objetivo de la validación de un método analítico es demostrar que es adecuado para el fin para el que se va a utilizar; por ello, el método analítico de este estudio se ha validado teniendo en cuenta las implicaciones que conlleva su uso. Los parámetros de linealidad, precisión, exactitud, sensibilidad y selectividad se han determinado de acuerdo con las ICH en los rangos de 0.156-5 μg/mL y 5-100 μg/mL, para la detección y cuantificación de la RAP a partir de muestras obtenidas de estudios de permeación *ex vivo*, utilizando la piel humana como matriz. La APR es insoluble en agua (226) y la mayoría de las técnicas descritas para la identificación de principios activos en muestras complejas requieren un tratamiento previo. El fluido receptor utilizado para las técnicas de permeación *in vitro* consistió en soluciones de transcutol:agua. El transcutol se utiliza habitualmente en las formulaciones dérmicas. Además, estudios anteriores han informado de la alta capacidad de solubilización del transcutol para la APR (Cs < 2.51~2.69 mg/mL) (227,228), y su uso como parte del fluido receptor para garantizar las *condiciones sink* en los estudios de liberación *in vitro* y estudios de permeación. La permeación del fármaco a través de la piel se determinó con la técnica de difusión celular de Franz y la membrana utilizada fue piel abdominal humana dermatomizada.

Los promotores de penetración evaluados han sido ampliamente estudiados y fueron seleccionados porque hay investigaciones que han informado que estos promotores aumentan la penetración del fármaco sin tener otras actividades farmacológicas en el organismo. Además, no son tóxicos, no irritan, no son alergénicos, son unidireccionales y son compatibles con los fármacos y excipientes de las formulaciones dérmicas, además de ser cosmetológicamente aceptables (97,229). Sin embargo, a pesar de su buen rendimiento en la mejora de la permeabilidad cutánea de los fármacos, todavía hay sustancias utilizadas como potenciadores de la penetración que pueden causar irritación cutánea o, en algunos casos, toxicidad cutánea *in vitro* en células HaCaT (230). La azona,

patentada en 1976, es el primer compuesto diseñado específicamente como potenciador de la penetración. Interactúa con los lípidos estructurales que componen el estrato córneo, permitiendo así el paso del fármaco, además de actuar desnaturalizando las proteínas y modificando el coeficiente de difusión del fármaco favoreciendo la permeabilidad a través de la piel (231,232). Los terpenos utilizados en este estudio, como careno, limoneno, mentona, nonano, α-pineno y escualeno, son compuestos orgánicos y diseñados en el laboratorio que despiertan un gran interés. Los terpenos son generalmente considerados como menos tóxicos y tienen un potencial de baja irritación en comparación con otras sustancias como los tensioactivos y otros potenciadores de la penetración sintéticos (233). Los terpenos son una clase de potenciadores de la permeación clínicamente aceptables y relativamente seguros para fármacos hidrofílicos hidrofílicos y lipofílicos. Los terpenos son de origen natural y, en general, son considerados *"seguros"* por la Administración Federal de Medicamentos de EE.UU., lo que les permite ofrecer ventajas sobre otros potenciadores como los alcoholes, los ácidos grasos, los sulfóxidos y la azona (234). En este estudio, el escualeno fue el promotor más eficaz para mejorar la permeabilidad de la APR a través de la piel abdominal humana. La cadena de ácido escualénico confiere una alta hidrofobicidad para la penetración en la piel de fármacos hidrofóbicos, como la APR. El escualeno reduce el daño oxidativo de los radicales libres radicales libres en la piel; además, este promotor está presente en un porcentaje de alrededor del 13% en el sebo que es producido por las glándulas sebáceas que corresponden a pequeñas glándulas presentes en la piel que segregan sebo en los folículos pilosos para lubricar la piel y el pelo en los animales. El escualeno se considera un gran emoliente en la naturaleza; se absorbe rápida y eficazmente en la piel (235–237).

Por tanto, estos resultados sugieren que la incorporación de escualeno en formulaciones dérmicas podría utilizarse como estrategia para mejorar la permeabilidad de la APR a través de a través del estrato córneo y su retención dentro de la piel, proporcionando alternativas terapéuticas tópicas alternativas terapéuticas tópicas con efectos secundarios reducidos para el tratamiento local de la psoriasis. El escualeno y los demás promotores de la penetración evaluados en este estudio fueron sustancias no tóxicas según los resultados obtenidos para la viabilidad celular en células de queratinocitos

HaCaT. Según varios estudios, los promotores de la penetración deben ser sustancias no tóxicas o irritantes, la absorción debe ser inmediata y unidireccional (113,238). Además, tras retirar el material de la membrana, el tejido debe recuperar inmediatamente sus propiedades de barrera y el promotor debe ser compatible con el fármaco y los excipientes farmacéuticos. Para la prueba de tolerancia *in vivo* a través de modelos animales, se utilizaron soluciones de APR junto con escualeno al 5%, como promotor de la penetración. Los parámetros colorimétricos evaluados mostraron que las soluciones de escualeno (con y sin fármaco) no son irritantes ni tóxicas al entrar en contacto con el dorso de la piel de los animales en comparación con el control positivo y eso se corroboró con las pruebas histológicas. Los resultados histológicos mostraron daños en los tejidos tras la aplicación de xilol; sin embargo, esto no se evidenció con las soluciones evaluadas. La evaluación consistente y reproducible del color es una de las técnicas más útiles en dermatología. Los dispositivos utilizados para este fin pueden cuantificar el color, el eritema y el bronceado en varios tipos de piel; los dispositivos contienen un espectrofotómetro que analiza las características espectrales de un color (239). Esta técnica se utiliza actualmente por su carácter no invasivo y permite caracterizar la piel lesionada de la no lesionada en pacientes con afectación cutánea; también se utiliza para evaluar la eficacia de los fármacos en la pigmentación de la piel (240).

CAPÍTULO 5

CONCLUSIONES

Los resultados de los estudios apoyan el uso tópico de APR-ME como una estrategia terapéutica atractiva en el tratamiento de la inflamación local de la piel. La formulación realizada resultó homogénea y transparente, exhibió un comportamiento newtoniano, permitiendo así una fácil administración vía spray o roll-on. Además, la alta tolerabilidad de APR-ME en voluntarios sanos gracias a su composición basada en excipientes aprobados para formulaciones dérmicas con alta biocompatibilidad con la piel. APR-ME demostró su capacidad de liberar el fármaco incorporado siguiendo un modelo cinético de primer orden, garantizando además un efecto antiinflamatorio efecto antiinflamatorio local con efectos adversos sistémicos reducidos debido a la alta retención del fármaco en la piel. Este potencial antiinflamatorio se evidenció por una reducción de la producción *in vitro* de IL-6 e IL-8, una disminución de la infiltración de células inflamatorias, un menor daño en el estrato córneo y una disminución de la expresión de citoquinas proinflamatorias como TNFα, IL -8 e IL-17 en el modelo *in vivo*. Asimismo, se evidenció que el uso de promotores de penetración favorece el paso de APR a través del estrato córneo. El escualeno presentó mejores resultados como potenciador de la penetración del apremilast a través del estrato córneo de una muestra de piel abdominal humana, lo que lo convierte en un excelente candidato para mejorar la permeabilidad del fármaco en el caso del desarrollo de una formulación tópica. Se confirmó que el escualeno es una sustancia no irritante, no tóxica y no alergénica que no provocó cambios como irritación o eritema al entrar en contacto con la piel en estudios experimentales con animales.

CAPÍTULO 6

ANEXOS

Como investigaciones anexas tenemos las siguiente:

Mini Review	**Apremilast Application as Treatment of Oral Ulcers in Behçet Syndrome** *Biomedical Journal of Scientific & Technical Research* 2021, 34 (5): 27076-27080
Communication	**Efficacy evaluation of a Microemulsion loaded with Apremilast for the Rosacea treatment** *Skin Forum* 2022

6.1. Mini Review

Journal	*Biomedical Journal of Scientific & Technical Research*
Volume	*34*
Issue	*5*
Published date	25 March 2021
ISSN:	1424-8247
DOI:	10.26717/BJSTR.2021.34.005605

Apremilast Application as Treatment of Oral Ulcers in Behçet Syndrome

Paulo Sarango-Granda[1,3], Lupe Carolina Espinoza[1,2], Mireia Mallandrich*[1,3] and Ana Cristina Calpena[1,3]

[1]Department of Pharmacy, Pharmaceutical Technology and Physical Chemistry, Faculty of Pharmacy and Food Sciences, University of Barcelona, Spain

[2]Departamento de Química y Ciencias Exactas, Universidad Técnica Particular de Loja, Ecuador

[3]Institute of Nanoscience and Nanotechnology (IN2UB), University of Barcelona, Spain

***Corresponding author:** Mireia Mallandrich, Department of Pharmacy, Pharmaceutical Technology and Physical Chemistry, Faculty of Pharmacy and Food Sciences, Institute of Nanoscience and Nanotechnology (IN2UB), University of Barcelona, Spain

Afiliaciones:

1. Department of Pharmacy, Pharmaceutical Technology and Physical Chemistry, Faculty of Pharmacy and Food Sciences, University of Barcelona, Spain
2. Departamento de Química y Ciencias Exactas, Universidad Técnica Particular de Loja, Ecuador
3. Institute of Nanoscience and Nanotechnology (IN$_2$UB), University of Barcelona, Spain

Mini Review

BIOMEDICAL Journal of Scientific & Technical Research

ISSN: 2574 -1241

DOI: 10.26717/BJSTR.2021.34.005605

Apremilast Application as Treatment of Oral Ulcers in Behçet Syndrome

Paulo Sarango-Granda[1,3], Lupe Carolina Espinoza[1,2], Mireia Mallandrich*[1,3] and Ana Cristina Calpena[1,3]

[1]*Department of Pharmacy, Pharmaceutical Technology and Physical Chemistry, Faculty of Pharmacy and Food Sciences, University of Barcelona, Spain*

[2]*Departamento de Química y Ciencias Exactas, Universidad Técnica Particular de Loja, Ecuador*

[3]*Institute of Nanoscience and Nanotechnology (IN2UB), University of Barcelona, Spain*

***Corresponding author:** Mireia Mallandrich, Department of Pharmacy, Pharmaceutical Technology and Physical Chemistry, Faculty of Pharmacy and Food Sciences, Institute of Nanoscience and Nanotechnology (IN2UB), University of Barcelona, Spain

ARTICLE INFO

Received: March 06, 2021

Published: March 25, 2021

Citation: P Sarango-Granda, Lupe Carolina E, Mireia M, Ana Cristina C. Apremilast Application as Treatment of Oral Ulcers in Behçet Syndrome. Biomed J Sci & Tech Res 34(5)-2021. BJSTR. MS.ID.005605.

Keywords: Behçet Disease; Behçet Syndrome; Oral Ulcers; Genital Ulcers; Apremilast; Inflammatory Disease

ABSTRACT

Several symptoms are present in the Behçet Syndrome, including oral ulcers, genital ulcers, skin lesions, eye injuries, severe problems such as meningitis, blood clots Inflammation of the digestive system and blindness can also occur. The Behçet Syndrome mainly affects countries of the Mediterranean basin, but it can also affect the Middle East, and the Far East, for instance. The prevalence in Western Europe and the United States is between 0.6 to 5.2 people per 100,000 inhabitants. The cause of Behçet Syndrome is still unknown, although some factors such as genetics, and that the environment may play a role. Currently, there is no cure for the Behçet Syndrome and the treatments are focused on alleviating the pain and preventing severe problems. Apremilast was approved by the FDA for the treatment of psoriatic arthritis and moderate to severe plaque psoriasis. Since 2019 it has also been used for the treatment of oral ulcers associated with Behçet's disease and there have been successful results in pain relief within a few weeks. However, further studies should be conducted.

Abbreviations: APR: Apremilast; AUC: Area Under The Curve; BD: Behçet Syndrome/ Behçet Disease; BDCAF: Behçet's Disease Current Activity Form; BDQOL: Behçet's Disease Quality of Life; BSAS: Behçet Syndrome Activity Score; CSs: Systemic Corticosteroids; IL: Interleukin; INF: Interferon; ISG: International Study Group; TNFα: Tumor Necrosis Factor-Alpha; USFDA: United States Food and Drug Administration

Mini Review

Behçet Syndrome (BD) is a disease characterized by complex, recurrent chronic and remitting inflammatory vasculitis of unknown etiology. It presents with recurrent episodes of oral, genital ulcers, skin lesions, eye injuries, among others [1], and it can cause more serious problems such as meningitis, blood clots, inflammation of the digestive system and blindness [2]. This disease can start with one or two of the symptoms indicated above, but as time passes, the rest of the symptoms are gradually triggered [3]. BD is known as the Silk Road disease because it affects all the countries of the Mediterranean Basin, the Middle East, and the Far East, although due to migratory movements it has become universal [4]. The highest prevalence occurs in countries such as Turkey (80-370 people per 100,000 population) [5] followed by Iran (80 people per 100,000 population) [6]. In Israel, Iraq, Saudi Arabia, China and Japan the prevalence is between 11.9 and 20 people per 100,000 inhabitants [7-10], while in Western Europe and the United States the prevalence is between 0.6 to 5.2 people per 100,000 inhabitants. It is noted that the prevalence in these countries increases depending on whether people are direct descendants of Middle Eastern countries [11-14] (Figure 1).

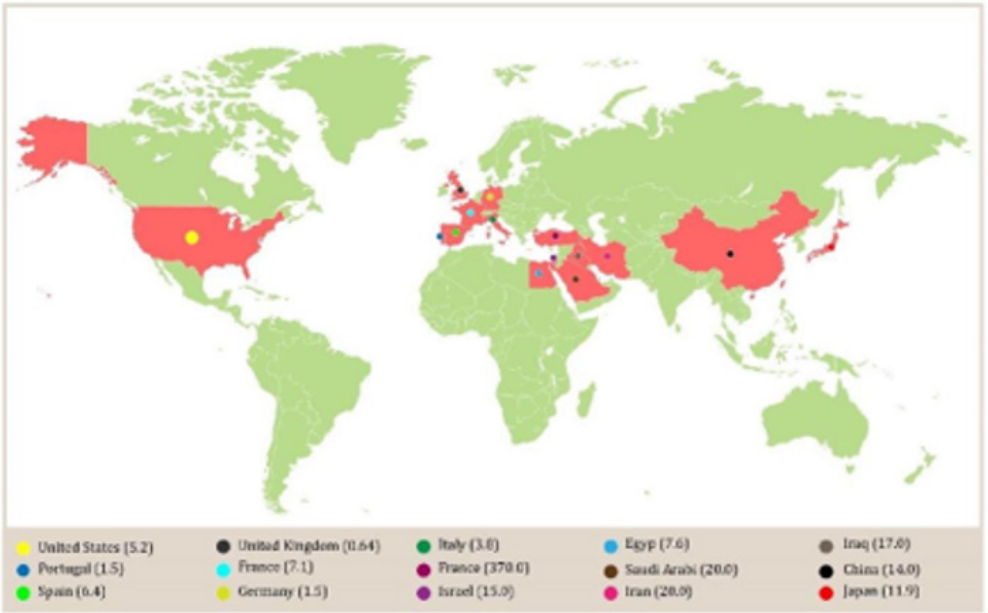

Figure 1: Prevalence of Behçet syndrome. Prevalence showed as with Behçet syndrome per 100 000 of population.

Although genetic and environmental factors are directly involved in the pathogenesis of BD, the main cause is still unknown, despite it being believed that the disease is due to an autoimmune process triggered by an infectious or environmental agent in a person who is genetically predisposed [15]. T cells have been found to be the major lymphocytes implicated in the pathogenesis of BD, and the IL-8 produced by T cells has been correlated with disease activity (including vascular) [16,17]. BD has also been considered an autoinflammatory disease [18] and this is corroborated due to the similarities with Crohn's Disease, which is considered an autoinflammatory disease [19,20]. A genome study conducted in BD patients reported an association for BD of Interleukin 4 (IL-4), Intelerukin 10 (IL-10), Interleukin 12 (IL-12), Interleukin 13 (IL-13), Interferon-γ (INF-γ) and IL23R – IL12RB2 loci. Similarly, two associations were identified in the 1p31.3 (IL23R-IL12RB2) and 1q32.1 (IL10) chromosomes, which predispose people with BD [21,22]. BD is associated with a range between IL23R and IL12RB2. An increase in Th1, Th17, CD4 + and CD8 + T cells was also found, and activity was observed in γδ + T cells in both serum and tissues of diagnosed patients with BD, suggesting that innate and adaptive immunity are involved in the pathogenesis of this disease [23,24]. The diagnosis of BD is not easy to detect in patients with oligosymptomatology. However, many authors apply their criteria or a combination thereof with the diagnostic criteria issued by the International Study Group (ISG). These criteria consist of the identification of clinical characteristics such as oral ulcers, genital ulcers, eye injuries, skin lesions and the pathergy test (Table 1). 97-99% of the cases detected with BD, mucocutaneous lesions represent the distinctive clinical manifestation, and genital ulcerations represent 85% [25-27].

Table 1: International Study Group Diagnostic Criteria for Behçet's Disease. Adapted from [25].

Criteria	Descriptions
Recurrent oral ulcerations	Minor aphthous, major aphthous, or herpetiform ulceration observed by physician or patient, which recurred at least 3 times in one 12-month period.
Plus 2 of the Following Criteria in the Absence of Other Clinical Explanations:	
Recurrent genital ulceration	Aphthous ulceration or scarring, observed by physician or patient.
Eye lesions	Anterior uveitis, posterior uveitis, or cells in vitreous on slit-lamp examination; or retinal vasculitis observed by an ophthalmologist.
Skin lesions	Erythema nodosum observed by physicians or patients, pseudo-folliculitis, or papulopustular lesions; or Acneiform nodules observed by physician in post- adolescent patients, not on corticosteroid treatment.
Positive pathergy test	Read by a physician at 24-48 h.

Currently, there is no cure for BD, however, there have been studies with various drugs to focus treatment on reducing pain and preventing more serious problems. For example, first-line therapy for the treatment of clinical manifestations such as mucocutaneous injuries includes colchicine and corticosteroids [28,29] has come forward. The effect of colchicine has been evaluated in some studies

for the treatment of BD. In one carried out by Davatchi et al with a total of 169 patients who met the international criteria for Behçet's disease, they were administered colchicine (1mg/tablet) at night for 4 months. Patients were randomized to colchicine or placebo; the results showed an improvement in oral and genital ulcers, pseudofolliculitis and erythema nodosum in patients who were treated with colchicine, that is, this drug significantly improved overall symptoms of the disease [30]. Systemic Corticosteroids (CSs) in many cases have been used for the treatment of BD, it is the case of Prednisolone that is used in doses of 0.5 - 1 mg/kg [31]. In a study carried out with 54 prescribed patients with intestinal BD, they were treated with CS and showed encouraging results due to complete remission of the disease in 46.3% of cases, unfortunately, after one year, 35.2% of patients showed corticosteroid dependence [32]. Corticosteroids are used to treat several of the manifestations of BD. However, many patients become resistant or dependent. Alpsoy et al determined the therapeutic efficacy of interferon α-2a for the treatment of BD, especially for mucocutaneous lesions, demonstrating its effectiveness [33]. Lesions that are resistant to these treatments include azathioprine, rituximab, rebamipide [34-37]. In addition, immunosuppressive drug combined therapies are used as they have demonstrated to be effective as interferon-α (INF-α), thalidomide, and blocking agents of tumor necrosis factor-alpha (TNFα) such as infliximab [38].

Apremilast as Treatment of Oral Ulcers Manifested in Behçet Syndrome

Apremilast (APR) is a small molecule approved by the United States Food and Drug Administration (USFDA) for the treatment of adults with psoriatic arthritis and moderate to severe plaque psoriasis and since 2019 it has been approved for the treatment of oral ulcers associated with Behçet's disease [39]. Clinical studies developed with apremilast have demonstrated its efficacy and safety against oral ulcers in BD patients [40]. A phase II clinical trial conducted in hospitals in Turkey and the United States between 2009 and 2011, with a total of 111 patients who met the criteria of the International Group for Behçet's Disease, mean age of between 37.3 ± 0.4 and a mean number of oral ulcers per patient at the start of the study of 3.1 ± 1.3 in the APR group and 3.2 ± 2.1 in the placebo group. Treatment consisted of the 30 mg dose of apremilast twice a day for 12 weeks and thereafter a 28-day observation after treatment. As a result, a significant reduction of oral ulcerations was obtained in the group treated with APR as opposed to the placebo group (0.5±1.0 vs. 2.1±2.6, p<0.001) [41-44]. Subsequently, between 2014 and 2017, a global study was conducted involving 53 centers in 10 countries that included Asia, Europe, the United States, Israel, Lebanon and Turkey. A total of 207 prescribed BD patients participated and in a 1:1 ratio they were randomly administered 30 mg of APR twice daily and placebo, for 12 weeks. This trial allowed the evaluation of the efficacy, tolerability and safety of APR. The main endpoint was the Area Under The Curve (AUC) for the number of oral ulcers up to 12 weeks. As a result, a significantly lower number of these ulcers was obtained for the group treated with APR compared to the control group, also, the reduction in pain evidenced the efficacy of the drug in the first weeks of treatment. Nausea, vomiting, abdominal pain, and diarrhea were some of the adverse reactions that the group treated with APR presented [45-47]. Recent studies carried out by Luca et al evaluated the efficacy and safety of Apremilast in 12 patients with BD who had recurrent ulcerations and/or intolerance to conventional therapies. Those who had uveitis and gastrointestinal involvement were excluded. The study demonstrated the efficacy of apremilast for oral ulcers and overall disease activity based on the Behçet Syndrome Activity Score (BSAS), Behçet's Disease Current Activity Form (BDCAF), Visual Analog Scale (VAS) and changes in the Behçet's Disease Quality of Life (BDQOL) at week 12. Diarrhea in three patients and suicidal ideation in one were the main adverse effects that occurred, which limited the study, so it was decided to suspend administration [48]. A retrospective study carried out by Lopalco et al in Italy, demonstrated the effectiveness of apremilast in obtaining clinical results similar to Luca et al, in 13 patients with BD who presented oral and genital ulcers refractory to multiple treatments, including TNF inhibitors [49].

Conclusion

Due to the nature of Behçet's disease, the studies carried out with apremilast suggest its employability in the treatment. However, it is necessary to carry out long-term studies and also evaluate other possible pharmaceutical forms and administration routes of the drug to improve its bioavailability.

Acknowledgement

We thank the Institute of Nanoscience and Nanotechnology (IN2UB) of the University of Barcelona for their support. The authors also want to thank Harry Paul for the English Language Editing.

Conflicts of Interest

There are no conflicts of interest to declare.

References

1. Emmi G, Bettiol A, Silvestri E, Di Scala G, Becatti M, et al. (2019) Vascular Behçet's Syndrome: An Update. Intern Emerg Med 14 (5): 645-652.
2. Nair J, Moots R (2017) Behcet's Disease. Clinical Medicine 17(1): 71-77.
3. Arayssi T (2004) New Insights into the Pathogenesis and Therapy of Behçet's Disease. Current Opinion in Pharmacology 4(2): 183-188.
4. Yazici H, Seyahi E, Hatemi G, Yazici Y (2018) Behçet Syndrome: A Contemporary View. Nat Rev Rheumatol 14(2): 107-119.
5. Ceylan Kalın Z, Sarıcaoğlu H, Yazici S, Aydoğan K, Bülbül Başkan E (2019) Clinical and Demographical Characteristics of Familial Behçet's Disease (Southeast Marmara Region). Dermatology 235(5): 407-412.

6. Davatchi F, Shahram F, Chams-Davatchi C, Shams H, Abdolahi BS, et al. (2019) Behcet's Disease in Iran: Analysis of 7641 Cases. Modern Rheumatology 29(6): 1023-1030.
7. Muhaya M, Lightman S, Ikeda E, Mochizuki M, Shaer B, et al. (2000) Behçet's Disease in Japan and in Great Britain: A Comparative Study. Ocul Immunol Inflamm 8(3): 141-148.
8. Chen Y, Cai J-F, Lin C-H, Guan J-L (2019) Demography of Vascular Behcet's Disease with Different Gender and Age: An Investigation with 166 Chinese Patients. Orphanet J Rare Dis 14(1): 88.
9. Alkazzaz AMH, Ebdan WR, Ghoben Mustafa K, Kareem ZT, Al-Harbi SJO (2020) Behçet's Disease in Iraq: New Insights into the Clinical and Epidemiologic Features in Middle-Euphrates Region. Expert Review of Clinical Immunology 16(1): 109-112.
10. Liu X, Gao F, Zhao C, Zhang M (2020) Clinical Features of Patients with Behcet's Uveitis. Chinese Journal of Ophthalmology 56(3): 217-223.
11. Sota J, Rigante D, Emmi G, Lopalco G, Orlando I, et al. (2020) Behçet's Syndrome in Italy: A Detailed Retrospective Analysis of 396 Cases Seen in 3 Tertiary Referral Clinics. Intern Emerg Med 15(6):1031-1039.
12. Wessman LL, Andersen LK, Davis MDP (2018) Incidence of Diseases Primarily Affecting the Skin by Age Group: Population-Based Epidemiologic Study in Olmsted County, Minnesota, and Comparison with Age-Specific Incidence Rates Worldwide. Int J Dermatol 57(9): 1021-1034.
13. Toledo-Samaniego N, Galeano-Valle F, Ascanio-Palomares P, González-Martínez B, Valencia-Kruszyna A, et al. (2020) Manifestaciones neurológicas en la enfermedad de Behçet: estudio de 57 pacientes. Medicina Clínica 154(12): 488-492.
14. Borhani-Haghighi A, Kardeh B, Banerjee S, Yadollahikhales G, Safari A, et al. (2020) Neuro-Behcet's Disease: An Update on Diagnosis, Differential Diagnoses, and Treatment. Multiple Sclerosis and Related Disorders 39: 101906.
15. Pay S, Şimşek İ, Erdem H, Dinç A (2007) Immunopathogenesis of Behçet's Disease with Special Emphasize on the Possible Role of Antigen Presenting Cells. Rheumatol Int 27(5): 417-424.
16. Greco A, De Virgilio A, Ralli M, Ciofalo A, Mancini P, et al. (2018) Behçet's Disease: New Insights into Pathophysiology, Clinical Features and Treatment Options. Autoimmunity Reviews 17(6): 567-575.
17. Zouboulis ChC, Katsantonis J, Ketteler R, Treudler R, Kaklamani E, et al. (2000) Adamantiades-Behçet's Disease: Interleukin-8 Is Increased in Serum of Patients with Active Oral and Neurological Manifestations and Is Secreted by Small Vessel Endothelial Cells. Archives of Dermatological Research 292(6): 279-284.
18. Gül A (2005) Behçet's Disease as an Autoinflammatory Disorder. Curr Drug Targets Inflamm Allergy 4(1): 81-83.
19. Valenti S, Gallizzi R, De Vivo D, Romano C (2017) Intestinal Behçet and Crohn's Disease: Two Sides of the Same Coin. Pediatr Rheumatol 15(1): 33.
20. Direskeneli H (2006) Autoimmunity vs Autoinflammation in Behcet's Disease: Do We Oversimplify a Complex Disorder? Rheumatology 45(12): 1461-1465.
21. Mizuki N, Meguro A, Ota M, Ohno S, Shiota T, et al. (2010) Genome-Wide Association Studies Identify IL23R-IL12RB2 and IL10 as Behçet's Disease Susceptibility Loci. Nat Genet 42(8): 703-706.
22. Aridogan BC, Yildirim M, Baysal V, Inaloz HS, Baz K, et al. (2003) Serum Levels of IL-4, IL-10, IL-12, IL-13 and FN-Gamma in Behçet's Disease. The Journal of Dermatology 30(8): 602-607.
23. Cho JH, Brant SR (2011) Recent Insights Into the Genetics of Inflammatory Bowel Disease. Gastroenterology 140(6): 1704-1712.
24. Remmers EF, Cosan F, Kirino Y, Ombrello MJ, Abaci N, et al. (2010) Genome-Wide Association Study Identifies Variants in the MHC Class I, IL10, and IL23R-IL12RB2 Regions Associated with Behçet's Disease. Nat Genet 42(8): 698-702.
25. (1990) International Study Group for Behcet's Disease. Criteria for Diagnosis of Behcet's Disease. The Lancet 335(8697): 1078-1080.
26. Kaklamani VG, Vaiopoulos G, Kaklamanis PG (1998) Behçet's Disease. Semin Arthritis Rheum 27(4): 197-217.
27. Al-Araji A, Kidd DP (2009) Neuro-Behçet's Disease: Epidemiology, Clinical Characteristics, and Management. The Lancet Neurology 8(2): 192-204.
28. Cabras M, Carrozzo M, Gambino A, Broccoletti R, Sciascia S, et al. (2020) Value of Colchicine as Treatment for Recurrent Oral Ulcers: A Systematic Review. J Oral Pathol Med 49(8): 731-740.
29. Djaballah-Ider F, Touil-Boukoffa C (2020) Effect of Combined Colchicine-Corticosteroid Treatment on Neutrophil/Lymphocyte Ratio: A Predictive Marker in Behçet Disease Activity. Inflammopharmacol 28(4): 819-829.
30. Davatchi F, Sadeghi Abdollahi B, Tehrani Banihashemi A, Shahram F, Nadji A, et al. (2009) Colchicine versus Placebo in Behçet's Disease: Randomized, Double-Blind, Controlled Crossover Trial. Modern Rheumatology 19(5): 542-549.
31. Kim DH, Cheon JH (2016) Intestinal Behçet's Disease: A True Inflammatory Bowel Disease or Merely an Intestinal Complication of Systemic Vasculitis? Yonsei Med J 57(1): 22-32.
32. Park JJ, Kim WH, Cheon JH (2013) Outcome Predictors for Intestinal Behçet's Disease. Yonsei Med J 54(5): 1084-1090.
33. Alpsoy E, Durusoy C, Yilmaz E, Ozgurel Y, Ermis O, et al. (2002) Interferon Alfa-2a in the Treatment of Behçet Disease: A Randomized Placebo-Controlled and Double-Blind Study. Arch Dermatol 138(4): 467-471.
34. Melikoglu M, Fresko I, Mat C, Ozyazgan Y, Gogus F, et al. (2005) Short-Term Trial of Etanercept in Behçet's Disease: A Double Blind, Placebo Controlled Study. J Rheumatol 32(1): 98-105.
35. Matsuda T, Ohno S, Hirohata S, Miyanaga Y, Ujihara H, et al. (2003) Efficacy of Rebamipide as Adjunctive Therapy in the Treatment of Recurrent Oral Aphthous Ulcers in Patients with Behçet's Disease. Drugs R&D 4(1): 19-28.
36. Saleh Z, Arayssi T (2014) Update on the Therapy of Behçet Disease. Therapeutic Advances in Chronic Disease 5(3): 112-134.
37. Yazici H, Pazarli H, Barnes CG, Tüzün Y, Özyazgan Y, et al. (1990) A Controlled Trial of Azathioprine in Behçet's Syndrome. The New England Journal of Medicine 322(5): 281-285.
38. Arida A, Fragiadaki K, Giavri E, Sfikakis PP (2011) Anti-TNF Agents for Behçet's Disease: Analysis of Published Data on 369 Patients. Seminars in Arthritis and Rheumatism 41(1): 61-70.
39. Zerilli T, Ocheretyaner E (2015) Apremilast (Otezla): A New Oral Treatment for Adults with Psoriasis and Psoriatic Arthritis. Drug Forecast 40(8): 495-500.
40. Takeno M (2020) Positioning of Apremilast in Treatment of Behçet's Disease. Modern Rheumatology 30(2): 219-224.
41. Hatemi G, Melikoglu M, Tunc R, Korkmaz C, Turgut Ozturk B, et al. (2015) Apremilast for Behçet's Syndrome-A Phase 2, Placebo-Controlled Study. N Engl J Med 372(16): 1510-1518.
42. Giácaman von der Weth MM, Tapial JM, Guillén BF, Ferrer DS, Sánchez-Carazo JL, et al. (2020) Complex Aphthae Treated With Apremilast. JCR: Journal of Clinical Rheumatology 26(3): e69-e70.
43. Cetin Gedik K, Romano M, Berard RA, Demirkaya E (2020) An Overview of Conventional and Recent Treatment Options for Behcet's Disease. Curr Treat Options in Rheum 6(17).

44. Maloney NJ, Zhao J, Tegtmeyer K, Lee EY, Cheng K (2020) Off-Label Studies on Apremilast in Dermatology: A Review. Journal of Dermatological Treatment 31(2): 131-140.

45. Hatemi G, Mahr A, Ishigatsubo Y, Song Y-W, Takeno M, et al. (2019) Trial of Apremilast for Oral Ulcers in Behçet's Syndrome. N Engl J Med 381(20): 1918-1928.

46. Leccese P, Ozguler Y, Christensen R, Esatoglu SN, Bang D, et al. (2019) Management of Skin, Mucosa and Joint Involvement of Behçet's Syndrome: A Systematic Review for Update of the EULAR Recommendations for the Management of Behçet's Syndrome. Seminars in Arthritis and Rheumatism 48(4): 752-762.

47. Onuora S (2020) Apremilast Reduces Behçet Oral Ulcers. Nature Reviews Rheumatology 16(2): 62.

48. De Luca G, Cariddi A, Campochiaro C, Vanni D, Boffini N, et al. (2020) Efficacy and Safety of Apremilast for Behçet's Syndrome: A Real-Life Single-Centre Italian Experience. Rheumatology 59(1): 171-175.

49. Lopalco G, Venerito V, Leccese P, Emmi G, Cantarini L, et al. (2019) Real-World Effectiveness of Apremilast in Multirefractory Mucosal Involvement of Behçet's Disease. Ann Rheum Dis 78(12): 1736-1737.

ISSN: 2574-1241

DOI: 10.26717/BJSTR.2021.34.005605

Mireia Mallandrich. Biomed J Sci & Tech Res

6.2. Comunicación

Evento:	*Skin Forum 2022 Annual Meeting*
Lugar:	Malmö, Suecia
Fecha:	21-22 Junio 2022

Afiliaciones:

a Department of Pharmacy, Pharmaceutical Technology and Physical-chemistry, University of Barcelona, Avda. Joan XXIII, 08028 Barcelona, Spain.

b Departamento de Química y Ciencias Exactas, Universidad Técnica Particular de Loja, 1101608, Loja, Ecuador.

c Institute of Nanoscience and Nanotechnology (IN2UB), University of Barcelona, 08028 Barcelona, Spain.

Efficacy evaluation of a Microemulsion loaded with Apremilast for the Rosacea treatment

Paulo Sarango-Granda[a,b,c], Lupe Carolina Espinoza[b,c], Mireia Mallandrich[a], Ana Calpena[a,c]

[a] Department of Pharmacy, Pharmaceutical Technology and Physical-chemistry, University of Barcelona, Avda. Joan XXIII, 08028 Barcelona, Spain.

[b] Departamento de Química y Ciencias Exactas, Universidad Técnica Particular de Loja, 1101608, Loja, Ecuador.

[c] Institute of Nanoscience and Nanotechnology (IN2UB), University of Barcelona, 08028 Barcelona, Spain.

Apremilast (APR) is an orally administered selective phosphodiesterase 4 inhibitor for the treatment of moderate to severe plaque psoriasis and active psoriatic arthritis. The low solubility and permeability of this drug make its dermal administration difficult. In preliminary studies, an apremilast-loaded microemulsion (APR-ME) was designed and characterized as a topical therapy for local skin inflammation. The results obtained in that study demonstrated an anti-inflammatory potential due to the decrease in IL-6 and IL-8 in an *in vitro* model and a decrease in IL-8, IL-17A and TNF cytokines in *in vivo* models with experimental animals. The objective of this study is to evaluate the topical anti-inflammatory potential of a microemulsion loaded with apremilast for the treatment of rosacea. For this, experimental models with rabbits were made. Inflammatory processes similar to those produced by rosacea were induced and APR-ME (1.5 mg/mL) was treated. The efficacy was evaluated through the concentrations of IL-6 and IL-8 present in rabbit tissue samples by the qPCR technique. Likewise, *in vivo*, a colorimetric evaluation was carried out to assess the physical change produced in the animal's skin. Finally, histological samples extracted from each animal after death were evaluated. The results obtained showed that the levels of IL-6 and IL-8 were decreased in the groups treated with APR-ME and the Reference product, the colorimetric evaluations showed that after exposure to APR-ME and the reference product, the physical condition of the skin surface after the decrease in redness, at the histological level there was also evidence of a decrease in inflammation and cellular infiltration, all these parameters evaluated were compared with a positive control group. Therefore, a

potential treatment for rosacea with the use of a microemulsion loaded with apremilast was evidenced.

References:

Sarango-Granda, P., Silva-Abreu, M., Calpena, A. C., Halbaut, L., Fábrega, M.-J., Rodríguez-Lagunas, M. J., Díaz-Garrido, N., Badia, J., & Espinoza, L. C. (2020). Apremilast Microemulsion as Topical Therapy for Local Inflammation: Design, Characterization and Efficacy Evaluation. Pharmaceuticals, 13(12), 484. https://doi.org/10.3390/ph13120484

Muto, Y., Wang, Z., Vanderberghe, M., Two, A., Gallo, R. L., & Di Nardo, A. (2014). Mast Cells Are Key Mediators of Cathelicidin-Initiated Skin Inflammation in Rosacea. Journal of Investigative Dermatology, 134(11), 2728-2736. https://doi.org/10.1038/jid.2014.222

EFFICACY EVALUATION OF A MICROEMULSION LOADED WITH APREMILAST FOR THE ROSACEA TREATMENT

Paulo Sarango-Granda[1,2,3], Lupe Carolina Espinoza[2], Mireia Mallandrich[1], Ana Calpena-Campmany [1,3]

[1] Department of Pharmacy, Pharmaceutical Technology, and Physical Chemistry, Faculty of Pharmacy and Food Sciences, University of Barcelona, Av. Joan XXIII 29-31, 08028 Barcelona, Spain
[2] Departamento de Química, Universidad Técnica Particular de Loja, 1101608 Loja, Ecuador.
[3] Institute of Nanoscience and Nanotechnology (IN2UB), University of Barcelona, 08028 Barcelona, Spain.

INTRODUCTION

Rosacea is a chronic disease that affects the skin and sometimes the eyes. It causes skin redness and pimples. Rosacea is more common among women and fair-skinned people. It usually affects middle-aged and older adults. In most cases, rosacea only affects the face. In most cases, rosacea only affects the face. Symptoms may include: Frequent redness of the face small red lines under the skin, acne, swelling of the nose, thickened skin, usually on the forehead, chin and cheeks. Many people with rosacea also have eye symptoms, such as redness, dryness, and itching. Sometimes eye problems occur. The cause of rosacea is not known. You may be more likely to have it if you redden easily or if rosacea runs in your family. Rosacea is not dangerous. There is no cure, but treatments can help. These include medicines and sometimes surgery [1]. Apremilast (APR) is an orally administered selective phosphodiesterase 4 inhibitor for the treatment of moderate to severe plaque psoriasis and active psoriatic arthritis. In preliminary studies [2], an apremilast-loaded microemulsion (APR-ME) was designed and characterized as a topical therapy for local skin inflammation.

AIM

The aim of this study is to evaluate the topical anti-inflammatory potential of a microemulsion loaded with apremilast for the treatment of rosacea.

MATERIALS AND METHODS

❑ ***Inflammation induction***

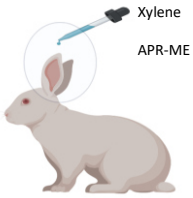

Xylene to inflame and APR-ME as treatment

❑ ***Microemulsion preparation***

APR-ME was prepared by titration method

❑ ***Colorimetric evaluation***

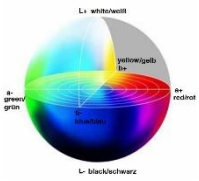

❑ ***Pro-Inflammatory cytokines***

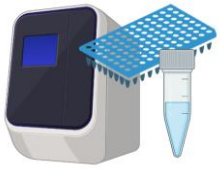

❑ ***Histological studies***

RESULTS

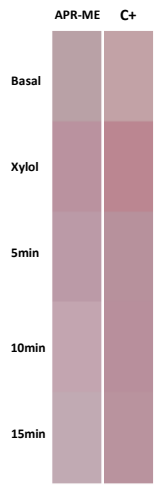

❑ ***Colorimetric evaluation***

	TREATMENT			CONTROL		
	R	G	B	R	G	B
BASAL	185	161	166	194	162	166
	178 - 205	153 - 173	159 - 171	188 - 208	152 - 175	159 - 177
XYLOL	186	146	159	187	134	145
	182 - 188	142 - 149	156 - 161	180 - 190	131 - 145	144 - 154
5 min	187	154	167	183	145	156
	186 - 188	148 - 155	162 - 167	180 - 183	141 - 147	152 - 161
10 min	195	165	176	184	143	156
	194 - 196	163 - 166	174 - 177	182 - 188	142 - 146	156 - 158
15 min	193	170	179	185	147	158
	183 - 196	149 - 171	162 - 180	183 - 188	146 - 150	157 - 161

❑ ***Pro-Inflammatory cytokines***

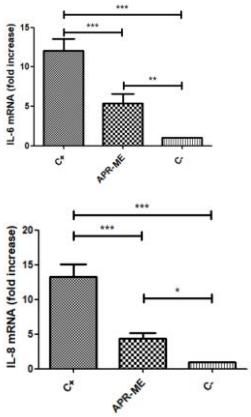

❑ ***Histological studies***

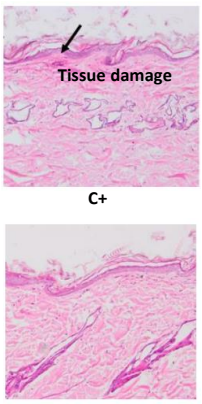

CONCLUSIONS

The results obtained showed that the levels of IL-6 and IL-8 were decreased in the groups treated with APR-ME, the colorimetric evaluations showed that after exposure to APR-ME, the physical condition of the skin surface after the decrease in redness, at the histological level there was also evidence of a decrease in inflammation and cellular infiltration, all these parameters evaluated were compared with a positive control group. Therefore, a potential treatment for rosacea with the use of a microemulsion loaded with apremilast was evidenced.

REFERENCES

1. Y., Wang, Z., Vanderberghe, M., Two, A., Gallo, R. L., & Di Nardo, A. (2014). Mast Cells Are Key Mediators of Cathelicidin-Initiated Skin Inflammation in Rosacea. Journal of Investigative Dermatology, 134(11), 2728-2736.
2. Sarango-Granda, P., Silva-Abreu, M., Calpena, A. C., Halbaut, L., Fábrega, M.-J., Rodríguez-Lagunas, M. J., Díaz-Garrido, N., Badia, J., & Espinoza, L. C. (2020). Apremilast Microemulsion as Topical Therapy for Local Inflammation: Design, Characterization and Efficacy Evaluation. Pharmaceuticals, 13(12), 484.

Skin Forum international skin science network

UNIVERSITAT DE BARCELONA

REFERENCIAS

1. Arts RJW, Joosten LAB, Netea MG. The Potential Role of Trained Immunity in Autoimmune and Autoinflammatory Disorders. Front Immunol [Internet]. 2018 [citado 28 de septiembre de 2022];9. Disponible en: https://www.frontiersin.org/articles/10.3389/fimmu.2018.00298
2. Isailovic N, Daigo K, Mantovani A, Selmi C. Interleukin-17 and innate immunity in infections and chronic inflammation. J Autoimmun. junio de 2015;60:1-11.
3. Ollen-Bittle N, Roseborough AD, Wang W, Wu JLD, Whitehead SN. Mechanisms and Biomarker Potential of Extracellular Vesicles in Stroke. Biology. 18 de agosto de 2022;11(8):1231.
4. Cristobo Bravo T, Quirós Viqueira O, Rodríguez Bencomo D. Actualización en la detección y manejo de la sepsis en el menor de un año. Rev Arch Méd Camagüey. octubre de 2015;19(5):512-27.
5. Wang WY, Tan MS, Yu JT, Tan L. Role of pro-inflammatory cytokines released from microglia in Alzheimer's disease. Ann Transl Med. junio de 2015;3(10):136.
6. Devarajan A, Shih D, Reddy ST. Inflammation, Infection, Cancer and All That…The Role of Paraoxonases. En: Camps J, editor. Oxidative Stress and Inflammation in Non-communicable Diseases - Molecular Mechanisms and Perspectives in Therapeutics [Internet]. Cham: Springer International Publishing; 2014 [citado 28 de septiembre de 2022]. p. 33-41. (Advances in Experimental Medicine and Biology). Disponible en: https://doi.org/10.1007/978-3-319-07320-0_5
7. Uttara B, Singh AV, Zamboni P, Mahajan RT. Oxidative stress and neurodegenerative diseases: a review of upstream and downstream antioxidant therapeutic options. Curr Neuropharmacol. marzo de 2009;7(1):65-74.
8. Anwikar S, Bhitre M. Study of the synergistic anti-inflammatory activity of Solanum xanthocarpum Schrad and Wendl and Cassia fistula Linn. Int J Ayurveda Res. julio de 2010;1(3):167-71.
9. González JRR. Inmunología: Biología y patología del sistema inmunitario. Editorial Médica Panamericana S.A.; 2010. 276 p.
10. Taylor FB. Staging of the pathophysiologic responses of the primate microvasculature to Escherichia coli and endotoxin: examination of the elements of the compensated response and their links to the corresponding uncompensated lethal variants. Crit Care Med. julio de 2001;29(7 Suppl):S78-89.
11. Fedosov DA, Gompper G. White blood cell margination in microcirculation. Soft Matter. 7 de mayo de 2014;10(17):2961-70.

12. Wilkinson PC. Chemotaxis. En: Delves PJ, editor. Encyclopedia of Immunology (Second Edition) [Internet]. Oxford: Elsevier; 1998 [citado 5 de enero de 2023]. p. 533-7. Disponible en: https://www.sciencedirect.com/science/article/pii/B012226765600150X
13. Gibson NJ. Cell adhesion molecules in context: CAM function depends on the neighborhood. Cell Adhes Migr. 2011;5(1):48-51.
14. Håkansson L, Adell G, Boeryd B, Sjögren F, Sjödahl R. Infiltration of mononuclear inflammatory cells into primary colorectal carcinomas: an immunohistological analysis. Br J Cancer. 1997;75(3):374-80.
15. Fleit HB. Chronic Inflammation. En: McManus LM, Mitchell RN, editores. Pathobiology of Human Disease [Internet]. San Diego: Academic Press; 2014 [citado 5 de enero de 2023]. p. 300-14. Disponible en: https://www.sciencedirect.com/science/article/pii/B9780123864567018086
16. Lonkar P, Dedon PC. Reactive species and DNA damage in chronic inflammation: reconciling chemical mechanisms and biological fates. Int J Cancer. 1 de mayo de 2011;128(9):1999-2009.
17. Daniel PB, Walker WH, Habener JF. Cyclic AMP signaling and gene regulation. Annu Rev Nutr. 1998;18:353-83.
18. Miki H, Van Heerden JA, Fitzpatrick LA. Chapter 7 - The Parathyroid Gland:: Regulation of Production of Parathyroid Hormone. En: Bittar EE, Bittar N, editores. Principles of Medical Biology [Internet]. Elsevier; 1997 [citado 5 de enero de 2023]. p. 191-205. (Molecular and Cellular Endocrinology; vol. 10). Disponible en: https://www.sciencedirect.com/science/article/pii/S1569258297800347
19. Bolger GB. The cAMP-signaling cancers: Clinically-divergent disorders with a common central pathway. Front Endocrinol. 13 de octubre de 2022;13:1024423.
20. Kamenetsky M, Middelhaufe S, Bank EM, Levin LR, Buck J, Steegborn C. Molecular details of cAMP generation in mammalian cells: a tale of two systems. J Mol Biol. 29 de septiembre de 2006;362(4):623-39.
21. Grigorenko B, Polyakov I, Nemukhin A. Mechanisms of ATP to cAMP Conversion Catalyzed by the Mammalian Adenylyl Cyclase: A Role of Magnesium Coordination Shells and Proton Wires. J Phys Chem B. 23 de enero de 2020;124(3):451-60.
22. Calebiro D, Maiellaro I. cAMP signaling microdomains and their observation by optical methods. Front Cell Neurosci. 2014;8:350.
23. Perrot CY, Sawada J, Komatsu M. Prolonged activation of cAMP signaling leads to endothelial barrier disruption via transcriptional repression of RRAS. FASEB J Off Publ Fed Am Soc Exp Biol. 18 de mayo de 2018;32(11):fj201700818RRR.
24. Kang W, Park S, Choi D, Son B, Park T. Activation of cAMP Signaling in Response to α-Phellandrene Promotes Vascular Endothelial Growth Factor Levels and Proliferation in Human Dermal Papilla Cells. Int J Mol Sci. 11 de agosto de 2022;23(16):8959.
25. Aslam M, Ladilov Y. Emerging Role of cAMP/AMPK Signaling. Cells. 17 de enero de 2022;11(2):308.

26. Oliveira RF, Terrin A, Di Benedetto G, Cannon RC, Koh W, Kim M, et al. The role of type 4 phosphodiesterases in generating microdomains of cAMP: large scale stochastic simulations. PloS One. 22 de julio de 2010;5(7):e11725.
27. Martinez A, Gil C. cAMP-specific phosphodiesterase inhibitors: promising drugs for inflammatory and neurological diseases. Expert Opin Ther Pat. diciembre de 2014;24(12):1311-21.
28. Gerbaud P, Taskén K, Pidoux G. Spatiotemporal regulation of cAMP signaling controls the human trophoblast fusion. Front Pharmacol. 2015;6:202.
29. McCahill AC, Huston E, Li X, Houslay MD. PDE4 associates with different scaffolding proteins: modulating interactions as treatment for certain diseases. Handb Exp Pharmacol. 2008;(186):125-66.
30. Charov K, Burkart MD. Chapter Sixteen - Quantifying protein-protein interactions of the acyl carrier protein with solvatochromic probes. En: Chenoweth DM, editor. Methods in Enzymology [Internet]. Academic Press; 2020 [citado 6 de enero de 2023]. p. 321-40. (Chemical Tools for Imaging, Manipulating, and Tracking Biological Systems: Diverse Methods for Prokaryotic and Eukaryotic Systems; vol. 638). Disponible en: https://www.sciencedirect.com/science/article/pii/S0076687920301282
31. cAMP and cGMP Signaling Cross-Talk | Circulation Research [Internet]. [citado 6 de enero de 2023]. Disponible en: https://www.ahajournals.org/doi/10.1161/circresaha.106.144501
32. Lu H, Liu Y, Greenberg JT. Structure-function analysis of the plasma membrane- localized Arabidopsis defense component ACD6. Plant J Cell Mol Biol. diciembre de 2005;44(5):798-809.
33. Lee HY, Seo YE, Lee JH, Lee SE, Oh S, Kim J, et al. Plasma membrane-localized plant immune receptor targets H+ -ATPase for membrane depolarization to regulate cell death. New Phytol. enero de 2022;233(2):934-47.
34. Bang J, Zippin JH. Cyclic adenosine monophosphate (cAMP) signaling in melanocyte pigmentation and melanomagenesis. Pigment Cell Melanoma Res. 2021;34(1):28-43.
35. Wang ZZ, Zhang Y, Zhang HT, Li YF. Phosphodiesterase: an interface connecting cognitive deficits to neuropsychiatric and neurodegenerative diseases. Curr Pharm Des. 2015;21(3):303-16.
36. Lugnier C. Cyclic nucleotide phosphodiesterase (PDE) superfamily: a new target for the development of specific therapeutic agents. Pharmacol Ther. marzo de 2006;109(3):366-98.
37. Mackenzie KF, Topping EC, Bugaj-Gaweda B, Deng C, Cheung YF, Olsen AE, et al. Human PDE4A8, a novel brain-expressed PDE4 cAMP-specific phosphodiesterase that has undergone rapid evolutionary change. Biochem J. 15 de abril de 2008;411(2):361-9.
38. Li H, Zhang Y, Liu M, Fan C, Feng C, Lu Q, et al. Targeting PDE4 as a promising therapeutic strategy in chronic ulcerative colitis through modulating mucosal homeostasis. Acta Pharm Sin B. enero de 2022;12(1):228-45.

39. Michalski JM, Golden G, Ikari J, Rennard SI. PDE4: a novel target in the treatment of chronic obstructive pulmonary disease. Clin Pharmacol Ther. enero de 2012;91(1):134-42.
40. Dastidar SG, Rajagopal D, Ray A. Therapeutic benefit of PDE4 inhibitors in inflammatory diseases. Curr Opin Investig Drugs Lond Engl 2000. mayo de 2007;8(5):364-72.
41. Li H, Zuo J, Tang W. Phosphodiesterase-4 Inhibitors for the Treatment of Inflammatory Diseases. Front Pharmacol. 17 de octubre de 2018;9:1048.
42. Lu Q kai, Fan C, Xiang C gui, Wu B, Lu H min, Feng C lan, et al. Inhibition of PDE4 by apremilast attenuates skin fibrosis through directly suppressing activation of M1 and T cells. Acta Pharmacol Sin. febrero de 2022;43(2):376-86.
43. McDonough W, Aragon IV, Rich J, Murphy JM, Abou Saleh L, Boyd A, et al. PAN-selective inhibition of cAMP-phosphodiesterase 4 (PDE4) induces gastroparesis in mice. FASEB J Off Publ Fed Am Soc Exp Biol. septiembre de 2020;34(9):12533-48.
44. Furlan V, Bren U. Insight into Inhibitory Mechanism of PDE4D by Dietary Polyphenols Using Molecular Dynamics Simulations and Free Energy Calculations. Biomolecules. 23 de marzo de 2021;11(3):479.
45. Ong WK, Gribble FM, Reimann F, Lynch MJ, Houslay MD, Baillie GS, et al. The role of the PDE4D cAMP phosphodiesterase in the regulation of glucagon-like peptide-1 release. Br J Pharmacol. junio de 2009;157(4):633-44.
46. Moore MJ, Kanter JR, Jones KC, Taylor SS. Phosphorylation of the catalytic subunit of protein kinase A. Autophosphorylation versus phosphorylation by phosphoinositide-dependent kinase-1. J Biol Chem. 6 de diciembre de 2002;277(49):47878-84.
47. Su Y, Dostmann WR, Herberg FW, Durick K, Xuong NH, Ten Eyck L, et al. Regulatory subunit of protein kinase A: structure of deletion mutant with cAMP binding domains. Science. 11 de agosto de 1995;269(5225):807-13.
48. White M. Mediators of inflammation and the inflammatory process. J Allergy Clin Immunol. marzo de 1999;103(3 Pt 2):S378-381.
49. Sharma JN, Mohsin SS. The role of chemical mediators in the pathogenesis of inflammation with emphasis on the kinin system. Exp Pathol. 1990;38(2):73-96.
50. D SM, N M, G K. Topical drug delivery systems: a patent review. Expert Opin Ther Pat [Internet]. 2016 [citado 29 de septiembre de 2022];26(2). Disponible en: https://pubmed.ncbi.nlm.nih.gov/26651499/?myncbishare=iesubarclib&otool=iesubarclib
51. Fore J. A review of skin and the effects of aging on skin structure and function. Ostomy Wound Manage. 1 de septiembre de 2006;52(9):24-35; quiz 36-7.
52. Romanovsky AA. Skin temperature: its role in thermoregulation. Acta Physiol Oxf Engl. marzo de 2014;210(3):498-507.
53. Souto EB, Fangueiro JF, Fernandes AR, Cano A, Sanchez-Lopez E, Garcia ML, et al. Physicochemical and biopharmaceutical aspects influencing skin permeation and role of SLN and NLC for skin drug delivery. Heliyon. 1 de febrero de 2022;8(2):e08938.

54. Rustin MHA. Andrews' Diseases of the Skin - Clinical Dermatology. Postgrad Med J. noviembre de 1990;66(781):984.

55. Ibrahim AAE, Bagherani N, Smoller B, Bagherani N, Reyes-Barron C. Anatomy and Organization of Human Skin. En: Smoller B, Bagherani N, editores. Atlas of Dermatology, Dermatopathology and Venereology: Cutaneous Anatomy, Biology and Inherited Disorders and General Dermatologic Concepts [Internet]. Cham: Springer International Publishing; 2022 [citado 6 de enero de 2023]. p. 109-32. Disponible en: https://doi.org/10.1007/978-3-319-53811-2_3

56. Diegel KL, Danilenko DM, Wojcinski ZW. Chapter 24 - The Integumentary System. En: Wallig MA, Haschek WM, Rousseaux CG, Bolon B, editores. Fundamentals of Toxicologic Pathology (Third Edition) [Internet]. Academic Press; 2018 [citado 6 de enero de 2023]. p. 791-822. Disponible en: https://www.sciencedirect.com/science/article/pii/B9780128098417000253

57. Kolarsick PAJ, Kolarsick MA, Goodwin C. Anatomy and Physiology of the Skin. J Dermatol Nurses Assoc. agosto de 2011;3(4):203.

58. White SD, Yager JA. Resident Dendritic Cells in the Epidermis: Langerhans Cells, Merkel Cells and Melanocytes. Vet Dermatol. marzo de 1995;6(1):1-8.

59. Yousef H, Alhajj M, Sharma S. Anatomy, Skin (Integument), Epidermis. En: StatPearls [Internet]. Treasure Island (FL): StatPearls Publishing; 2022 [citado 13 de febrero de 2022]. Disponible en: http://www.ncbi.nlm.nih.gov/books/NBK470464/

60. Velasquez D, Pineda C, Cano M, Suarez N, Moises G, Usuga I, et al. Soluciones terapéuticas para la reconstrucción de la dermis y la epidermis. Oportunidades en el medio antioqueño. 1 de junio de 2008;2.

61. Kosodo Y, Huttner WB. Basal process and cell divisions of neural progenitors in the developing brain. Dev Growth Differ. abril de 2009;51(3):251-61.

62. Evans MJ. BASAL CELLS. En: Laurent GJ, Shapiro SD, editores. Encyclopedia of Respiratory Medicine [Internet]. Oxford: Academic Press; 2006 [citado 6 de enero de 2023]. p. 229-33. Disponible en: https://www.sciencedirect.com/science/article/pii/B0123708796000417

63. Joffe R, Plaza JA, Kajoian A. Tip Chapter: Histology and Physiology of the Skin. En: Costa AD, editor. Minimally Invasive Aesthetic Procedures : A Guide for Dermatologists and Plastic Surgeons [Internet]. Cham: Springer International Publishing; 2020 [citado 6 de enero de 2023]. p. 179-92. Disponible en: https://doi.org/10.1007/978-3-319-78265-2_26

64. Chu DH. Chapter 7. Development and Structure of Skin. En: Goldsmith LA, Katz SI, Gilchrest BA, Paller AS, Leffell DJ, Wolff K, editores. Fitzpatrick's Dermatology in General Medicine [Internet]. 8.ª ed. New York, NY: The McGraw-Hill Companies; 2012 [citado 6 de enero de 2023]. Disponible en: accessmedicine.mhmedical.com/content.aspx?aid=56021404

65. Michniak-Kohn BB, Wertz PW, Al-Khalili M, Meidan VM. 3 - Skin: Physiology and Penetration Pathways. En: Rosen MR, editor. Delivery System Handbook for Personal Care and Cosmetic Products [Internet]. Norwich, NY: William Andrew Publishing; 2005 [citado 6 de enero de

2023]. p. 77-100. (Personal Care & Cosmetic Technology). Disponible en: https://www.sciencedirect.com/science/article/pii/B9780815515043500080

66. Gay D, Plikus MV, Treffeisen E, Wang A, Cotsarelis G. Chapter 75 - Cutaneous Epithelial Stem Cells. En: Lanza R, Langer R, Vacanti J, editores. Principles of Tissue Engineering (Fourth Edition) [Internet]. Boston: Academic Press; 2014 [citado 6 de enero de 2023]. p. 1581-94. Disponible en: https://www.sciencedirect.com/science/article/pii/B9780123983589000756

67. Singh R. Basal Cells in the Epidermis and Epidermal Differentiation. Stem Cell Rev Rep. agosto de 2022;18(6):1883-91.

68. Wertz PW. Chapter 5 - Changes in Epidermal Lipids and Sebum Secretion with Aging. En: Dayan N, editor. Skin Aging Handbook [Internet]. Norwich, NY: William Andrew Publishing; 2009 [citado 6 de enero de 2023]. p. 91-104. (Personal Care & Cosmetic Technology). Disponible en: https://www.sciencedirect.com/science/article/pii/B9780815515845500090

69. Jalian HR, Takahashi S, Kim J. 7.32 - Overview of Dermatological Diseases. En: Taylor JB, Triggle DJ, editores. Comprehensive Medicinal Chemistry II [Internet]. Oxford: Elsevier; 2007 [citado 6 de enero de 2023]. p. 935-55. Disponible en: https://www.sciencedirect.com/science/article/pii/B008045044X002352

70. Monteiro-Riviere NA, Filon FL. Chapter 15 - Skin. En: Fadeel B, Pietroiusti A, Shvedova AA, editores. Adverse Effects of Engineered Nanomaterials (Second Edition) [Internet]. Academic Press; 2017 [citado 6 de enero de 2023]. p. 357-80. Disponible en: https://www.sciencedirect.com/science/article/pii/B978012809199900015X

71. Gilaberte Y, Prieto-Torres L, Pastushenko I, Juarranz Á. Chapter 1 - Anatomy and Function of the Skin. En: Hamblin MR, Avci P, Prow TW, editores. Nanoscience in Dermatology [Internet]. Boston: Academic Press; 2016 [citado 6 de enero de 2023]. p. 1-14. Disponible en: https://www.sciencedirect.com/science/article/pii/B978012802926800001X

72. Woo WM. Skin Structure and Biology. En: Imaging Technologies and Transdermal Delivery in Skin Disorders [Internet]. John Wiley & Sons, Ltd; 2019 [citado 6 de enero de 2023]. p. 1-14. Disponible en: https://onlinelibrary.wiley.com/doi/abs/10.1002/9783527814633.ch1

73. Scott DW, Miller WH. CHAPTER 1 - Structure and Function of the Skin. En: Scott DW, Miller WH, editores. Equine Dermatology (Second Edition) [Internet]. Saint Louis: W.B. Saunders; 2011 [citado 6 de enero de 2023]. p. 1-34. Disponible en: https://www.sciencedirect.com/science/article/pii/B9781437709209000019

74. Miller T. Chapter 14 - Clinical Testing to Uphold an Anti-aging Claim. En: Dayan N, editor. Skin Aging Handbook [Internet]. Norwich, NY: William Andrew Publishing; 2009 [citado 6 de enero de 2023]. p. 363-89. (Personal Care & Cosmetic Technology). Disponible en: https://www.sciencedirect.com/science/article/pii/B9780815515845500181

75. Lefèvre-Utile A, Braun C, Haftek M, Aubin F. Five Functional Aspects of the Epidermal Barrier. Int J Mol Sci. enero de 2021;22(21):11676.

76. Maynard RL, Downes N. Chapter 24 - The Skin or the Integument. En: Maynard RL, Downes N, editores. Anatomy and Histology of the Laboratory Rat in Toxicology and Biomedical Research [Internet]. Academic Press; 2019 [citado 6 de enero de 2023]. p. 303-15. Disponible en: https://www.sciencedirect.com/science/article/pii/B9780128118375000241

77. Haskell H. Introduction. En: Busam KJ, editor. Dermatopathology [Internet]. Philadelphia: W.B. Saunders; 2010 [citado 6 de enero de 2023]. p. 1-8. (Foundations in Diagnostic Pathology). Disponible en: https://www.sciencedirect.com/science/article/pii/B9780443066542000184

78. Boissy RE. The melanocyte. Its structure, function, and subpopulations in skin, eyes, and hair. Dermatol Clin. abril de 1988;6(2):161-73.

79. Barbieri JS, Wanat K, Seykora J. Skin: Basic Structure and Function. En: McManus LM, Mitchell RN, editores. Pathobiology of Human Disease [Internet]. San Diego: Academic Press; 2014 [citado 6 de enero de 2023]. p. 1134-44. Disponible en: https://www.sciencedirect.com/science/article/pii/B9780123864567035012

80. Fenner J, Clark RAF. Chapter 1 - Anatomy, Physiology, Histology, and Immunohistochemistry of Human Skin. En: Albanna MZ, Holmes IV JH, editores. Skin Tissue Engineering and Regenerative Medicine [Internet]. Boston: Academic Press; 2016 [citado 6 de enero de 2023]. p. 1-17. Disponible en: https://www.sciencedirect.com/science/article/pii/B9780128016541000012

81. Nguyen AV, Soulika AM. The Dynamics of the Skin's Immune System. Int J Mol Sci. enero de 2019;20(8):1811.

82. Blauvelt A. Langerhans Cells. En: Delves PJ, editor. Encyclopedia of Immunology (Second Edition) [Internet]. Oxford: Elsevier; 1998 [citado 6 de enero de 2023]. p. 1528-32. Disponible en: https://www.sciencedirect.com/science/article/pii/B0122267656004060

83. Maurer D, Stingl G. CHAPTER 5 - Langerhans cells. En: Lotze MT, Thomson AW, editores. Dendritic Cells (Second Edition) [Internet]. London: Academic Press; 2001 [citado 6 de enero de 2023]. p. 35-cp1. Disponible en: https://www.sciencedirect.com/science/article/pii/B9780124558519500444

84. Khan S, Ruutu M, Thomas R, Bhardwaj N. 9 - Dendritic Cells. En: Firestein GS, Budd RC, Gabriel SE, McInnes IB, O'Dell JR, editores. Kelley's Textbook of Rheumatology (Ninth Edition) [Internet]. Philadelphia: W.B. Saunders; 2013 [citado 6 de enero de 2023]. p. 117-133.e6. Disponible en: https://www.sciencedirect.com/science/article/pii/B9781437717389000098

85. Haniffa M, Collin M, Ginhoux F. Chapter One - Ontogeny and Functional Specialization of Dendritic Cells in Human and Mouse. En: Murphy KM, Merad M, editores. Advances in Immunology [Internet]. Academic Press; 2013 [citado 6 de enero de 2023]. p. 1-49. (Development and Function of Myeloid Subsets; vol. 120). Disponible en: https://www.sciencedirect.com/science/article/pii/B9780124170285000016

86. Sundberg JP, Nanney LB, Fleckman P, King LE. 23 - Skin and Adnexa. En: Treuting PM, Dintzis SM, editores. Comparative Anatomy and Histology [Internet]. San Diego: Academic Press; 2012

[citado 6 de enero de 2023]. p. 433-55. Disponible en: https://www.sciencedirect.com/science/article/pii/B9780123813619000238

87. Yousef H, Miao JH, Alhajj M, Badri T. Histology, Skin Appendages. En: StatPearls [Internet]. Treasure Island (FL): StatPearls Publishing; 2022 [citado 6 de enero de 2023]. Disponible en: http://www.ncbi.nlm.nih.gov/books/NBK482237/

88. Dellambra E, Dimri GP. Chapter 7 - Cellular Senescence and Skin Aging. En: Dayan N, editor. Skin Aging Handbook [Internet]. Norwich, NY: William Andrew Publishing; 2009 [citado 6 de enero de 2023]. p. 129-48. (Personal Care & Cosmetic Technology). Disponible en: https://www.sciencedirect.com/science/article/pii/B9780815515845500119

89. Prost-Squarcioni C, Fraitag S, Heller M, Boehm N. [Functional histology of dermis]. Ann Dermatol Venereol. enero de 2008;135(1 Pt 2):1S5-20.

90. Carroll RG. 2 - The Integument. En: Carroll RG, editor. Elsevier's Integrated Physiology [Internet]. Philadelphia: Mosby; 2007 [citado 6 de enero de 2023]. p. 11-7. Disponible en: https://www.sciencedirect.com/science/article/pii/B978032304318250008X

91. Nafisi S, Maibach HI. Chapter 3 - Skin penetration of nanoparticles. En: Shegokar R, Souto EB, editores. Emerging Nanotechnologies in Immunology [Internet]. Boston: Elsevier; 2018 [citado 6 de enero de 2023]. p. 47-88. (Micro and Nano Technologies). Disponible en: https://www.sciencedirect.com/science/article/pii/B9780323400169000038

92. Menon GK, Dryer L, Kalafsky R. Chapter 11 - Approaches to the Development of Cosmetic Products to Counter the Effects of Skin Aging. En: Dayan N, editor. Skin Aging Handbook [Internet]. Norwich, NY: William Andrew Publishing; 2009 [citado 6 de enero de 2023]. p. 265-90. (Personal Care & Cosmetic Technology). Disponible en: https://www.sciencedirect.com/science/article/pii/B9780815515845500156

93. Fong M, Crane JS. Histology, Mast Cells. En: StatPearls [Internet]. Treasure Island (FL): StatPearls Publishing; 2022 [citado 6 de enero de 2023]. Disponible en: http://www.ncbi.nlm.nih.gov/books/NBK499904/

94. Möllerherm H, Meier K, Schmies K, Fuhrmann H, Naim HY, von Köckritz-Blickwede M, et al. Differentiation and Functionality of Bone Marrow-Derived Mast Cells Depend on Varying Physiologic Oxygen Conditions. Front Immunol. 2017;8:1665.

95. Yong LC. The mast cell: origin, morphology, distribution, and function. Exp Toxicol Pathol Off J Ges Toxikol Pathol. diciembre de 1997;49(6):409-24.

96. Xie F, Chai JK, Hu Q, Yu YH, Ma L, Liu LY, et al. Transdermal permeation of drugs with differing lipophilicity: Effect of penetration enhancer camphor. Int J Pharm. 30 de junio de 2016;507(1-2):90-101.

97. Kováčik A, Kopečná M, Vávrová K. Permeation enhancers in transdermal drug delivery: benefits and limitations. Expert Opin Drug Deliv. 1 de febrero de 2020;17(2):145-55.

98. Sugino M, Todo H, Sugibayashi K. [Skin permeation and transdermal delivery systems of drugs: history to overcome barrier function in the stratum corneum]. Yakugaku Zasshi. diciembre de 2009;129(12):1453-8.

99. Alkilani AZ, McCrudden MTC, Donnelly RF. Transdermal Drug Delivery: Innovative Pharmaceutical Developments Based on Disruption of the Barrier Properties of the Stratum Corneum. Pharmaceutics. diciembre de 2015;7(4):438-70.

100. Lademann J, Otberg N, Richter H, Jacobi U, Schaefer H, Blume-Peytavi U, et al. [Follicular penetration. An important pathway for topically applied substances]. Hautarzt Z Dermatol Venerol Verwandte Geb. abril de 2003;54(4):321-3.

101. Denis F, Alain S, Ploy MC. [New routes of administration: epidermal, transcutaneous mucosal ways of vaccination]. Med Sci MS. abril de 2007;23(4):379-85.

102. Ranade VV. Drug delivery systems. 6. Transdermal drug delivery. J Clin Pharmacol. mayo de 1991;31(5):401-18.

103. Samad A, Ullah Z, Alam MI, Wais M, Shams MS. Transdermal drug delivery system: patent reviews. Recent Pat Drug Deliv Formul. junio de 2009;3(2):143-52.

104. Deb PK, Kokaz SF, Abed SN, Paradkar A, Tekade RK. Chapter 6 - Pharmaceutical and Biomedical Applications of Polymers. En: Tekade RK, editor. Basic Fundamentals of Drug Delivery [Internet]. Academic Press; 2019 [citado 6 de enero de 2023]. p. 203-67. (Advances in Pharmaceutical Product Development and Research). Disponible en: https://www.sciencedirect.com/science/article/pii/B9780128179093000066

105. Mishra DK, Pandey V, Maheshwari R, Ghode P, Tekade RK. Chapter 15 - Cutaneous and Transdermal Drug Delivery: Techniques and Delivery Systems. En: Tekade RK, editor. Basic Fundamentals of Drug Delivery [Internet]. Academic Press; 2019 [citado 6 de enero de 2023]. p. 595-650. (Advances in Pharmaceutical Product Development and Research). Disponible en: https://www.sciencedirect.com/science/article/pii/B9780128179093000157

106. Bibi N, Ahmed N, Khan GM. Chapter 21 - Nanostructures in transdermal drug delivery systems. En: Andronescu E, Grumezescu AM, editores. Nanostructures for Drug Delivery [Internet]. Elsevier; 2017 [citado 6 de enero de 2023]. p. 639-68. (Micro and Nano Technologies). Disponible en: https://www.sciencedirect.com/science/article/pii/B978032346143600021X

107. Roy J. 13 - New pharmaceutical technology and pharmaceuticals. En: Roy J, editor. An Introduction to Pharmaceutical Sciences [Internet]. Woodhead Publishing; 2011 [citado 6 de enero de 2023]. p. 349-56. (Woodhead Publishing Series in Biomedicine). Disponible en: https://www.sciencedirect.com/science/article/pii/B9781907568527500132

108. Liu C, Quan P, Fang L. Effect of drug physicochemical properties on drug release and their relationship with drug skin permeation behaviors in hydroxyl pressure sensitive adhesive. Eur J Pharm Sci Off J Eur Fed Pharm Sci. 10 de octubre de 2016;93:437-46.

109. Keberle H. Physico-chemical factors of drugs affecting absorption, distribution, and excretion. Acta Pharmacol Toxicol (Copenh). 1971;29 Suppl 3:30-47.

110. Chandrasekaran SK, Shaw JE. Factors influencing the percutaneous absorption of drugs. Curr Probl Dermatol. 1978;7:142-55.

111. Yu YQ, Yang X, Wu XF, Fan YB. Enhancing Permeation of Drug Molecules Across the Skin via Delivery in Nanocarriers: Novel Strategies for Effective Transdermal Applications. Front Bioeng Biotechnol [Internet]. 2021 [citado 6 de enero de 2023];9. Disponible en: https://www.frontiersin.org/articles/10.3389/fbioe.2021.646554

112. Lopes LB, Garcia MTJ, Bentley MVLB. Chemical penetration enhancers. Ther Deliv. 2015;6(9):1053-61.

113. Ita K. Chapter 5 - Chemical permeation enhancers. En: Ita K, editor. Transdermal Drug Delivery [Internet]. Academic Press; 2020 [citado 13 de febrero de 2022]. p. 63-96. Disponible en: https://www.sciencedirect.com/science/article/pii/B9780128225509000053

114. Gupta R, Dwadasi BS, Rai B, Mitragotri S. Effect of Chemical Permeation Enhancers on Skin Permeability: In silico screening using Molecular Dynamics simulations. Sci Rep. 6 de febrero de 2019;9(1):1456.

115. Qi QM, Duffy M, Curreri AM, Balkaran JPR, Tanner EEL, Mitragotri S. Comparison of Ionic Liquids and Chemical Permeation Enhancers for Transdermal Drug Delivery. Adv Funct Mater. 2020;30(45):2004257.

116. Kolb L, Ferrer-Bruker SJ. Atopic Dermatitis. En: StatPearls [Internet]. Treasure Island (FL): StatPearls Publishing; 2022 [citado 6 de enero de 2023]. Disponible en: http://www.ncbi.nlm.nih.gov/books/NBK448071/

117. Fishbein AB, Silverberg JI, Wilson EJ, Ong PY. Update on Atopic Dermatitis: Diagnosis, Severity Assessment, and Treatment Selection. J Allergy Clin Immunol Pract. enero de 2020;8(1):91-101.

118. Schneider L, Tilles S, Lio P, Boguniewicz M, Beck L, LeBovidge J, et al. Atopic dermatitis: a practice parameter update 2012. J Allergy Clin Immunol. febrero de 2013;131(2):295-299.e1-27.

119. Margolis JS, Abuabara K, Bilker W, Hoffstad O, Margolis DJ. Persistence of mild to moderate atopic dermatitis. JAMA Dermatol. junio de 2014;150(6):593-600.

120. Kasemsarn P, Bosco J, Nixon RL. The Role of the Skin Barrier in Occupational Skin Diseases. Curr Probl Dermatol. 2016;49:135-43.

121. Kezic S, Jakasa I. Filaggrin and Skin Barrier Function. Curr Probl Dermatol. 2016;49:1-7.

122. Drislane C, Irvine AD. The role of filaggrin in atopic dermatitis and allergic disease. Ann Allergy Asthma Immunol. enero de 2020;124(1):36-43.

123. David Boothe W, Tarbox JA, Tarbox MB. Atopic Dermatitis: Pathophysiology. Adv Exp Med Biol. 2017;1027:21-37.

124. Rho NK, Kim WS, Lee DY, Lee JH, Lee ES, Yang JM. Immunophenotyping of inflammatory cells in lesional skin of the extrinsic and intrinsic types of atopic dermatitis. Br J Dermatol. julio de 2004;151(1):119-25.

125. Weidinger S, Beck LA, Bieber T, Kabashima K, Irvine AD. Atopic dermatitis. Nat Rev Dis Primer. 21 de junio de 2018;4(1):1-20.

126. Ho AW, Kupper TS. T cells and the skin: from protective immunity to inflammatory skin disorders. Nat Rev Immunol. agosto de 2019;19(8):490-502.
127. Luger T, Amagai M, Dreno B, Dagnelie MA, Liao W, Kabashima K, et al. Atopic dermatitis: Role of the skin barrier, environment, microbiome, and therapeutic agents. J Dermatol Sci. junio de 2021;102(3):142-57.
128. Farshchian M, Daveluy S. Rosacea. En: StatPearls [Internet]. Treasure Island (FL): StatPearls Publishing; 2022 [citado 6 de enero de 2023]. Disponible en: http://www.ncbi.nlm.nih.gov/books/NBK557574/
129. Oge' LK, Muncie HL, Phillips-Savoy AR. Rosacea: Diagnosis and Treatment. Am Fam Physician. 1 de agosto de 2015;92(3):187-96.
130. Rainer BM, Fischer AH, Luz Felipe da Silva D, Kang S, Chien AL. Rosacea is associated with chronic systemic diseases in a skin severity-dependent manner: results of a case-control study. J Am Acad Dermatol. octubre de 2015;73(4):604-8.
131. Woo YR, Lim JH, Cho DH, Park HJ. Rosacea: Molecular Mechanisms and Management of a Chronic Cutaneous Inflammatory Condition. Int J Mol Sci. 15 de septiembre de 2016;17(9):1562.
132. The innate and adaptive immune systems [Internet]. InformedHealth.org [Internet]. Institute for Quality and Efficiency in Health Care (IQWiG); 2020 [citado 6 de enero de 2023]. Disponible en: https://www.ncbi.nlm.nih.gov/books/NBK279396/
133. Jang HM, Park JY, Lee YJ, Kang MJ, Jo SG, Jeong YJ, et al. TLR2 and the NLRP3 inflammasome mediate IL-1β production in Prevotella nigrescens-infected dendritic cells. Int J Med Sci. 2021;18(2):432-40.
134. Emmi G, Bettiol A, Silvestri E, Di Scala G, Becatti M, Fiorillo C, et al. Vascular Behçet's syndrome: an update. Intern Emerg Med. agosto de 2019;14(5):645-52.
135. Nair J, Moots R. Behcet's disease. Clin Med. 2017;17(1):71-7.
136. Arayssi T. New insights into the pathogenesis and therapy of Behçet's disease. Curr Opin Pharmacol. abril de 2004;4(2):183-8.
137. Ceylan Kalın Z, Sarıcaoğlu H, Yazici S, Aydoğan K, Bülbül Başkan E. Clinical and Demographical Characteristics of Familial Behçet's Disease (Southeast Marmara Region). Dermatology. 2019;235(5):407-12.
138. Davatchi F, Shahram F, Chams-Davatchi C, Shams H, Abdolahi BS, Nadji A, et al. Behcet's disease in Iran: Analysis of 7641 cases. Mod Rheumatol. 2 de noviembre de 2019;29(6):1023-30.
139. Muhaya M, Lightman S, Ikeda E, Mochizuki M, Shaer B, McCluskey P, et al. Behçet's disease in Japan and in Great Britain: a comparative study. Ocul Immunol Inflamm. 2000;8(3):141-8.
140. Chen Y, Cai JF, Lin CH, Guan JL. Demography of vascular Behcet's disease with different gender and age: an investigation with 166 Chinese patients. Orphanet J Rare Dis. diciembre de 2019;14(1):88.

141. Alkazzaz AMH, Ebdan WR, Ghoben MustafaK, Kareem ZT, Al-Harbi SJO. Behçet's disease in Iraq: new insights into the clinical and epidemiologic features in Middle-Euphrates region. Expert Rev Clin Immunol. 2 de enero de 2020;16(1):109-12.

142. Liu X, Gao F, Zhao C, Zhang M. Clinical features of patients with Behcet's uveitis. Chin J Ophthalmol. 2020;56(3):217-23.

143. Sota J, Rigante D, Emmi G, Lopalco G, Orlando I, Tosi GM, et al. Behçet's syndrome in Italy: a detailed retrospective analysis of 396 cases seen in 3 tertiary referral clinics. Intern Emerg Med [Internet]. 2020 [citado 24 de abril de 2020]; Disponible en: http://link.springer.com/10.1007/s11739-019-02248-4

144. Wessman LL, Andersen LK, Davis MDP. Incidence of diseases primarily affecting the skin by age group: population-based epidemiologic study in Olmsted County, Minnesota, and comparison with age-specific incidence rates worldwide. Int J Dermatol. 2018;57(9):1021-34.

145. Toledo-Samaniego N, Galeano-Valle F, Ascanio-Palomares P, González-Martínez B, Valencia-Kruszyna A, Demelo-Rodríguez P. Manifestaciones neurológicas en la enfermedad de Behçet: estudio de 57 pacientes. Med Clínica. 2020;1-5.

146. Borhani-Haghighi A, Kardeh B, Banerjee S, Yadollahikhales G, Safari A, Sahraian MA, et al. Neuro-Behcet's disease: An update on diagnosis, differential diagnoses, and treatment. Mult Scler Relat Disord. abril de 2020;39:101906.

147. Pay S, Şimşek İ, Erdem H, Dinç A. Immunopathogenesis of Behçet's disease with special emphasize on the possible role of antigen presenting cells. Rheumatol Int. 15 de febrero de 2007;27(5):417-24.

148. Greco A, De Virgilio A, Ralli M, Ciofalo A, Mancini P, Attanasio G, et al. Behçet's disease: New insights into pathophysiology, clinical features and treatment options. Autoimmun Rev. junio de 2018;17(6):567-75.

149. Zouboulis ChC, Katsantonis J, Ketteler R, Treudler R, Kaklamani E, Hornemann S, et al. Adamantiades-Behçet's disease: interleukin-8 is increased in serum of patients with active oral and neurological manifestations and is secreted by small vessel endothelial cells. Arch Dermatol Res. 2000;292(6):279-84.

150. Valenti S, Gallizzi R, De Vivo D, Romano C. Intestinal Behçet and Crohn's disease: two sides of the same coin. Pediatr Rheumatol. 2017;15(1):33.

151. Direskeneli H. Autoimmunity vs autoinflammation in Behcet's disease: do we oversimplify a complex disorder? Rheumatology. 18 de agosto de 2006;45(12):1461-5.

152. Mizuki N, Meguro A, Ota M, Ohno S, Shiota T, Kawagoe T, et al. Genome-wide association studies identify IL23R-IL12RB2 and IL10 as Behçet's disease susceptibility loci. Nat Genet. agosto de 2010;42(8):703-6.

153. Aridogan BC, Yildirim M, Baysal V, Inaloz HS, Baz K, Kaya S. Serum Levels of IL-4, IL-10, IL-12, IL-13 and IFN-Gamma in Behçet's Disease. J Dermatol. agosto de 2003;30(8):602-7.

154. Cho JH, Brant SR. Recent Insights Into the Genetics of Inflammatory Bowel Disease. Gastroenterology. mayo de 2011;140(6):1704-1712.e2.

155. Remmers EF, Cosan F, Kirino Y, Ombrello MJ, Abaci N, Satorius C, et al. Genome-wide association study identifies variants in the MHC class I, IL10, and IL23R-IL12RB2 regions associated with Behçet's disease. Nat Genet. agosto de 2010;42(8):698-702.

156. Cabras M, Carrozzo M, Gambino A, Broccoletti R, Sciascia S, Baldovino S, et al. Value of colchicine as treatment for recurrent oral ulcers: a systematic review. J Oral Pathol Med [Internet]. 13 de abril de 2020 [citado 24 de abril de 2020]; Disponible en: http://doi.wiley.com/10.1111/jop.13020

157. Djaballah-Ider F, Touil-Boukoffa C. Effect of combined colchicine-corticosteroid treatment on neutrophil/lymphocyte ratio: a predictive marker in Behçet disease activity. Inflammopharmacology [Internet]. 29 de marzo de 2020 [citado 24 de abril de 2020]; Disponible en: http://link.springer.com/10.1007/s10787-020-00701-x

158. Hatemi G, Mahr A, Ishigatsubo Y, Song YW, Takeno M, Kim D, et al. Trial of Apremilast for Oral Ulcers in Behçet's Syndrome. N Engl J Med. 2019;381(20):1918-28.

159. Giácaman von der Weth MM, Tapial JM, Guillén BF, Ferrer DS, Sánchez-Carazo JL, Ninet VZ. Complex Aphthae Treated With Apremilast. JCR J Clin Rheumatol. abril de 2020;26(3):e69.

160. Cetin Gedik K, Romano M, Berard RA, Demirkaya E. An Overview of Conventional and Recent Treatment Options for Behcet's Disease. Curr Treat Options Rheumatol [Internet]. 28 de marzo de 2020 [citado 24 de abril de 2020]; Disponible en: http://link.springer.com/10.1007/s40674-020-00143-0

161. Maloney NJ, Zhao J, Tegtmeyer K, Lee EY, Cheng K. Off-label studies on apremilast in dermatology: a review. J Dermatol Treat. 17 de febrero de 2020;31(2):131-40.

162. De Luca G, Cariddi A, Campochiaro C, Vanni D, Boffini N, Tomelleri A, et al. Efficacy and safety of apremilast for Behçet's syndrome: a real-life single-centre Italian experience. Rheumatology. 1 de enero de 2020;59(1):171-5.

163. Schafer P. Apremilast mechanism of action and application to psoriasis and psoriatic arthritis. Biochem Pharmacol. junio de 2012;83(12):1583-90.

164. Padda IS, Bhatt R, Parmar M. Apremilast. En: StatPearls [Internet]. Treasure Island (FL): StatPearls Publishing; 2022 [citado 6 de enero de 2023]. Disponible en: http://www.ncbi.nlm.nih.gov/books/NBK572078/

165. Young M, Roebuck HL. Apremilast, an oral phosphodiesterase 4 (PDE4) inhibitor: A novel treatment option for nurse practitioners treating patients with psoriatic disease. J Am Assoc Nurse Pract. diciembre de 2016;28(12):683-95.

166. Bissonnette R, Pariser DM, Wasel NR, Goncalves J, Day RM, Chen R, et al. Apremilast, an oral phosphodiesterase-4 inhibitor, in the treatment of palmoplantar psoriasis: Results of a pooled analysis from phase II PSOR-005 and phase III Efficacy and Safety Trial Evaluating the Effects

of Apremilast in Psoriasis (ESTEEM) clinical trials in patients with moderate to severe psoriasis. J Am Acad Dermatol. julio de 2016;75(1):99-105.

167. Keating GM. Apremilast: A Review in Psoriasis and Psoriatic Arthritis. Drugs. marzo de 2017;77(4):459-72.

168. Viswanath V, Joshi P, Lawate P, Tare D, Dhoot D, Mahadkar N, et al. An Open-Label, Randomized, Prospective, Comparative, Three-Arm Clinical Trial to Evaluate the Safety and Effectiveness of Apremilast with Three Different Titration Methods in Patients with Chronic Plaque Psoriasis in India. Psoriasis Auckl NZ. 2022;12:53-61.

169. Schett G, Sloan VS, Stevens RM, Schafer P. Apremilast: a novel PDE4 inhibitor in the treatment of autoimmune and inflammatory diseases. Ther Adv Musculoskelet Dis. octubre de 2010;2(5):271-8.

170. Meier-Schiesser B, Mellett M, Ramirez-Fort MK, Maul JT, Klug A, Winkelbeiner N, et al. Phosphodiesterase-4 Inhibition Reduces Cutaneous Inflammation and IL-1β Expression in a Psoriasiform Mouse Model but Does Not Inhibit Inflammasome Activation. Int J Mol Sci. 28 de noviembre de 2021;22(23):12878.

171. Bianchi L, Del Duca E, Romanelli M, Saraceno R, Chimenti S, Chiricozzi A. Pharmacodynamic assessment of apremilast for the treatment of moderate-to-severe plaque psoriasis. Expert Opin Drug Metab Toxicol. septiembre de 2016;12(9):1121-8.

172. Langley A, Beecker J. Management of Common Side Effects of Apremilast. J Cutan Med Surg. julio de 2018;22(4):415-21.

173. Karimkhani Aksut C, Dellavalle RP, Naghavi M. 181 Global skin disease morbidity and mortality: An update from the Global Burden of Disease Study 2013. J Invest Dermatol. mayo de 2017;137(5):S31.

174. Seth D, Cheldize K, Brown D, Freeman EE. Global Burden of Skin Disease: Inequities and Innovations. Curr Dermatol Rep. septiembre de 2017;6(3):204-10.

175. Zhang X jie, Wang A ping, Shi T ying, Zhang J, Xu H, Wang D qiu, et al. The psychosocial adaptation of patients with skin disease: a scoping review. BMC Public Health. diciembre de 2019;19(1):1404.

176. Zamora NV, Valerio-Morales IA, Lopez-Olivo MA, Pan X, Suarez-Almazor ME. Phosphodiesterase 4 inhibitors for psoriatic arthritis. Cochrane Musculoskeletal Group, editor. Cochrane Database Syst Rev [Internet]. 15 de octubre de 2016 [citado 5 de mayo de 2020]; Disponible en: http://doi.wiley.com/10.1002/14651858.CD012401

177. Lopalco G, Venerito V, Leccese P, Emmi G, Cantarini L, Lascaro N, et al. Real-world effectiveness of apremilast in multirefractory mucosal involvement of Behçet's disease. Ann Rheum Dis. diciembre de 2019;78(12):1736-7.

178. European Medicines Agency. ICH Q2 (R1) Validation of analytical procedures: text and methodology [Internet]. European Medicines Agency. 2018 [citado 15 de julio de 2020].

Disponible en: https://www.ema.europa.eu/en/ich-q2-r1-validation-analytical-procedures-text-methodology

179. Kulkarni P, Deshpande A. Analytical Methods for Determination of Apremilast from Bulk, Dosage Form and Biological Fluids: A Critical Review. Crit Rev Anal Chem. 5 de febrero de 2020;1-10.

180. Wadhwa J, Nair A, Kumria R. Self-emulsifying therapeutic system: a potential approach for delivery of lipophilic drugs. Braz J Pharm Sci. septiembre de 2011;47(3):447-65.

181. Abbasi S, Amiri-Rigi A. Microemulsions as Nano-Carriers for Nutraceuticals: Current Trends and the Future Outlook. EC Nutr. 2017;12(1):46-50.

182. Fernández-Campos F, Clares Naveros B, López Serrano O, Alonso Merino C, Calpena Campmany AC. Evaluation of novel nystatin nanoemulsion for skin candidosis infections: Nystatin nanoemulsion for skin candidosis. Mycoses. enero de 2013;56(1):70-81.

183. Espinoza LC, Silva-Abreu M, Calpena AC, Rodríguez-Lagunas MJ, Fábrega MJ, Garduño-Ramírez ML, et al. Nanoemulsion strategy of pioglitazone for the treatment of skin inflammatory diseases. Nanomedicine Nanotechnol Biol Med. julio de 2019;19:115-25.

184. Gué E, Since M, Ropars S, Herbinet R, Le Pluart L, Malzert-Fréon A. Evaluation of the versatile character of a nanoemulsion formulation. Int J Pharm. febrero de 2016;498(1-2):49-65.

185. Elmataeeshy ME, Sokar MS, Bahey-El-Din M, Shaker DS. Enhanced transdermal permeability of Terbinafine through novel nanoemulgel formulation; Development, in vitro and in vivo characterization. Future J Pharm Sci. junio de 2018;4(1):18-28.

186. Szumała P. Structure of Microemulsion Formulated with Monoacylglycerols in the Presence of Polyols and Ethanol. J Surfactants Deterg. 2015;18:97-106.

187. Ciurlizza C, Fernández F, Calpena AC, Lázaro R, Parra A, Clares B. Semisolid formulations containing cetirizine: human skin permeation and topical antihistaminic evaluation in a rabbit model. Arch Dermatol Res. octubre de 2014;306(8):711-7.

188. Ali MS, Alam MS, Alam N, Siddiqui MR. Preparation, Characterization and Stability Study of Dutasteride Loaded Nanoemulsion for Treatment of Benign Prostatic Hypertrophy. 2014;16.

189. Zhang Z, McClements DJ. Overview of Nanoemulsion Properties: Stability, Rheology, and Appearance. En: Nanoemulsions [Internet]. Elsevier; 2018 [citado 5 de mayo de 2020]. p. 21-49. Disponible en: https://linkinghub.elsevier.com/retrieve/pii/B9780128118382000023

190. Mehrnia MA, Jafari SM, Makhmal-Zadeh BS, Maghsoudlou Y. Rheological and release properties of double nano-emulsions containing crocin prepared with Angum gum, Arabic gum and whey protein. Food Hydrocoll. mayo de 2017;66:259-67.

191. Salamanca C, Barrera-Ocampo A, Lasso J, Camacho N, Yarce C. Franz Diffusion Cell Approach for Pre-Formulation Characterisation of Ketoprofen Semi-Solid Dosage Forms. Pharmaceutics. 5 de septiembre de 2018;10(3):148.

192. Dahan A, Miller JM. The Solubility–Permeability Interplay and Its Implications in Formulation Design and Development for Poorly Soluble Drugs. AAPS J. junio de 2012;14(2):244-51.

193. Mallandrich M, Fernández-Campos F, Clares B, Halbaut L, Alonso C, Coderch L, et al. Developing Transdermal Applications of Ketorolac Tromethamine Entrapped in Stimuli Sensitive Block Copolymer Hydrogels. Pharm Res. agosto de 2017;34(8):1728-40.

194. Lai J, Maibach HI. Experimental models in predicting topical antifungal efficacy: practical aspects and challenges. Skin Pharmacol Physiol. 2009;22(5):231-9.

195. Abd E, Yousef SA, Pastore MN, Telaprolu K, Mohammed YH, Namjoshi S, et al. Skin models for the testing of transdermal drugs. Clin Pharmacol Adv Appl. 19 de octubre de 2016;8:163-76.

196. Schafer PH, Chen P, Fang L, Wang A, Chopra R. The Pharmacodynamic Impact of Apremilast, an Oral Phosphodiesterase 4 Inhibitor, on Circulating Levels of Inflammatory Biomarkers in Patients with Psoriatic Arthritis: Substudy Results from a Phase III, Randomized, Placebo-Controlled Trial (PALACE 1). J Immunol Res [Internet]. 2015 [citado 8 de noviembre de 2020];2015. Disponible en: https://www.ncbi.nlm.nih.gov/pmc/articles/PMC4417944/

197. Messamore E, Yao JK. Phospholipid, arachidonate and eicosanoid signaling in schizophrenia. OCL. enero de 2016;23(1):D112.

198. Kiezel-Tsugunova M, Kendall AC, Nicolaou A. Fatty acids and related lipid mediators in the regulation of cutaneous inflammation. Biochem Soc Trans. 19 de febrero de 2018;46(1):119-29.

199. Hwang PA, Hung YL, Chien SY. Inhibitory activity of Sargassum hemiphyllum sulfated polysaccharide in arachidonic acid-induced animal models of inflammation. J Food Drug Anal. marzo de 2015;23(1):49-56.

200. Kawahara K, Hohjoh H, Inazumi T, Tsuchiya S, Sugimoto Y. Prostaglandin E2-induced inflammation: Relevance of prostaglandin E receptors. Biochim Biophys Acta BBA - Mol Cell Biol Lipids. abril de 2015;1851(4):414-21.

201. Veras HNH, Araruna MKA, Costa JGM, Coutinho HDM, Kerntopf MR, Botelho MA, et al. Topical Antiinflammatory Activity of Essential Oil of *Lippia sidoides* Cham: Possible Mechanism of Action: LIPPIA SIDOIDES. Phytother Res. febrero de 2013;27(2):179-85.

202. Toda K, Tsukayama I, Nagasaki Y, Konoike Y, Tamenobu A, Ganeko N, et al. Red-kerneled rice proanthocyanidin inhibits arachidonate 5-lipoxygenase and decreases psoriasis-like skin inflammation. Arch Biochem Biophys. febrero de 2020;108307.

203. Pincelli C, Schafer PH, French LE, Augustin M, Krueger JG. Mechanisms Underlying the Clinical Effects of Apremilast for Psoriasis. 2018;17(8):6.

204. da Silva BAF, da Costa RHS, Fernandes CN, Leite LHI, Ribeiro-Filho J, Garcia TR, et al. HPLC profile and antiedematogenic activity of Ximenia americana L. (Olacaceae) in mice models of skin inflammation. Food Chem Toxicol. septiembre de 2018;119:199-205.

205. Tang SC, Liao PY, Hung SJ, Ge JS, Chen SM, Lai JC, et al. Topical application of glycolic acid suppresses the UVB induced IL-6, IL-8, MCP-1 and COX-2 inflammation by modulating NF-κB signaling pathway in keratinocytes and mice skin. J Dermatol Sci. junio de 2017;86(3):238-48.

206. De Vry CG, Valdez M, Lazarov M, Muhr E, Buelow R, Fong T, et al. Topical Application of A Novel Immunomodulatory Peptide, RDP58, Reduces Skin Inflammation in the Phorbol Ester-Induced Dermatitis Model. J Invest Dermatol. 1 de septiembre de 2005;125(3):473-81.

207. Schüler R, Brand A, Klebow S, Wild J, Veras FP, Ullmann E, et al. Antagonization of IL-17A Attenuates Skin Inflammation and Vascular Dysfunction in Mouse Models of Psoriasis. J Invest Dermatol. marzo de 2019;139(3):638-47.

208. Go HN, Lee SH, Cho HJ, Ahn JR, Kang MJ, Lee SY, et al. Effects of chloromethylisothiazolinone/methylisothiazolinone (CMIT/MIT) on Th2/Th17-related immune modulation in an atopic dermatitis mouse model. Sci Rep. diciembre de 2020;10(1):4099.

209. Lubrano E, Scriffignano S, Perrotta FM. TNF-alpha inhibitors for the six treatment targets of psoriatic arthritis. Expert Rev Clin Immunol. 2 de diciembre de 2019;15(12):1303-12.

210. Mootoo A, Stylianou E, Reljic MAA and R. TNF-α in Tuberculosis: A Cytokine with a Split Personality. Inflamm Allergy - Drug Targets Discontin. 2009;8(1):53-62.

211. Chu WM. Tumor necrosis factor. Cancer Lett. enero de 2013;328(2):222-5.

212. Liu Y, Yang G, Zhang J, Xing K, Dai L, Cheng L, et al. Anti-TNF-α monoclonal antibody reverses psoriasis through dual inhibition of inflammation and angiogenesis. Int Immunopharmacol. septiembre de 2015;28(1):731-43.

213. Lin ZM, Ma M, Li H, Qi Q, Liu YT, Yan YX, et al. Topical administration of reversible SAHH inhibitor ameliorates imiquimod-induced psoriasis-like skin lesions in mice via suppression of TNF-α/IFN-γ-induced inflammatory response in keratinocytes and T cell-derived IL-17. Pharmacol Res. 1 de marzo de 2018;129:443-52.

214. Ozawa M, Terui T, Tagami H. Localization of IL-8 and Complement Components in Lesional Skin of Psoriasis vulgaris and Pustulosis palmaris et plantaris. Dermatology. 2005;211(3):249-55.

215. Kondo S, Kono T, Sauder DN, McKenzie RC. IL-8 gene expression and production in human keratinocytes and their modulation by UVB. J Invest Dermatol. noviembre de 1993;101(5):690-4.

216. Bernardini N, Skroza N, Tolino E, Mambrin A, Anzalone A, Balduzzi V, et al. IL-17 and its role in inflammatory, autoimmune, and oncological skin diseases: state of art. Int J Dermatol. abril de 2020;59(4):406-11.

217. Beringer A, Noack M, Miossec P. IL-17 in Chronic Inflammation: From Discovery to Targeting. Trends Mol Med. marzo de 2016;22(3):230-41.

218. Medvedeva IV, Stokes ME, Eisinger D, LaBrie ST, Ai J, Trotter MWB, et al. Large-scale Analyses of Disease Biomarkers and Apremilast Pharmacodynamic Effects. Sci Rep. diciembre de 2020;10(1):605.

219. Villanueva-Martínez A, Hernández-Rizo L, Ganem-Rondero A. Evaluating two nanocarrier systems for the transdermal delivery of sodium alendronate. Int J Pharm. mayo de 2020;582:119312.

220. Alalaiwe A, Lin CF, Hsiao CY, Chen EL, Lin CY, Lien WC, et al. Development of flavanone and its derivatives as topical agents against psoriasis: The prediction of therapeutic efficiency through skin permeation evaluation and cell-based assay. Int J Pharm. mayo de 2020;581:119256.

221. Duplan H, Nocera T. Hydratation cutanée et produits hydratants. Ann Dermatol Vénéréologie. mayo de 2018;145(5):376-84.

222. Tomita Y, Akiyama M, Shimizu H. Stratum corneum hydration and flexibility are useful parameters to indicate clinical severity of congenital ichthyosis. Exp Dermatol. agosto de 2005;14(8):619-24.

223. Schario M, Tomova-Simitchieva T, Lichterfeld A, Herfert H, Dobos G, Lahmann N, et al. Effects of two different fabrics on skin barrier function under real pressure conditions. J Tissue Viability. mayo de 2017;26(2):150-5.

224. Zhang Q, Murawsky M, LaCount T, Kasting GB, Li SK. Transepidermal water loss and skin conductance as barrier integrity tests. Toxicol In Vitro. septiembre de 2018;51:129-35.

225. Fujimura T, Shimotoyodome Y, Nishijima T, Sugata K, Taguchi H, Moriwaki S. Changes in hydration of the stratum corneum are the most suitable indicator to evaluate the irritation of surfactants on the skin. Skin Res Technol. febrero de 2017;23(1):97-103.

226. Madan JR, Khobaragade S, Dua K, Awasthi R. Formulation, optimization, and in vitro evaluation of nanostructured lipid carriers for topical delivery of Apremilast. Dermatol Ther [Internet]. mayo de 2020 [citado 10 de diciembre de 2020];33(3). Disponible en: https://onlinelibrary.wiley.com/doi/abs/10.1111/dth.13370

227. Sarango-Granda P, Silva-Abreu M, Calpena AC, Halbaut L, Fábrega MJ, Rodríguez-Lagunas MJ, et al. Apremilast Microemulsion as Topical Therapy for Local Inflammation: Design, Characterization and Efficacy Evaluation. Pharmaceuticals. diciembre de 2020;13(12):484.

228. Shakeel F, Haq N, Alanazi FK, Alsarra IA. Solubility and thermodynamics of apremilast in different mono solvents: Determination, correlation and molecular interactions. Int J Pharm. mayo de 2017;523(1):410-7.

229. Amin S, Kohli K, Khar RK, Mir SR, Pillai KK. Mechanism of In Vitro Percutaneous Absorption Enhancement of Carvedilol by Penetration Enhancers. Pharm Dev Technol. enero de 2008;13(6):533-9.

230. Chen J, Jiang QD, Wu YM, Liu P, Yao JH, Lu Q, et al. Potential of Essential Oils as Penetration Enhancers for Transdermal Administration of Ibuprofen to Treat Dysmenorrhoea. Mol Basel Switz. 7 de octubre de 2015;20(10):18219-36.

231. Hadgraft J, Peck J, Williams DG, Pugh WJ, Allan G. Mechanisms of action of skin penetration enhancers/retarders: Azone and analogues. Int J Pharm. septiembre de 1996;141(1-2):17-25.

232. Haq A, Michniak-Kohn B. Effects of solvents and penetration enhancers on transdermal delivery of thymoquinone: permeability and skin deposition study. Drug Deliv. 1 de enero de 2018;25(1):1943-9.

233. Sapra B, Jain S, Tiwary A. Sapra B, Jain S, Tiwary AK. Percutaneous permeation enhancement by terpenes: mechanistic view.AAPS J 10(1): 120-32. AAPS J. 1 de febrero de 2008;10:120-32.

234. Fox LT, Gerber M, Plessis JD, Hamman JH. Transdermal Drug Delivery Enhancement by Compounds of Natural Origin. Molecules. diciembre de 2011;16(12):10507-40.

235. Gref R, Deloménie C, Maksimenko A, Gouadon E, Percoco G, Lati E, et al. Vitamin C–squalene bioconjugate promotes epidermal thickening and collagen production in human skin. Sci Rep. diciembre de 2020;10(1):16883.

236. Pragst F, Auwärter V, Kießling B, Dyes C. Wipe-test and patch-test for alcohol misuse based on the concentration ratio of fatty acid ethyl esters and squalene CFAEE/CSQ in skin surface lipids. Forensic Sci Int. julio de 2004;143(2-3):77-86.

237. Huang ZR, Lin YK, Fang JY. Biological and Pharmacological Activities of Squalene and Related Compounds: Potential Uses in Cosmetic Dermatology. Mol Basel Switz. 1 de febrero de 2009;14:540-54.

238. Herman A, Herman AP. Essential oils and their constituents as skin penetration enhancer for transdermal drug delivery: a review. J Pharm Pharmacol. 2015;67(4):473-85.

239. Ly BCK, Dyer EB, Feig JL, Chien AL, Del Bino S. Research Techniques Made Simple: Cutaneous Colorimetry: A Reliable Technique for Objective Skin Color Measurement. J Invest Dermatol. enero de 2020;140(1):3-12.e1.

240. Nam GW, Baek JH, Koh JS, Hwang JK. The seasonal variation in skin hydration, sebum, scaliness, brightness and elasticity in Korean females. Skin Res Technol. febrero de 2015;21(1):1-8.